SUNFLOWER YIELD ESTIMATION USING SYNTHETIC APERTURE RADAR AND OPTICAL DATA

SENTETİK AÇIKLIKLI RADAR VE OPTİK VERİLER KULLANILARAK AYÇİÇEĞİ VERİM TAHMİNİ

İREM ECEM ASLAN

ASSOC. PROF. DR. SAYGIN ABDİKAN

Supervisor

Submitted to

Graduate School of Science and Engineering of Hacettepe University

as a Partial Fulfilment to the Requirements

for the Award of the Degree of Master of Science

in Geomatics Engineering

2023

ABSTRACT

SUNFLOWER YIELD ESTIMATION USING SYNTHETIC APERTURE RADAR AND OPTICAL DATA

İrem Ecem ASLAN

Master of Science, Department of Geomatics Engineering

Supervisor: Assoc. Prof. Dr. Saygın ABDİKAN

2023

The scope of the presented thesis, it is aimed to obtain highly accurate yield estimation by applying Artificial Neural Networks (ANN) and Simple Linear Regression (SLR) methods on sunflower parcels in a certain area using Sentinel-1 Synthetic Aperture Radar (SAR) and Sentinel-2 optical satellite images. The 2018 Sentinel-1 and Sentinel-2 satellite images of the sunflower farming region in the Zile district of Tokat province were examined. First, the Normalized Difference Vegetation Index (NDVI), Normalized Difference Vegetation Red-Edge-1 (NDVIR1), Optimized Soil-Adjusted Vegetation Index (OSAVI), and Inverted Red-edge Chlorophyll Index (IRECI) were obtained from Sentinel-2 satellite images. Then, the correlations between these indices and reference yield data were examined separately. The highest correlation in all examined vegetation indices examined was determined on 30 June, 8 July, and 10 July. Using the SLR method, OSAVI (R^2=0.75 RMSE=22.47 kg) gave the best result during the heading period on 30 June. However, when the indices are processed as a single input value in the ANN method, the best result is obtained from NDVI (R^2=0.76 RMSE=22.07 kg) in the 30 June heading period. The ANN method gave

better results than the linear regression method on all dates. The best estimation study was made with the ANN method in the NDVI and NDVIR1. When the four indices were processed together as input values, the best result was again obtained during the heading period on 30 June (R^2=0.78 RMSE=21.59 kg). In the ANN method, it was concluded that using the indices together as inputs reduces the error rate in yield estimation. The phenological stages and yield values of the sunflower plant were determined with high accuracy by the ANN method. Secondly, backscattering and coherence values obtained from Sentinel-1 satellite images produced close values in both VH and VV polarizations in most of the dates considered, but in the ANN method, VV polarization produced better values than VH polarization. When the yield estimation was made with the backscatter values, the best result in the ANN method was obtained in the VV polarization on June 29 (R^2=0,09 RMSE=42,46 kg). When the yield is estimated with the coherence values, the best result was obtained on the 5th of July-11th in the VV polarization (R^2=0.01 RMSE=46.24 kg). The results showed higher errors compared to optical data. When the R^2 value and the average RMSE are compared with the values obtained from the indices values, it is seen that the contribution of the backscatter and coherence values is very little or not in the yield estimation. The use of backscatter and coherence values alone in the yield estimation is not recommended for this study. Lastly, when the values obtained from optical and SAR satellites are used together, the best result was obtained during the heading period between 29 June - 5 July (R^2=0.67 RMSE=26.83 kg). The estimated yield values were found with acceptable accuracy. However, the values did not improve.

Keywords : Sunflower, Sentinel-1, Sentinel-2, ANN, Yield estimation

ÖZET

SENTETİK AÇIKLIKLI RADAR VE OPTİK VERİLER KULLANILARAK AYÇİÇEĞİ VERİM TAHMİNİ

İrem Ecem ASLAN

Yüksek Lisans, Geomatik Mühendisliği Bölümü

Tez Danışmanı: Doç. Dr. Saygın ABDİKAN

2023

Sunulan tez kapsamında, Sentinel-1 Sentetik Açıklı Radar (SAR) ve Sentinel-2 optik uydu görüntülerini kullanarak belirli bir alandaki ayçiçeği parsellerinde Yapay Sinir Ağları yöntemi (YSA) ve Lineer Regresyon yöntemi uygulanarak verim tahmininin yüksek doğrulukla elde edilmesi hedeflenmiştir. Tokat ilinin Zile ilçesinde yer alan ayçiçeği tarım bölgesinin 2018 yılına ait Sentinel-1 ve Sentinel-2 uydu görüntüleri incelenmiştir. İlk önce, Sentinel-2 uydu görüntülerinden Normalleştirilmiş Fark Bitki Örtüsü İndeksi (NDVI), Normalleştirilmiş Fark Bitki Örtüsü Kırmızı Kenar 1 İndeksi (NDVIR1), Optimize Edilmiş Toprak Ayarlı Bitki Örtüsü İndeksi (OSAVI) ve Ters Kırmızı Kenarlı Klorofil İndeksi (IRECI) elde edilmiştir. Daha sonra bu indeksler ile referans verim değerleri arasındaki korelasyonlara ayrı ayrı bakılmıştır. İncelenen tüm bitki indekslerinde en yüksek korelasyon 30 Haziran, 8 Temmuz ve 10 Temmuz tarihlerinde elde edilen verilerle belirlenmiştir. Lineer regresyon metodunda en iyi sonucu, OSAVI (R^2=0,75 RMSE=22,47 kg) 30 Haziran tarihinde çiçek tablası oluşum döneminde vermiştir. Ancak, YSA yönteminde indeksler tek girdi değeri olarak işleme alındığında , en iyi sonuç 30 Haziran tarihinde çiçek tablası oluşum döneminde NDVI'dan (R^2=0,76 RMSE= 22,07 kg) alınmıştır. YSA yöntemi, lineer regresyon metodundan tüm tarihlerde daha iyi sonuç vermiştir. En iyi tahmin çalışması NDVI

ve NDVIR1 verileriyle sinir ağı yöntemiyle yapılmıştır. Dört indeks birlikte girdi değeri olarak işleme girdiğinde, en iyi sonuç 30 Haziran (R^2=0,78 RMSE= 21,59 kg) tarihinde yine çiçek tablası oluşum döneminde alınmıştır. YSA yönteminde, indekslerin girdi olarak birlikte kullanılması, verim tahmininde hata oranını azalttığı sonucuna varılmıştır. YSA yöntemi ile ayçiçeği bitkisinin fenolojik aşamaları ve verim değerleri yüksek doğrulukla belirlenmiştir. Daha sonra, Sentinel-1 uydu görüntülerinden geri saçılım ve uyumluluk değerleri hem VH hemde VV polarizasyonunda üretilmiştir. Ele alınan çoğu tarihte, incelenen polarizasyonlar birbirlerine yakın değerler üretmiştir ancak YSA yönteminde, VV polarizasyonu VH polarizasyonuna göre daha iyi değerler üretmiştir. Geri saçılım değerlerleri ile verim tahmini yapıldığında, YSA metodunda en iyi sonuç 29 Haziran VV polarizasyonunda alınmıştır (R^2=0,09 RMSE= 42,46 kg). Uyumluluk değerleri ile verim tahmini yapıldığında en iyi sonuç 5 Temmuz-11 Temmuz tarihinde VV polarizasyonunda alınmıştır (R^2= 0,01 RMSE= 46,24 kg). Bulunan sonuçlar kabul edilebilir doğrulukta bulunmamıştır. R^2 değeri ve ortalama RMSE, indeks değerlerinde elde edilen değerlerle kıyaslandığında geri saçılım ve uyumluluk değerlerinin verim tahmininde katkısnın çok az yada olmadığı görülmüştür. Geri saçılım ve uyumluluk değerlerinin tek başına verim tahmininde kullanılması bu çalışma için önerilmemektedir. YSA yöntemiyle, optik ve SAR uydularından elde ettiğimiz değerler birlikte kullanıldığında, en iyi sonuç 29 Haziran- 5 Temmuz tarihinde çiçek tablası oluşum döneminde alınmıştır (R^2=0,67 RMSE= 26,83 kg). Tahmin edilen verim değerleri, kabul edilebilir doğrulukta bulunmuştur. Ancak değerler iyileşmemiştir.

Anahtar Kelimeler: Ayçiçeği, Sentinel-1, Sentinel-2, YSA, Verim tahmini

ACKNOWLEDGEMENTS

CONTENTS

LIST OF TABLES

LIST OF FIGURES

LIST OF ABBREVIATIONS

SAR: Synthetic Aperture RADAR

VIs: Vegetation Indices

NDVI: Normalized Difference Vegetation Index

NDVIre1: Normalized Difference Vegetation Index Red-edge 1

OSAVI: Optimized Soil-Adjusted Vegetation Index

IRECI: Inverted Red-edge Chlorophyll Index

RDVI1: Red Edge Difference Vegetation Index

SLR: Simple Linear Regression

ANN: Artificial Neural Networks

R^2: Coefficient of Determination

RMSE: Root Mean Square Error

MLR: Multiple Linear Regression

CNN: Convolutional Neural Networks

SVR: Support Vector Regression

RFR: Random Forest Regression

UAV: Unmanned Aerial Vehicle

PLSR: Partial Least Squares Regression

XGBoost: Extreme Gradient Boosting

BBCH: Biologische Bundesanstalt, Bundessortenamt and CHemical industry

SIs: Salinity Indices

EC: Electrical Conductivity

LAI: Leaf Area Index

SSC: Soil Salt Content

Kg: Kilogram

VV: Vertical-Vertical

VH: Vertical-Horizontal

1. INTRODUCTION

1.1 Purpose and Scope

It has become very difficult to ensure food safety, due to the increasing population and negative meteorological effects. Therefore, it is very important to provide the timely processing of agricultural products and reliable information about crop development. The evolving era and technology aim to learn as quickly as possible, reliably, and easily. For this, remote sensing technologies, which provide us with the necessary facilities and are used in smart agriculture applications, seem to be a very good option. Remote sensing technology by satellite is providing more and more accurate and reliable results by using various methods for these requirements. One of the most widely used areas of remote sensing techniques is agricultural applications. Such as the phenological time of the plant, yield estimation, creating a product mold, increasing product yield, and determining soil salinity [1]. For example, vegetable oils are especially important in people's nutrition. Sunflower (Helianthus annuus L.), is one of the world's leading sources of vegetable oil production. It is an oilseed plant with a wide planting area and production in the world. The sunflower plant can grow in moist and dry conditions and provides easy adaptation to the soil. This is the advantage of the sunflower plant [2]. The ongoing climate changes around the world are causing extreme temperatures, drought, and salinity, which are certain stress components in agriculture. These effects decrease the yield and cause crop loss [3]. Particularly, salinity is one of the factors leading to a decrease in sunflower production by more than 60% worldwide [4]. The salinity tolerance of sunflower is 8.4 dS / m− 1, and an increase in each salinity unit relative to the tolerance level reduces the yield amount of sunflower seeds by about 5% [5]. Therefore, it is very important to get the maximum yield from the sunflower plant. The use of remote sensing techniques has become quite widespread in order to make faster and more reliable yield estimates.

Crop yield estimation is seen as an important requirement for taking precautions against drought in advance, ensuring food security for many years, monitoring plant agriculture in fast and large areas, and increasing the well-being of farmer families. In crop yield estimation studies, yield estimation is most often performed

based on land reports, but this method is a time-consuming, costly method with a high tendency to error [6]. Crop yield estimation and growth phases can be performed with both optical and Synthetic Aperture RADAR (SAR) satellites. Optical and SAR data can be used together to complement each other, depending on the study's conditions. Optical sensors operating in the optical wavelength portion of the electromagnetic spectrum are placed in satellite systems that allow viewing all or part of the earth. Different spectra represent different landforms. They can be distinguished by processing satellite images. These high resolution images are highly preferred in agricultural applications due to their low cost, ease of processing, and short-term reproducibility. Vegetation indices are obtained by different combinations formed between different bands in optical satellite images and the proportioning of these combinations to each other. Vegetation indices play a crucial role in monitoring changes in vegetation [7]. In yield estimation studies, vegetation indices are preferred because they give highly accurate results. The most widely used of these is the Normalized Difference Vegetation Index (NDVI), presented in 1974 [8]. Different vegetation index types can be used in crop yield estimation studies and other agricultural application studies. The vegetation index types to be used should be determined by the purpose of the study [9,10]. The Optimized Soil-Adjusted Vegetation Index (OSAVI) is one of the indices that, like the NDVI, is used as a predictive indicator of crop growth. Product phenology plays an important role as a series of growth stages and in determining the grain yield of a single product property [11]. The study conducted by Marino and Alvino (2019) also confirmed the ability of OSAVI to take into account the brightness of the soil [11]. The Inverted Red-Edge Chlorophyll Index (IRECI) highlights the amount of chlorophyll. Frampton et al. (2013) evaluated the biophysical variables with Sentinel-2 images. They stated that the IRECI was better than the NDVI in measuring the chlorophyll content of the canopy and showed high performance in the study [12]. Optical satellite images have also some disadvantages. As the optical satellites have passive sensors, they use the sun as an energy source and are affected by weather conditions, and can not be used at night. SAR satellite images are formed by determining the ratio between the electromagnetic energy sent to the earth's surface and the electromagnetic energy returned to a receiver [13]. The satellite sends the energy generated by itself to the Earth, and the energy scattered back is detected and recorded numerically through an antenna. The

energy returned to the sensor is called backscatter [14]. Backscatter is an important quantity that shows the reflectance values of the parcels opened on the radar image relative to each other. It is used as an important value in determining the different phenological stages of the crop in agricultural monitoring applications [15]. For example, Nasirzadehdizaji et al. (2021), confirmed that there is a high correlation between the backscatter value obtained from the Sentinel-1 radar satellite image and the growth stage of the crops [15]. The coherence value produced from several SAR images at different times can be used as a quantification to determine the signal-to-noise ratio [16]. For example, Amherdt et al. (2022) investigated the contribution of the coherence value to the backscatter value obtained from the Sentinel-1 satellite image for soybean and maize analysis. Consequently, C-band and VV polarized data may be a suitable parameter to map soybean and maize, while adding coherence to the backscatter information. However, they concluded that when the preferred variables for classification are a combination of dual-polarized (VV and VH) backscattering, it is not relevant to add coherence because of less enhancement and high computing overhead [17]. Unlike optical satellites, SAR satellites use their energy sources. They may perform day or night and are unaffected by the weather, but radar systems, display errors due to topographic effects, and speckle-noise effects on images are disadvantageous compared to optical systems and their processing and evaluation are a bit more complex [18].

Due to the various limitations of optical and SAR satellites in yield estimation studies, there is a growing interest in the joint use of both for agricultural purposes. For this purpose, there are many studies in which optical and radar satellites are used together in agricultural applications [18]. Fiezal et al. (2016) estimated the yield of crop maize plants using the artificial neural network method using optical (Spot-4/5, Formosat-2) and microwave (TerraSAR-X, Radarsat-2) satellite images. They determined that for the maize plant, the optical satellite gave the best estimation result in the red wavelength, and the adaptation of the backscatter values remained lower in the yield estimation [19]. In their study, Ranjan and Parida (2021) tried to estimate the yield estimation of rice crops using three different methods using MODIS satellite from optical satellites and Sentinel-1 satellite images from radar satellites together. As a result of this, they stated that when they

used the Multiple Linear Regression (MLR) models according to the optical image, they got better results than the radar image based on the SAR satellite [22]. The preferred method as well as the satellite image used in crop yield estimation studies can positively affect yield estimation. Artificial Neural Networks (ANN) and linear regression are broadly preferred in agricultural applications, especially for yield prediction. Simple Linear regression (SLR) is a conventional method, it establishes a linear relationship between satellite images and vegetation indices, phenological stages of plants can be examined and yield estimation can be studied. ANN is a relatively new method compared to the SLR method [23]. ANN symbolically represents interconnected processing neurons or nodes in the human brain, and is used to develop the relationships between variables and the models created [24]. ANN is a trial and error method that has many features of the human brain, it is a method that learns with experience, they make new inferences by reducing the previously learned information to general. In many studies, it has been stated that the inferences made with this method give high accuracy. Ballesteros et al. (2020) used multispectral images obtained with an Unmanned Aerial Vehicle (UAV) and compared the ANN and other linear modeling techniques to estimate the yield of the Vineyard. As a result, they stated that the ANN technique gave much better results than other SLR models [25]. Ashapure et al. (2020) presented a machine-learning approach for cotton yield estimation which has been developed using multi-temporal remote sensing image acquired by a UAV system. Three categories of product attributes generated from UAS data were used in the proposed model's ANN to predict efficiency. The performance of the ANN model was compared with Support Vector Regression (SVR) and Random Forest Regression (RFR). The comparison results revealed that the ANN model performs better than SVR and RFR. It was stated that the ANN model technique of their cotton yield estimation is a safe model that can be used in crop yield estimation [26].

1.2. Aim of the thesis

The study aims to obtain accurate yield estimation and phenological time by applying the ANN method on sunflower parcels in a certain area using Sentinel-1C-band data and multi-spectral Sentinel-2 satellite images. In addition, it is aimed to examine the relationship between vegetation indices calculated by creating time

series and yield. The main objectives of the research can be listed in detail as follows;

- Performing high-accuracy yield analysis using optical and radar satellites together with NDVI and NDVIre1, which are highly accurate spectral index options in the field of agriculture, and IRECI and OSAVI, which are index types that have not been studied much before.
- Investigation of the contribution of Sentinel-1 and Sentinel-2 satellites in achieving high accuracy results in yield analysis with the ANN method.
- Investigation of the effects of using vertical-vertical (VV) and vertical-horizontal (VH) images of SAR satellite.
- Contribution of coherence feature derived from multi-temporal VV and VH data.
- Determination of the most appropriate phenological time in yield estimation.
- In addition, it is aimed to investigate to what extent this study can contribute to local institutions and organizations.

In this study, using backscatter, and coherence of Sentinel-1 and 4 vegetation indices of Sentinel-2 satellite data will be produced separately for each image. By using the ANN method, yield estimation will be made on the test parcels where the sunflower plant gives the highest correlation in the phenological growing stage. The SLR and ANN methods were compared.

1.3 Thesis Structure

There are seven chapters in the thesis. The first part presents the role of remote sensing in agriculture and summarizes the purpose of the study. The second part includes the studies done with optical and SAR satellite images in the past and reveals the difference in this study. The third part covers the study area and materials and examines the optical and SAR satellites and the data we obtained from these satellite images. In the fourth part, the preprocessing steps of satellite images are explained. The fifth part examines the result of the study separately and together for optical and SAR satellites. The sixth chapter includes discussion, and the seventh and final chapter contains general conclusions and future work.

2. RELATED WORK

In the literature, there are many studies on agricultural product detection by remote sensing methods. These studies are promising for agricultural product detection. Therefore, in recent years, like all other agricultural products, studies on the sunflower plant have increased.

In the field of crop agriculture, many different studies such as yield estimation, creation of time series, determination of phenological phases of the product, length determination, estimation of leaf area index, and determination of soil salinity have been carried out and different methods have been developed. Sometimes only optical images, sometimes SAR satellite images, and sometimes both satellite images were used in the studies and the results were examined. These studies carried out cover different remote sensing techniques and different methods from the past to the present.

Fieuzal and Baup (2016) estimated leaf area index (LAI) and crop height (CH) of sunflower plant using optical and SAR satellite images from selected sunflower fields from Southwest France. They used TerraSAR-X, Radarsat-2, Alos, Formosat-2 and Spot-4/5 satellites and benefited from NDVI and Modified Triangular Vegetation Index (MTVI2). As a result, they obtained the highest results for L_{HH}, C_{HH} polarization and NDVI for LAI and CH. But, they stated that more analysis is required to obtain more accurate and precise results [27].

Wenzhi et al. (2017) also investigated the effectiveness of statistical models created by Partial Least Squares Regression (PLSR) and ANN in predicting the yield of sunflower plants. Data from two years of sunflower field trials on plant growth under various salt levels and nitrogen (N) application rates were utilized to calibrate and validate statistical models in Hetao Irrigation District, Inner Mongolia, China. Precise indices as inputs for the estimation of seed yield with the PLSR model, all measured indices used in comparison with a comparable accuracy (Root Mean Square Error (RMSE) = 0.81 t ha-1 and Coefficient of Determination (R^2) = 0.77) (RMSE) = 0.93 t ha-1, R^2 = 0.69). They concluded that ANN outperforms PLSR for estimated yield in different combinations, therefore it is a method that can be used to determine yield [28].

Ameline et al. (2018) estimated the yield of maize plants using an agro-meteorological model, using data from the Southwest of France, using Landsat-8 optical satellite imagery and Sentinel-1 SAR satellite image. As a result, they stated that the estimation was lower with the use of these two satellites together, but it was an acceptable result [20].

Narin (2019), determined NDVI and NDVIre1 from Sentinel-2 images gave high accuracy when RMSE values are taken into account in the phenological stages of sunflower crop yield estimation by linear regression method [6].

Narin et al. (2021), examined the relationship between NDVIred and NDVI obtained from the Sentinel-2 satellite. They examined Linear Regression, Convolutional Neural Networks (CNN), and ANN techniques using vegetation indices and estimated the yield of sunflower plants. As a result of this study, they obtained the best results with the CNN approach using NDVI with RMSE 20,874 Kg/da on 30 June 2018 and stated that there was no critical difference between the indices, and they obtained the finest outputs with the CNN method [29].

Alebele et al. (2021) estimated rice grain yield by Gaussian kernel regression method with Sentinel-1 interferometric coherence data using the red edge difference vegetation index (RDVI1) and various indices obtained from Sentinel-2 optical satellite images. As a result, they concluded that the coherence values can be used in the analysis of phenology levels of the crop and the Gaussian kernel method can be used as a preferred method in yield estimation studies [21].

Narin and Abdikan (2022) determined the phenological growing stages of the sunflower plant and estimated the yield by utilizing the seasonal Sentinel-2 images and producing ten different indices from these images. They reported that the best estimate was made by NDVI on 30 June (RMSE=10.80 kg/da and R^2=0.74). They came to the conclusion that Sentinel-2 satellite data might be utilized to monitor the growth of the sunflower plant and to gather yield information roughly three months prior to harvest. [30].

Amankulova et al. (2022) used Sentinel-2 images to determine sunflower yield with RFR, in the study they conducted in Mezohegyes, Hungary. They used Sentinel-2 images obtained between April and September. They stated that the best time to estimate sunflower yield from Sentinel-2 images was between 85 and 105 days at

the flowering stage, with high accuracy with RMSE values ranging from 121.9 to 284.5 kg/ha for different test areas. They concluded that they could predict sunflower yield 3-4 months before harvest [31].

Cui et al. (2022) studied to estimate soil salinity under sunflower cover by taking aerial images of four growing stages of sunflowers from six study areas between July and September 2021 in Hetao Irrigation Zone in Inner Mongolia Province, China, with a UAV. They investigated the correlation between vegetation indices (VIs), salinity indices (SIs), electrical conductivity (EC), leaf area index (LAI), plant height (H), three crop parameters and Soil Salt Content (SSC). Optimal parameters were determined and the SSC prediction model was created using ANN, Radom Forest, and MLR algorithms, respectively. As a result, they determined that ANN and Random Forest method outperform MLR in SSC prediction application and ANN is the best prediction model for the four growth stages of sunflowers [32].

Khalifani et al. (2022), determined sunflower seed yield in both normal and salinity stressed conditions, using MLR, ANN, and CNN approaches. They then determined the most effective parameters defined in both conditions. As a result, they concluded that head diameter parameter was the characteristic of sunflower seeds that had the most influence, and that, when compared to MLR and ANN, the CNN approach provided the most accurate prediction for sunflower seed [33].

Bognár et al. (2022) determined the yield estimation of corn, winter wheat, sunflower, and rapeseed in Hungary with 16 different vegetation indices using the MODIS optical satellite. As a result, they concluded that the yield accuracy can be increased by adding meteorological data [34].

A.Sadenova et al. (2022) conducted a study in East Kazakhstan applying the Gaussian function and Levenberg-Marquardt approach, they determined the yield of sunflower with NDVI over a 7 day period. They determined that the estimation error, depending on the week, varied between 0.67% and 10.7% each year, for the examined period. This was considered a respectable accuracy in seasonal analysis [35].

Abdikan et al. (2023), used Sentinel-1 and Sentinel-2 satellite images, to estimate the crop height of sunflowers. They used SLR, MLR, ANN, EXtreme Gradient

Boosting (XGBoost), and CNN methods. As a result, the best models in all four methods were constructed using rvh, concluding that NDVIred contributed more from their previous work than NDVI. They determined that the ANN gave the minimum error (RMSE = 3.083 cm) for the stem elongation span, while the second best result was given at the flowering stage of the CNN (RMSE = 8.731 cm) [36].

3. STUDY AREA AND MATERIALS

This study was carried out on 48 sunflower parcels in the south of the Zile district of Tokat province. Study area parcels were taken from the study of Narin (2019) [6]. Sentinel-1 with Sentinel-2 satellite images, which contain 48 sunflower parcels, were downloaded taking into account certain periods. The coherence and backscatter values were obtained from the Sentinel-1 image and the four index values (NDVI, NDVR1, IRECI, and OSAVI) were obtained from the Sentinel-2 satellite image. In this section, the study area, the phenological stages of the sunflower plant, and the satellites used are explained in detail.

3.1 The Study Area

The test site was chosen from the cropland of Tokat province located between the Fatih and Kurşunlu villages of the Zile district. Zile is one of the oldest settlements in Anatolia, it is Turkey's 169th-largest district in terms of area [37]. Zile Province is between 39° 52' and 40° 55' north latitudes and 35° 27' and 37° 39' east longitudes.

Zile district is located 67 kilometers west of Tokat province in the central Black Sea. The weather in the region is hot and dry during the summer season and snowy and cold in winter. From June to September the weather is hot. From December to February the weather is cold. It is usually rainy in April, May, June, November, and December.
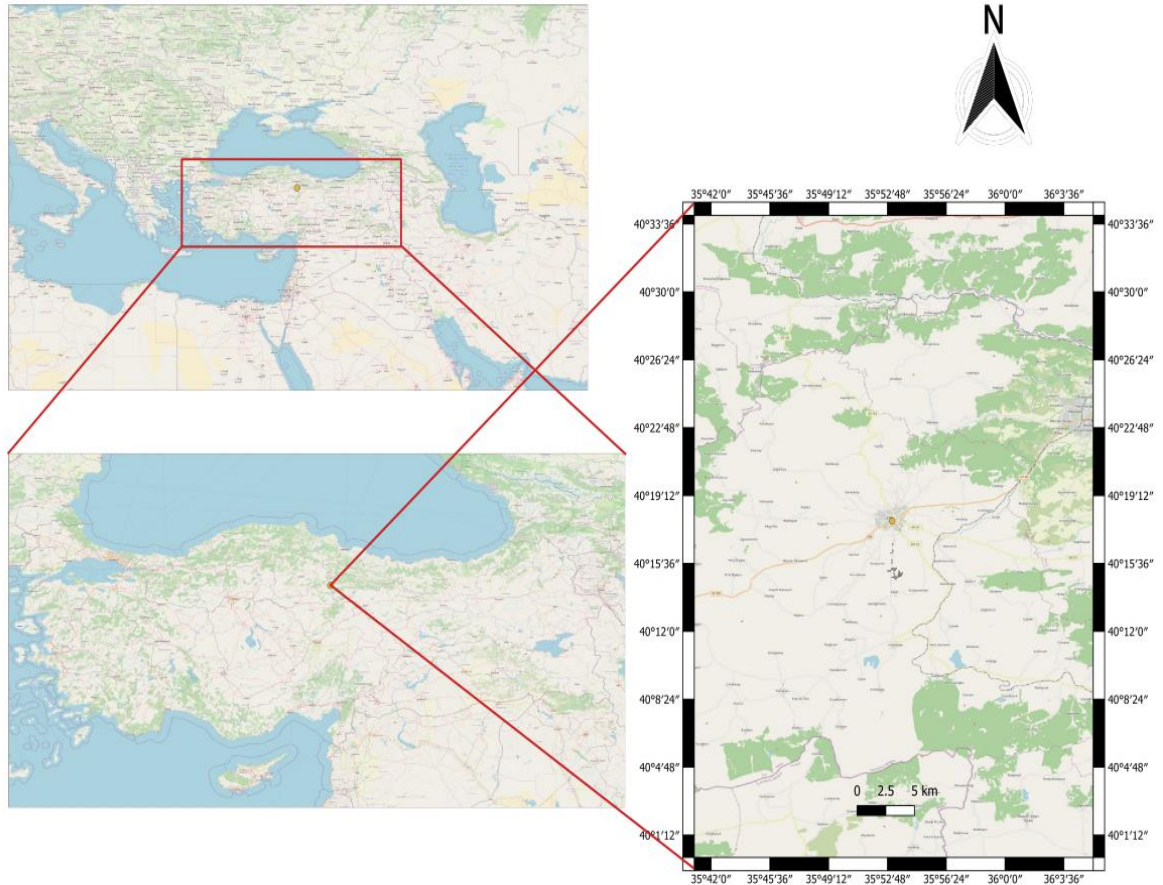
Figure 3.1. Tokat Province Zile District

The average air temperatures of the Zile district by month are shown in Figure 3.2 [38].
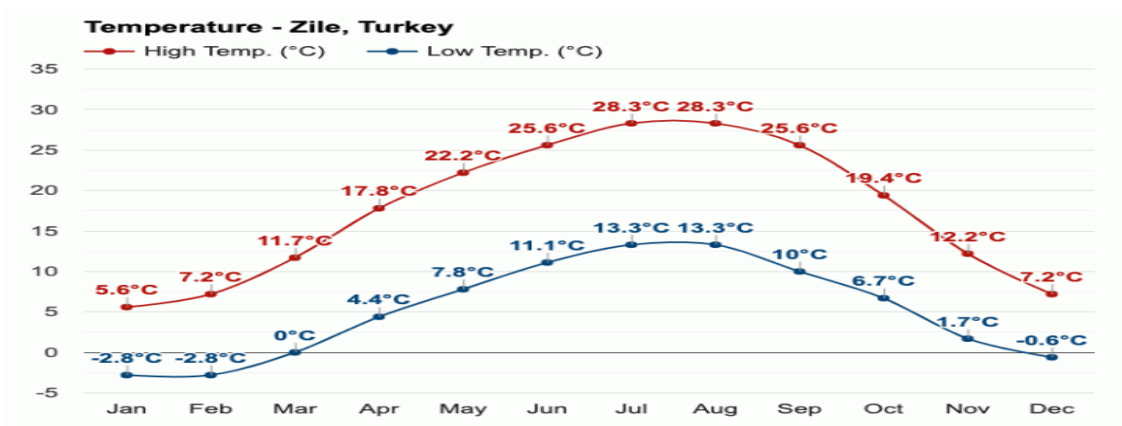
Figure 3.2. Average Air Temperatures of Zile District

The average cloudy, sunny, and rainy days of Zile District are shown in Figure 2.3 [39].
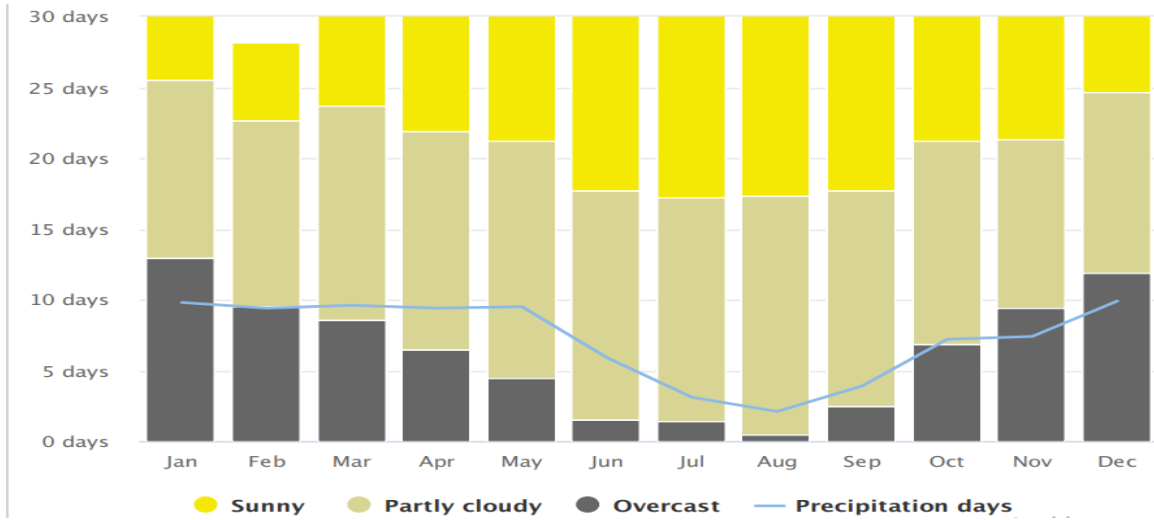
Figure 3.3. Cloudy, sunny, and rainy days in the Zile District

The cadastral borders of 48 sunflower parcels, which are considered the study area, between Fatih and Kurşunlu villages, on the Google Earth image (blue polygons) are shown in Figure 2.4.
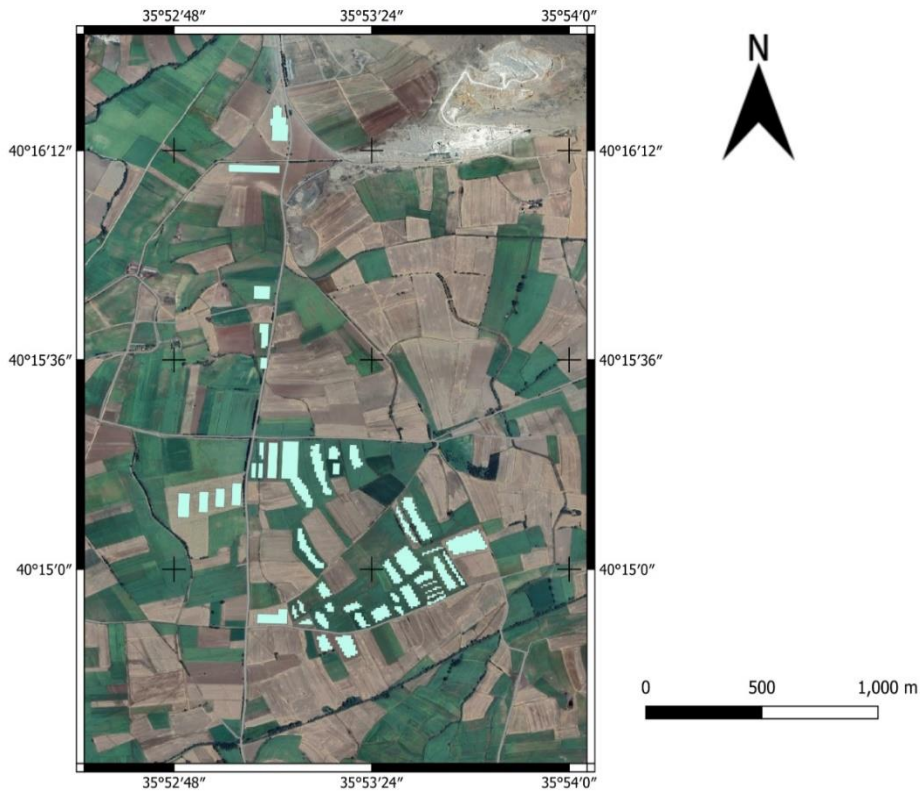
Figure 3.4. Google Earth view of 48 parcels of the sunflower field

3.2 Phenological Stages of the Sunflower Plant

Sunflower, which has a wide cultivation area and production in the world, is also used as an important raw material in the oil industry, cosmetics, and chemical industries. It is a nutritious animal feed due to its high content of protein, carbohydrates, fat, and phosphorus [40]. In 2021, 49.27 million tons of sunflower was produced. And most of it was used for oil production [41]. The sunflower plant is an annual and summer plant. It is grown in temperate climatic regions where the average temperature in July does not fall below 18-19 °C. It is a relatively drought-resistant plant due to its strong and deep root system. Sunflower does not like very humid areas, in case of high relative humidity, it is affected by the negative effects of diseases that cause rot [42]. Sunflowers can adapt to different soil types. For example, it can grow in sandy or clay soils. Deep, and rich in organic matter, alluvial soils are very suitable for sunflower cultivation, but it is difficult to grow in soils with high salinity. For the germination of sunflowers, the minimum soil temperature should be 8-10 °C. Sunflower is resistant to cold, but it is highly affected by frost which occurs when the temperature drops below -4 °C [43].

The appearance of the sunflower plant at each stage is shown in Figure 3.5.

1	2	3	4
5	6	7	8
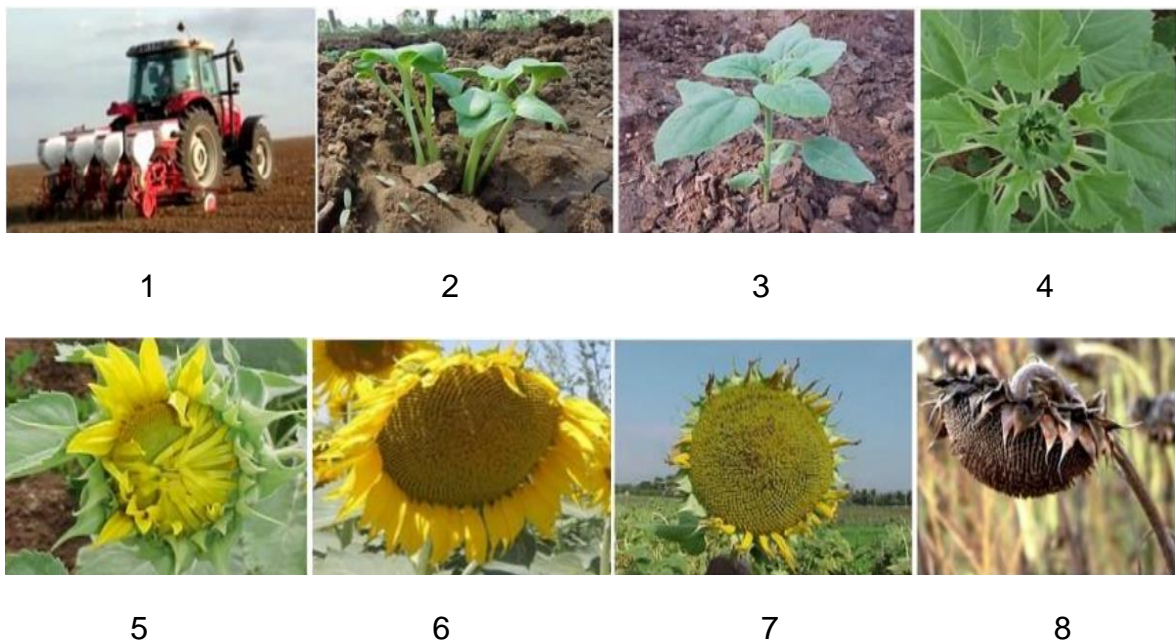
Figure 3.5. The view of the sunflower plant at each stage [6].

The stages shown in Figure 3.5 were evaluated in the code scale of Biologische Bundesanstalt, Bundessortenamt and CHemical industry(BBCH). The BBCH code

is classified under 8 main headings. These are the stages of soil preparation-planting, leaf development, root elongation, flower tray formation, flowering, fruit ripening, ripening, and harvesting, respectively [44]. The planting of the sunflower plant is usually done in early April-mid-May. Early sowing significantly increases yield. Harvest operations are applied at the end of August and the beginning of September. Approximately four months later from the planting process, the sunflower plant begins to be harvested [6]. Yield information for each parcel is given in the appendices.

3.3 Optical Remote Sensing Data

In the study, 23 level-2A optical images of Sentinel-2 satellites from 2018 were used. The selected display dates cover the leaf development stage of the sunflower plant through to the harvest stage. Selected optical image dates are shown in Table 3.1.

Tablo 3.1: Available optical image dates

Satellite name	Image Date	Satellite Name	Image Date
Sentinel-2A	26 April 2018	Sentinel-2B	13 June 2018
Sentinel-2A	29 April 2018	Sentinel-2B	30 June 2018
Sentinel-2B	4 May 2018	Sentinel-2A	8 July 2018
Sentinel-2B	14 May 2018	Sentinel-2B	10 July 2018
Sentinel-2B	16 May 2018	Sentinel-2A	18 July 2018
Sentinel-2B	24 May 2018	Sentinel-2A	25 July 2018
Sentinel-2A	26 May 2018	Sentinel-2A	14 August 2018
Sentinel-2B	3 June 2018	Sentinel-2A	17 August 2018
Sentinel-2A	5 June 2018	Sentinel-2A	24 August 2018
Sentinel-2A	8 June 2018	Sentinel-2A	27 August 2018
Sentinel-2B	10 June 2018	Sentinel-2B	1 September 2018
		Sentinel-2A	13September 2018

The Sentinel-2 satellite is a Multi-Spectral image acquisition satellite used to provide optical images supported by European Space Agency (ESA). Multi-spectral images obtained by satellite sensors can display visible and infrared wavelengths separately. The satellite has 13 spectral bands which have various spatial resolutions [45]. Each image representing a wavelength range is called a band. Sentinel-2 is frequently preferred in monitoring applications because of its high imaging frequency, spatial resolution options, and coverage area [13]. As the spatial resolution increases, it becomes easier to detect the reflection values of objects. The distinguishability of objects from each other is increased, therefore, interpretation becomes easier. The size of the objects affects the reflection values of the pixels that make up the image [46]. The reflection properties of objects participate in the reflection value of pixels and these values are used in determining the phenological stage of the plant and in yield estimation studies.

In this study, Sentinel-2A and Sentinel-2B satellites that started their operations in 2015 and 2017, respectively were used together. These missions are placed in the same orbit at 180 degrees from each other. This ensures that a 10-day return visit cycle is completed in 5 days [47]. The band characteristics of both satellites are shown in Table 3.2.

Table 3.2: Spectral properties of Sentinel-2A/B satellites.

Band Name	SENTINEL-2					
	Sentinel-2A			Sentinel-2B		
	Resolution (m)	Wavelength (nm)	Band Width (nm)	Resolution (m)	Wavelength (nm)	Band Width (nm)
1	60	442.7	27	60	442.2	45
2	10	496.6	98	10	492.1	98
3	10	560.0	45	10	559	46
4	10	664.5	38	10	665	39
5	20	703.9	19	20	703.8	20
6	20	740.2	18	20	739.1	18

7	20	782.5	28	20	779.7	28
8	10	835.1	145	10	833	133
8a	20	864.8	33	20	864	32
9	60	945.1	26	60	943.2	27
10	60	1373.5	75	60	1376.9	76
11	20	1613.7	143	20	1610.4	141
12	20	2202.4	242	20	2185.7	238

Sentinel-2 satellites provide images at different levels. Level-1C has Top-Of-Atmosphere reflectance. The pre-processing steps should be applied to images at the level of Level-1C and the image should be improved [48]. Therefore, Level-2A data with Bottom-Of-Atmosphere reflectance have been also distributed. In this study, Level-2A level images were used and no additional pre-processing steps were applied.

In this study, four different indices were used. The indices and bands used are shown in Table 3.3.

Table 3.3: Indices and Equations

Index Name	Equations	Reference
NDVI	(B8-B4)/(B8+B4)	Rouse et al. 1973
NDVIR1	(B8-B5)/(B8+B5)	Gitelson et al. 1994
OSAVI	(B8-B4)/(B8+B4+0.16)	Rondeaux et al. 1996
IRECI	(B7-B4)/(B5/B6)	Rondeaux et al. 2013

Vegetation indices are used to increase the distinguishability of land cover in agricultural applications. They are frequently used because high accuracy results are obtained in yield estimation studies and other agricultural applications [29, 35]. With the increase in spectral resolution of optical sensors, new indices have started to be produced by proportioning the bands to each other and they have been tried

according to the purpose of the study. Among these indices, OSAVI and IRECI indices are some of these indices. While the IRECI index highlights the amount of chlorophyll, the OSAVI index is more prominent in grain yield estimation studies [11].

3.4 SAR Remote Sensing Data

The backscatter value is measured to distinguish objects from each other. Low backscatter on a surface or object causes a low pixel value to result in a dark near-black color, while high backscatter results in a high pixel value, causing the pixel color to appear close to white [49]. The amount of backscatter is a variable that can change. This change also depends on some parameters. These are radar system parameters (frequency, polarization, incidence angle of reflected signals) and target system parameters (surface roughness ratio, geometric shape, moisture).

3.4.1 Frequency

Frequency is used to understand the depth to go under the surface of an object and to measure the surface roughness in absolute (relative) terms [50]. The wavelengths used in microwave active systems alter according to the response of the targets in the specified ranges. The X band between the 2.4 cm and 3.75 cm wavelength range is backscattered from the surface of the targets and is mostly used for military purposes. The C band, with wavelengths between 3.75 and 7.5 cm, has the ability to reach the near-surface areas of the objects. The L band wavelength with a range from 15 to 30 cm is especially suitable for the ground under the vegetation, etc. accessing such objects [51]. In this study, Sentinel-1 C band (λ = 5.5 cm, 5.404 GHZ) images were used.

3.4.2 Polarization

The electromagnetic wave's polarization shows which way the electric field vector is moving. Polarizations can be horizontal (H), vertical (V), or both horizontal and vertical. The polarization combinations are VV, VH, HH, and HV. The first letter in the notations indicates the polarization of the transmitted radiation and the second letter indicates the polarization of the received radiation.

3.4.3. The Angle Of Incidence Of Reflected Signals

The angle of incidence is the angle between the normal of the received surface and the direction of the reflected signal. Increasing or decreasing the angle affects the backscatter value. The higher the angle of incidence, the smoother the surface appears, resulting in reduced backscatter and darker images. A decrease in the angle of incidence causes an increase in backscatter and therefore a lighter gray value [52].

3.4.4. The Effect Of Roughness And The Geometric Structure Of The Surface

Surface roughness is a parameter that determines the interaction of its energy with the ground surface. Surface roughness refers to the height differences of the object from the plane. If the height difference of the surface is smaller than the radar wavelength, the surface is perceived as smooth, but when the height difference reaches the wavelength, the surface is perceived as rough. Rough surfaces scatter incoming energy equally in all directions, and most of the scattered energy can be recorded by radar systems. As the scattered energy increases the pixel value, rough surfaces often appear in light tones. Smooth surfaces, on the other hand, reflect the incoming energy without scattering, and only a small amount of the sent energy can return to the sensor. For this reason, smooth surfaces often appear dark. For example, characteristic shape and geometrical differences in terrestrial surfaces increase the ratio of roughness. The amount and strength of the returning signals are detected at high levels of brightness. Sea and lake surfaces are calm and smooth environments apart from meteorological factors such as wind and precipitation. For this reason, the transmitted signals reflect properly in these regions and are not backscattered to the sensor. For this reason, they appear black and smooth on the radar image. But in windy weather, the geometry of the waves and the mobility of the surface increases the back reflection, the brightness increases, and as a result, light gray tones can be widely seen in a certain texture in the radar image. Surface backscattering is explained by the relationship between the wavelength of the transmitted electromagnetic energy and the surface roughness [53]. In remote sensing, the scattering angle and the angle of incidence are the same, because, in radar systems, the receiving antenna and the antenna sending electromagnetic energy are in the same place. For this reason, backscatter values are considered in remote sensing.

3.4.5. Moisture

18

The interaction of radar signals with the surface can vary depending on moisture and precipitation. Backscattering increases as the moisture content of the object increases, so surfaces such as soil and vegetation appear brighter when they are wet (moist) than when they are dry. When objects are dry, the surface appears smooth and radar energy can travel from the surface to the depths and appear dark, regardless of whether it is a homogeneous surface such as soil, sand and ice, or causing excessive backscatter such as vegetation, forest cover [13]. Sea and lake surfaces are excluded from this situation. Because these regions consist only of water and the signals reflect properly in these regions. For this reason, wetlands always appear darker than normal areas.

The coherence value, obtained from two different satellite images at different times, was also calculated using the same satellite images for this study. The coherence value is a black-and-white image that takes a value between zero and one. In the image, bright areas have high coherence which indicates the similarity of the two data and dark areas have low coherence which shows the changed areas.

The Sentinel-1 is one of the observation satellites mission of the Copernicus program within the European Union. It consists of the Sentinel-1A and Sentinel-1B constellations, which were sent into orbit in April 2014 and April 2016, respectively. Both satellites were launched into orbit from Soyuz rockets in Kourou, French Guiana [54]. The Sentinel-1 satellite has dual polarization, 12-day imaging frequency, and free product supply. Sentinel-1A and Sentinel-1B can be used to reduce the temporal resolution to 6 days in the equator. Sentinel-1 satellite is used in many different areas such as monitoring agricultural lands, detecting and tracking ships, monitoring the marine environment, and quickly mapping the area in case of natural disasters [55]. Sentinel-1 satellites are displayed in four reception modes at different processing levels given in Table 3.4. Radar images are available in two Level-1 products. Single Look Complex (SLC) data are the first level images after signal processing. In SLC images, each pixel consists of a real and imaginary number. On the other hand, Ground Range Detected (GRD) data has only amplitude information [13]. In this study, descending orbit, IW mode SLC process level radar images, VV and VH polarizations are used in the WGS-84 coordinate system.

Table 3.4: Sentinel-1 beam modes features [56].

Mode	Arrival Angle	Resolution	Strip Width	Polarization(H= Horizontal V = Vertical)
Stripmap (SM)	20-45	5 x 5 m²	80 km	HH+HV, VH+VV, HH, VV
Interferometric Wide swath (IW)	29-46	5 x 20 m²	250 km	HH+HV, VH+VV, HH, VV
Extra Wide Swath (EW)	19-47	20 x 40 m²	400 km	HH+HV, VH+VV, HH, VV
Wave (WV)	22-35-35-38	5 x 5 m²	20x20 km	HH, VV

In the study, 26 Sentinel-1 radar images from 2018 were used. There is a 6-day time difference between the dates. For each date, both VH and VV polarizations were used. Backscattering values of individual pixels were calculated from each image and coherence value was generated for each pixel value from the coherence images obtained from two separate images with a 6-day difference between them. Radar image acquisition dates are shown in Table 3.4. These dates include the leaf development stage of the sunflower plant and the dates until the harvest stage.

Table 3.5: Avaible SAR image dates

Satellite name	Image Date	Satellite Name	Image Date
Sentinel-1B	24 April 2018	Sentinel-1A	11 July 2018
Sentinel-1A	30 April 2018	Sentinel-1B	17 July 2018
Sentinel-1B	6 May 2018	Sentinel-1A	23 July 2018
Sentinel-1A	12 May 2018	Sentinel-1B	29 July 2018
Sentinel-1B	18 May 2018	Sentinel-1A	4 August 2018
Sentinel-1A	24 May 2018	Sentinel-1B	10 August 2018
Sentinel-1B	30 May 2018	Sentinel-1A	16 August 2018

Sentinel-1A	5 June 2018	Sentinel-1B	22 August 2018
Sentinel-1B	11 June 2018	Sentinel-1A	28 August 2018
Sentinel-1A	17 June 2018	Sentinel-1B	3 September 2018
Sentinel-1B	23 June 2018	Sentinel-1A	9 September 2018
Sentinel-1A	29 June 2018	Sentinel-1B	15 September 2018
Sentinel-1B	5 July 2018	Sentinel-1A	21 September 2018

4. METHODOLOGY

In this part of the study, the process steps performed in the study are explained in order and the workflow of the study is given in Figure 4.1. The pre-processing steps

of Sentinel-1 satellite images and the pre-processing steps to create coherence images are also explained in detail. In addition, the working principle and features of the ANN method used in the study are mentioned.

In the study, first, vegetation indices were produced using Sentinel-2 optical images. Since Level-2A of Sentinel-2 images are used in the thesis, no pre-processing step has been applied. In the SNAP program, reflectance values were obtained from the sunflower plots opened on the index image. The reflectance values of the sunflower parcels were calculated separately for each index for 48 sunflower parcels. By taking the average of the calculated reflectance values within the parcel borders, for each parcel single value was calculated for each index.

In the study, the reference yield values for each parcel were obtained from the farmers in the field by traditional methods [6]. Then, the correlation between the reference yield values and the reflection values was examined and the dates with the highest correlation were determined. After the 48 parcels were divided into 4 groups of 12 on these dates. Three linear function sets were used for a test set to be created. This is because each group is used as a test and four linear functions can be obtained. The yield of the sunflower plant on the dates with the highest correlation was estimated by SLR and ANN methods and then compared with the reference yield values.

As a second step, the pre-processing steps of Sentinel-1 satellite images were made and the images were improved. The SNAP program was used to perform the pre-processing steps. 48 sunflower parcels were opened on the processed images and backscatter values were determined separately for each parcel on the dates determined in this way. The parcel image values were calculated by taking the average of the backscatter values of 48 parcels calculated separately for each date. Then, the correlation between the backscatter values and the reference yield values was examined. On the dates of the highest correlation, 48 parcels were divided into 4 groups of 12 each, and three linear function sets were used for a test set to be created. Then, the processed Sentinel-1 satellite images were divided into pairs with a 6-day time difference between them, and coherence images were created after the pre-processing steps. The coherence values of 48 parcels were calculated for each date from the created coherence images. The dates with the highest correlation were also divided into 4 groups of 48 parcels of 12 each. Three

linear regression function sets were used for a test set to be created. Then, yield estimation was made using SLR and ANN methods and compared with the reference values.
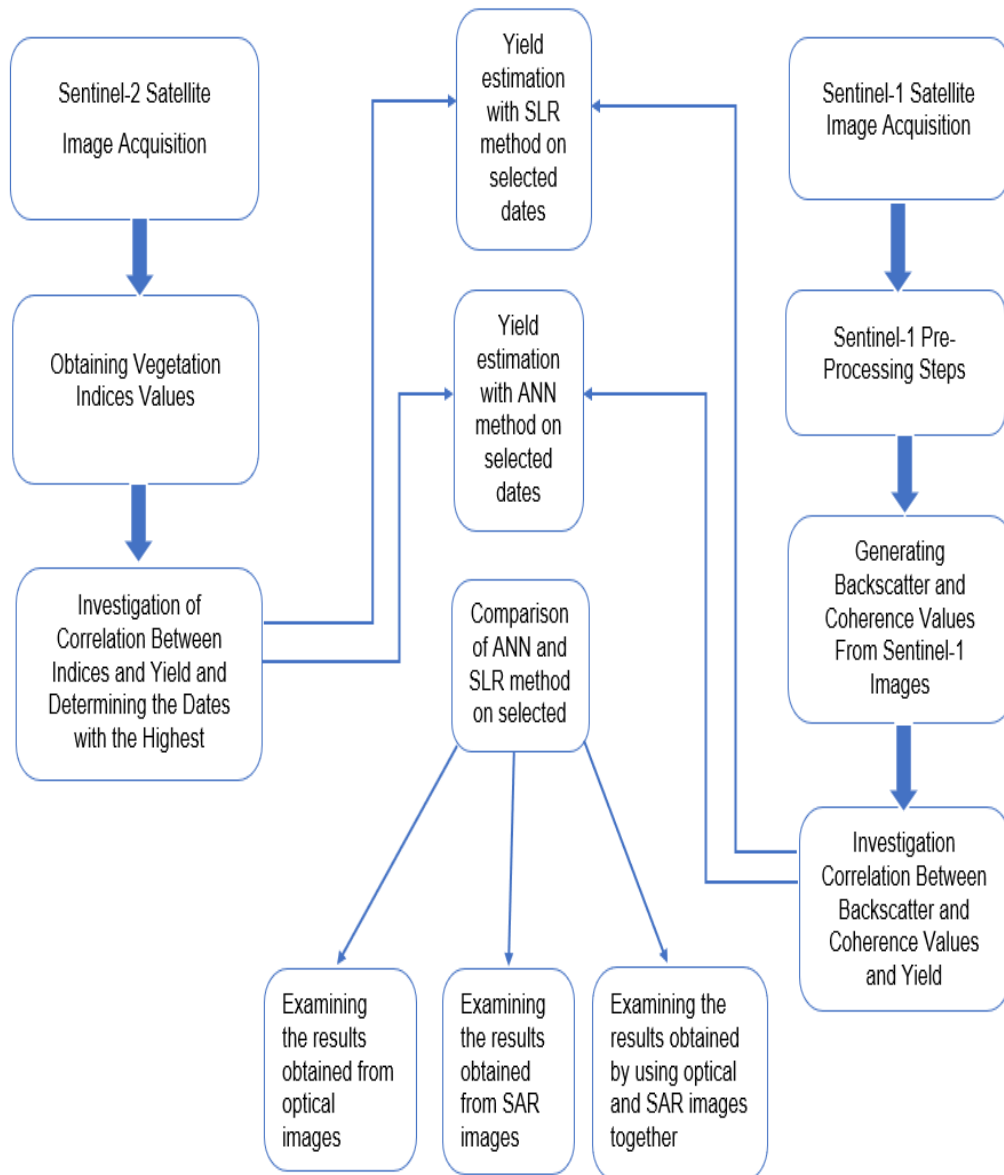
Figure 4.1. Workflow chart for this study**.**

4.1 Data Pre-processing

Satellite images contain systematic or unsystematic errors in their structure. Therefore, they need some fixes before they can be used in an application. These processes are generally defined as pre-processing steps. Because these processes form the basis for obtaining information from images in the next steps and are performed before the 'image processing and analysis steps. The pre-processing steps include geometric correction, which ensures geographical compatibility between the satellite image and the measured information, and radiometric correction, which aims to eliminate reflections that are not representative of the object in the detected image. Geometric Correction is the processing step of removing the effects of geometric distortion in the satellite image and fitting the image to a defined geographical location. The point coordinates in the image to be corrected are defined by the coordinates of the ground control points, such as latitude and longitude. This process is called rectification. Matching the same points of two images or correcting one image according to the other is called geometric registration. Radiometric Correction is the process that eliminates the atmospheric effects that cause false perceptions in the satellite image and makes the objects detected by the sensors prominent. Electromagnetic radiation signals coming from the sun and detected by the satellite detector after hitting the earth, undergo change due to gases and aerosols in the atmosphere as they pass through the atmosphere, so it is necessary to calibrate the image by applying some pre-processing steps to the image. This is called the atmospheric effect [57]. The preprocessing steps of the coherence image production from the SLC level of Sentinel-1 data were described below and shown in Figure 4.2.

Sentinel-1 Pre-Processing Steps	Pre-processing steps to create a coherence image
Opening of the Sentinel-1 satellite image in the SNAP program	Opening of two separate Sentinel-1 satellite images in the SNAP program
Opening of 48 sunflower parcels on the image	Opening of 48 sunflower parcels on the image
S-1 Tops-Split	S-1 Tops-Split
Apple Orbit File	Apple Orbit File
Calibration	S-1 Back Geocoding
S-1 Tops Deburst	Coherence Estimation
Multilooking	S-1 Tops Deburst
Speckle Filter	Multilooking
Subset	Terrain Correction
Terrain Correction	Recording the image as Geotiff
Db conversion	
Recording the image as Geotiff	

Figure 4.2 Sentinel-1 backscatter and coherence pre-processing

S-1 Tops-Split

First of all, because the SLC satellite image size is big, the area covering 48 sunflower parcels was selected with the help of Google Earth. The area to be studied has been cropped to a smaller size.

Apple Orbit File

Apply orbit file module was used to eliminate orbital errors of the image and to perform precise orbital calibration. This step allows for accurate image geocoding using the trajectory files contained in the metadata of each product [58].

Calibration

Calibration can be impaired in images taken under the influence of space conditions. The purpose of this step is to remove the complexity from the SAR data so that the values of pixels can be directly attributed to backscattering [59]. In this step, VH and VV polarization are used together. Outputsigma0 and outputbeta0 band types were selected and the next step was taken.

S-1 Tops Deburst

This step is done to integrate the data and the workspace is prepared. Burst images from all subscales of the image are resampled. Therefore, it is a necessary step.

Multilooking

This processing step is done to reduce the multiple views in the image that deteriorate under space conditions. This step, which is done to make the image clearer, increases the radiometric resolution and reduces the spatial resolution [60]. As a result of this process, a less noisy image is obtained. Therefore, it is a necessary step to take. This step has been applied for bands in both VH and VV polarization. It has been selected as the Number of Range Looks 4. It was selected as the Number of azimuth looks 1. The average number of ground resolution square pixels was taken as 14.33 m.

Single Product Speckle Filter

Spots on the satellite image are caused by the salt and pepper noise that occurs as a result of random constructive and destructive interference throughout the image [13]. In this study, the image was first subjected to multi-look processing and then the Refined Lee filter was applied to reduce speckles. The Refined Lee filter preserves the edges while averaging the satellite image. The filter takes into account the Local Linear Minimum Mean Square Error (LLMMSE) estimation

within edge-aligned windows, providing better preservation of details in an image [61]. The image on each date was then cropped at the same coordinates to cover the workspace.

Range Doppler Terrain Correction

In the Terrain Correction step, natural geometric distortions (i.e. foreshortening, overlapping, and shadow) in the SAR image are corrected using the digital elevation model (DEM) and image geocoding is performed [62]. Geocoding converts the range geometry of the image to the coordinate system of a map. Land geocoding; requires the use of a DEM to correct for local SAR geometric distortions [63]. In this process step, the bilinear interpolation method was used and the pixel size was sampled to a 10 m X 10 m spatial resolution. CDEM was used as DEM. SAR geometric distortions have been corrected and the image has been geocoded. After this process step, the pixel digital values in the obtained bands were converted to radar backscatter (dB) values. The formula used for this transformation is given in Equation 1. With this logarithmic transformation, the back reflection coefficients that do not have a unit value are converted to dB values [64].

$$\beta_{db}{}^0 = 10 * \log_{10}(\beta 0) \tag{1}$$

With these operations performed separately for each image date, the backscatter values of 48 parcels were calculated in both VH and VV polarization for each date. The image was recorded in GeoTIFF format and the image was made ready. After these pre-processing steps were performed, the backscatter values were calculated separately in both VH and VV polarization for each date and each parcel based on the images that were made ready. In order to produce coherence images from Sentinel-1 satellite images from two different times, Sentinel-1 satellite images of 26 different dates were divided into pairs with a 6-day time difference between them. Display dates divided into groups are shown in Table 2.8.

S-1 Back Geocoding

This step was applied one by one to group images to combine images from two different dates with orbit corrected and cropped to obtain a single image. In this step, SRTM 3Sec was used as the DEM. Bilinear interpolation was used as the resampling method. Then, these processes were printed and a stack image was obtained.

Coherence

At this stage, this process step was carried out to make coherence estimation from the stack image pairs. The coherence range size is selected as 10, coherence azimuth size is selected as 3. DEM was not changed, again SRTM 3Sec was chosen and other parameters were used without changing. In order to improve the coherence of images created after this processing step, the deburst, multilooking and terrain correction processing steps used to improve the Sentinel-1 images were applied to these images without changing the previously used parameters and the images were improved. Coherence values from these images covering the same area and 48 sunflower parcels were calculated separately for each parcel in both VH and VV polarization.

Table: 4.1: Image dates to calculate coherence value

24 April- 30 April 2018	5 July- 11 July 2018
30 April- 6 May 2018	11 July- 17 July 2018
6 May- 12 May 2018	17 July- 23 July 2018
12 May- 18 May 2018	23 July- 29 July 2018
18 May- 24 May 2018	29 July- 4 August 2018
24 May-30 May 2018	4 August- 10 August 2018
30 May- 5 June 2018	10 August- 16 August 2018
5 June- 11 June 2018	16 August- 22 August 2018
11 June- 17 June 2018	22 August- 28 August 2018
17 June- 23 June 2018	28 August- 3 September 2018
23 June- 29 June 2018	3 September- 9 September 2018
29 June- 5 July 2018	9 September- 15 September 2018

4.2. Artificial Neural Network

ANN method is a learning method, that can produce new information, create new information, and automatically make predictions without any assistance. ANN

consists of artificial cells connected to each other. It is accepted that these cells are connected and each connection has a value. The most basic task of the ANN is to predict an output set that corresponds to an input set shown to it. The high accuracy of this estimated output set is the most important feature of ANN. An ANN consists of three layers. These; are the input layer, hidden layer and output layers. The visual figure containing the layers and connections of the neural network is shown in 4.2.1. The input and output layers contain nodes corresponding to the input and output variables, respectively. The number of hidden nodes determines the number of connections between inputs and outputs and may vary depending on the particular problem. If too many nodes are used, then the ANN can be overtrained, causing it to memorize the training data, resulting in poor predictions [65]. Therefore, the number of hidden layers and the number of neurons in the hidden layer can only be decided by a trial because this method is a trial and error method.
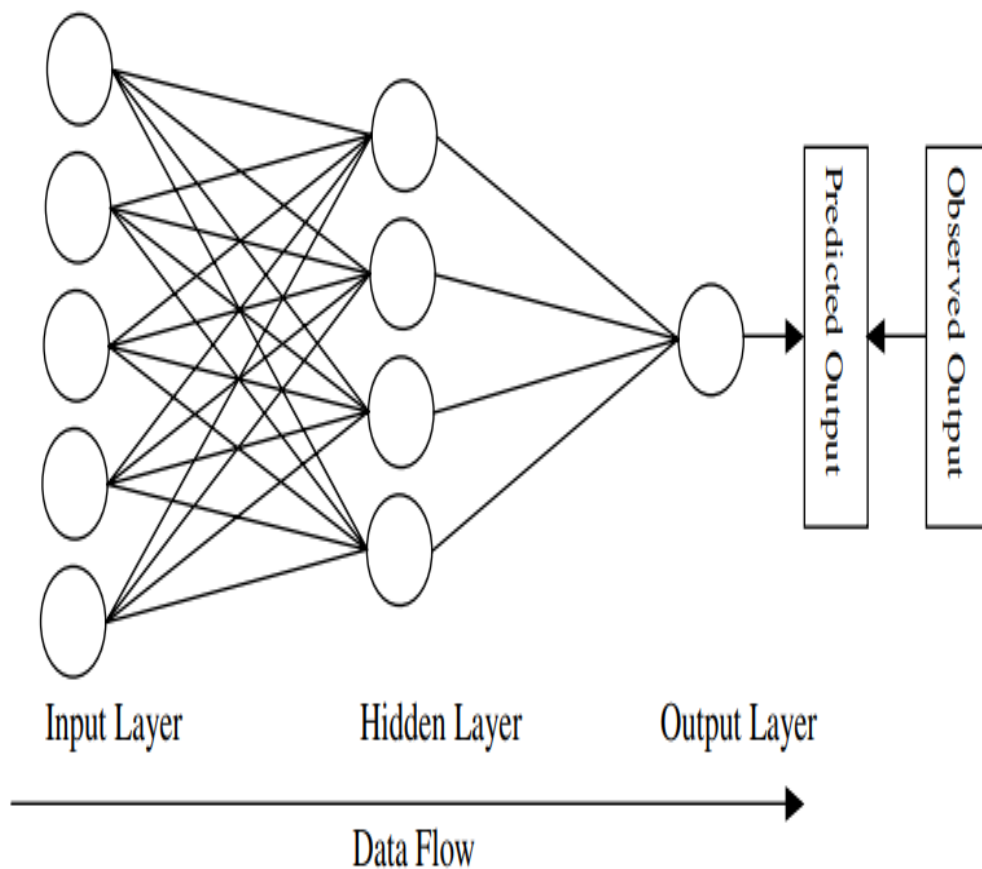
Figure 4.3. Layers and connections of an artificial neural network

It is the basic principle to determine various input and output parameters in yield estimation with ANN. In this study, the MATLAB program was used when making transactions with ANN. 36 parcels of 48 sunflower parcels were used as input parameters. As an output parameter, the previously determined reference yield values of the same parcels were also used. Then, the parcels were divided into groups among themselves and decoupled as test and training data respectively, and accuracy analyses were applied to all parcels.

5. RESULTS

5.1. Results of Optical Data

In the study, the phenological stages of the sunflower plant were identified using vegetation indices derived from Sentinel-2 data. The average reflection of the 48 parcels graph for the four indices studied is shown in Figure 5.1.
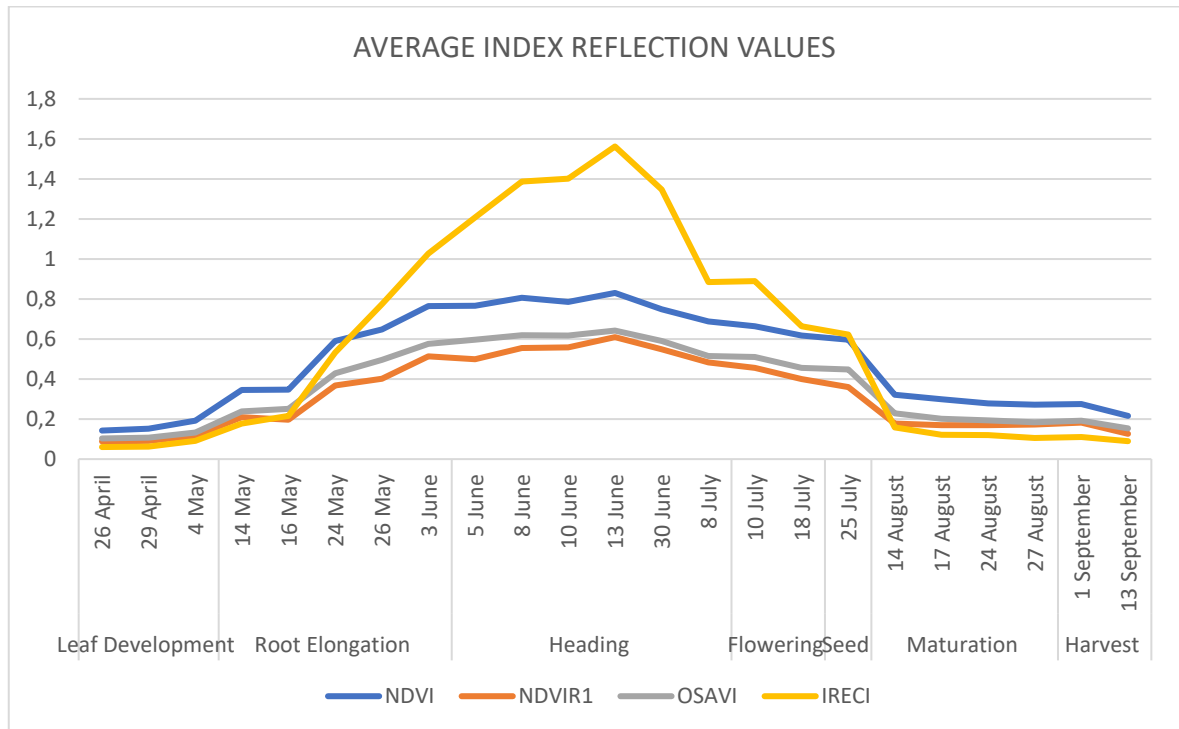
Figure 5.1. Reflection values of the indices for the 48 parcels

According to Figure 5.1, it was observed that the reflectance value of the sunflower plant increased in all four indices from the end of April to the middle of June. From the end of June to September, a decrease was observed in the reflectance values. The month of June, when the reflectance value increases, covers the first stage before flowering occurs.

The correlation between the reflectance values and vegetation indices obtained from 23 satellite images taken from Sentinel-2 satellites and the predetermined reference yield values obtained from the field was examined for 48 parcels. The correlation between reference yield and indices is given in Figure 5.2. Looking at the correlation for the four indices examined, it was determined that the dates with

the highest correlation were 30 June, 8 July, and 10 July. For these dates, the highest correlation is given in Table 5.1.
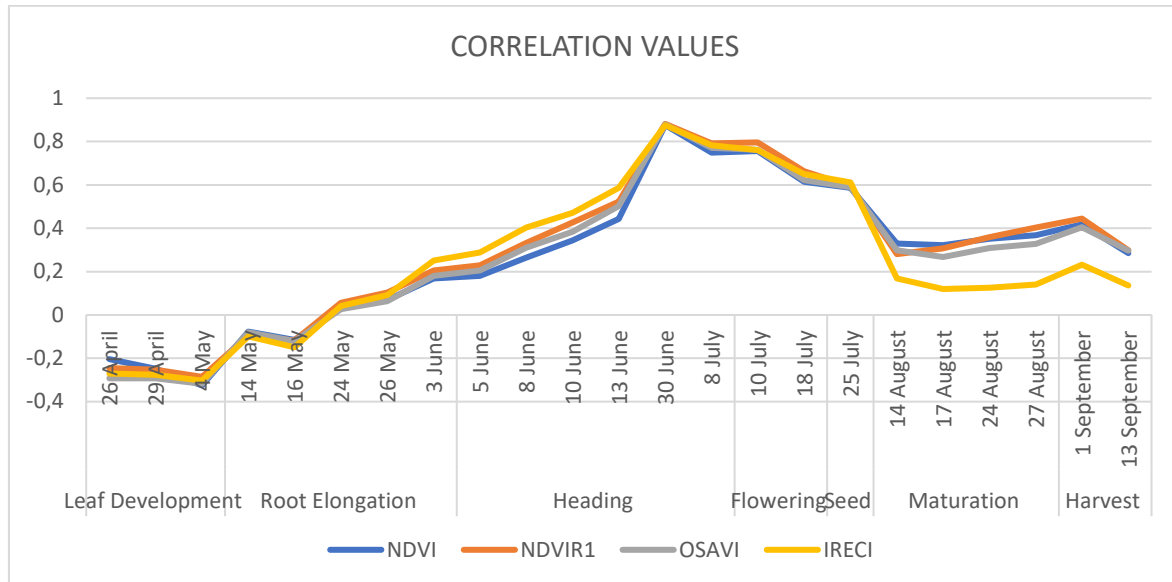
Figure 5.2. Correlation values between reference yield and indices.

Table 5.1: Correlation values between reference yield values and indices on 30 June, 8 July, and 10 July 2018. The highest correlation values date is shown in red and the lowest correlation values are in blue for each date.

	30 June 2018	8 July 2018	10 July 2018
NDVI	0,876	0,749	0,756
NDVIR1	0,882	0,792	0,796
OSAVI	0,879	0,772	0,762
IRECI	0,875	0,783	0,760

In the study, the yield was first obtained from the reflectance values of the indices using the SLR. RMSE values were calculated for each index on 30 June, 8 July, and 10 July. Calculated RMSE and average RMSE for each group are given in Figure 5.3.
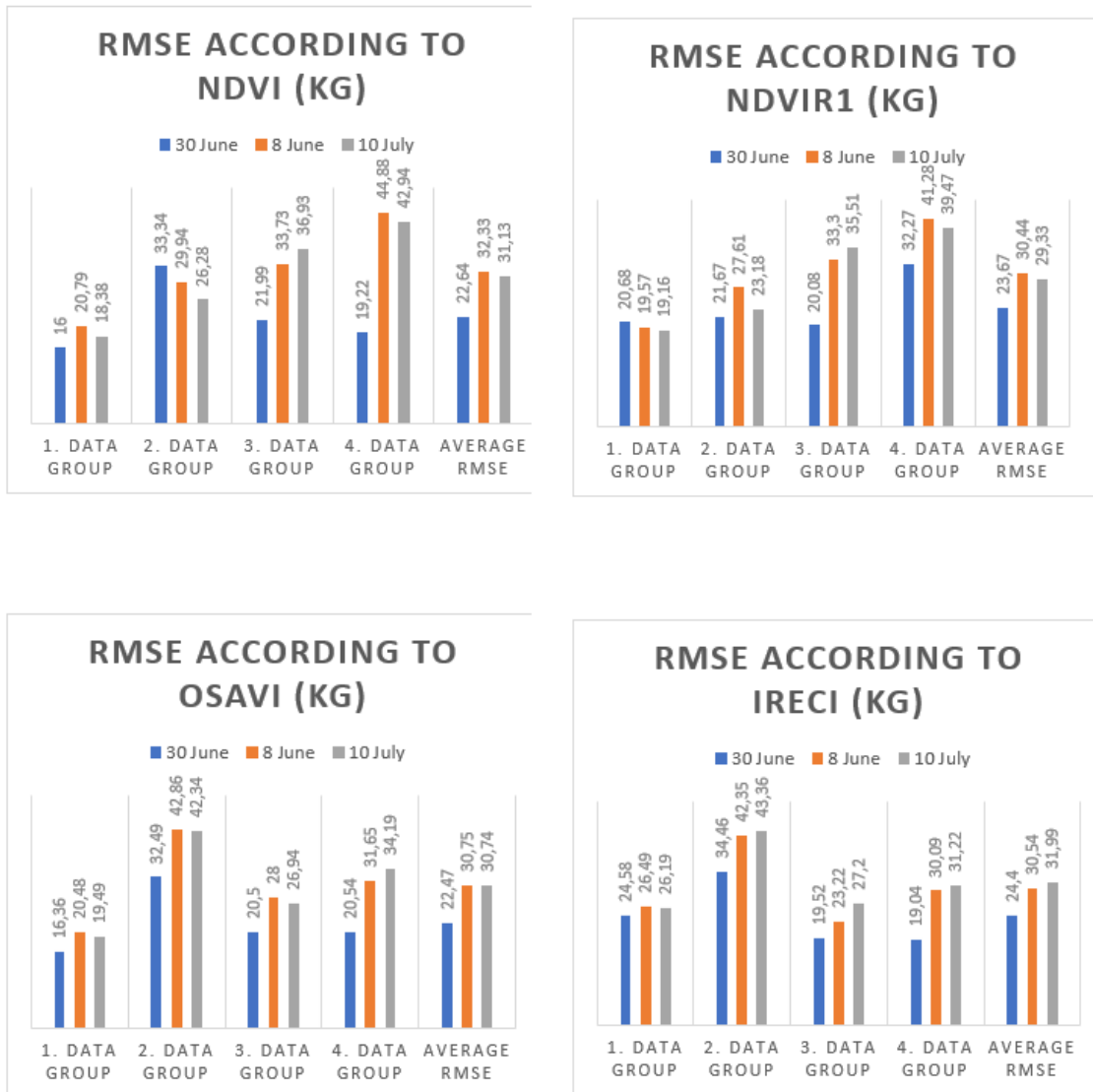
Figure 5.3. RMSE of each data and average RMSE values were calculated using the SLR method.

Looking at the average of RMSE values, in the SLR, the OSAVI gave the best result for the date of 30 June (Figure 5.3). NDVIR1 gave the best result for 8 July. The index that gave the best results for July 10 was again the NDVIR1. ANN method was used as the next step and yield values were obtained with this method. The yield values obtained by these two different methods were compared with the reference yield values. Details are given in the appendices [Appendix A]. In the ANN method, firstly, each index value was processed separately for each group as a single input. The number of inputs is taken as 1. The output number is taken as 1. The number of iterations was determined as 1000. The number of hidden layers was tried by trial and error method and different combinations were tried

and the value that gave the best result was taken as the basis. The number of hidden layers and RMSE selected when used indices are processed as inputs alone are given in Table 5.2. The lowest error values for each date are shown in bold.

Table 5.2: The number of hidden layers and RMSE selected when indices are used as input values alone.

30 June NDVI		8 July NDVI		10 July NDVI	
Hidden Layer Number	Average RMSE	Hidden Layer Number	Average RMSE	Hidden Layer Number	Average RMSE
2	23,68	**2**	**29,17**	**2**	**30,95**
3	24,45	3	30,12	3	31,03
4	24,82	4	29,8	4	31,67
5	**22,07**	5	29,71	5	31,52
30 June NDVIR1		8 July NDVIR1		10 July NDVIR1	
Hidden Layer Number	Average RMSE	Hidden Layer Number	Average RMSE	Hidden Layer Number	Average RMSE
2	25,62	**2**	**27,53**	**2**	**24,31**
3	28,4	3	28,43	3	25,7
4	27,53	4	31,03	4	27,87
5	**22,71**	5	30,13	5	28,01
30 June OSAVI		8 July OSAVI		10 July OSAVI	
Hidden Layer Number	Average RMSE	Hidden Layer Number	Average RMSE	Hidden Layer Number	Average RMSE
2	23,4	2	33,03	2	30,91
3	23,89	3	32,51	3	33,87

4	23,34	4	32,44	4	32,76
5	**22,32**	**5**	30,28	**5**	**28,41**

30 June IRECI		8 July IRECI		10 July IRECI	
Hidden Layer Number	Average RMSE	Hidden Layer Number	Average RMSE	Hidden Layer Number	Average RMSE
2	25,12	2	30,45	2	29,42
3	29,44	3	34,03	3	29,4
4	28,41	4	30,81	4	30,97
5	**23,86**	**5**	**27,59**	**5**	**28,67**

When each index value is processed as a single input, the calculated RMSE for each group and the average RMSE on 30 June, 8 July, and 10 July are given in Figure 5.4.
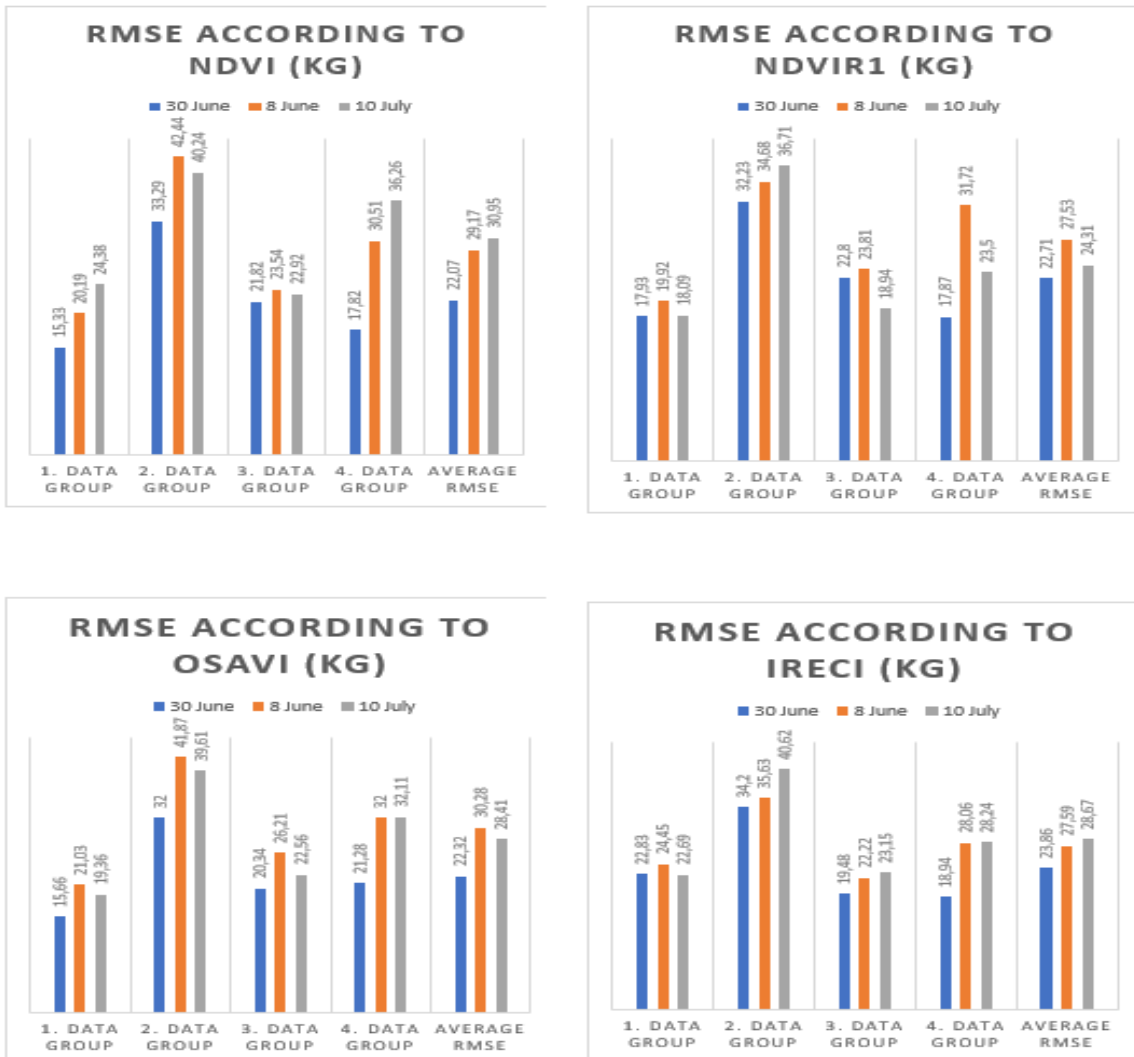
Figure 5.4. RMSE of each data and average RMSE values were calculated using the ANN method.

When examining the average RMSE values, in the ANN method, on June 30, the NDVI gave the best results. The index that gave the best results on July 8 and 10 was the NDVIR1 (Figure 5.4). When all indices are examined together, the RMSE calculated for each group in SLR and the average RMSE are given in Figure 5.5.

RMSE CALCULATED WITH THE SLR METHOD FOR ALL INDICES (KG)

Legend: 30 June, 8 June, 10 July

Data Group	30 June	8 June	10 July
1. DATA GROUP	19,4	21,83	20,8
2. DATA GROUP	33,14	42,85	42,03
3. DATA GROUP	20,92	27,19	25,9
4. DATA GROUP	19,72	32,19	34,46
AVERAGE RMSE	23,3	31,01	30,8
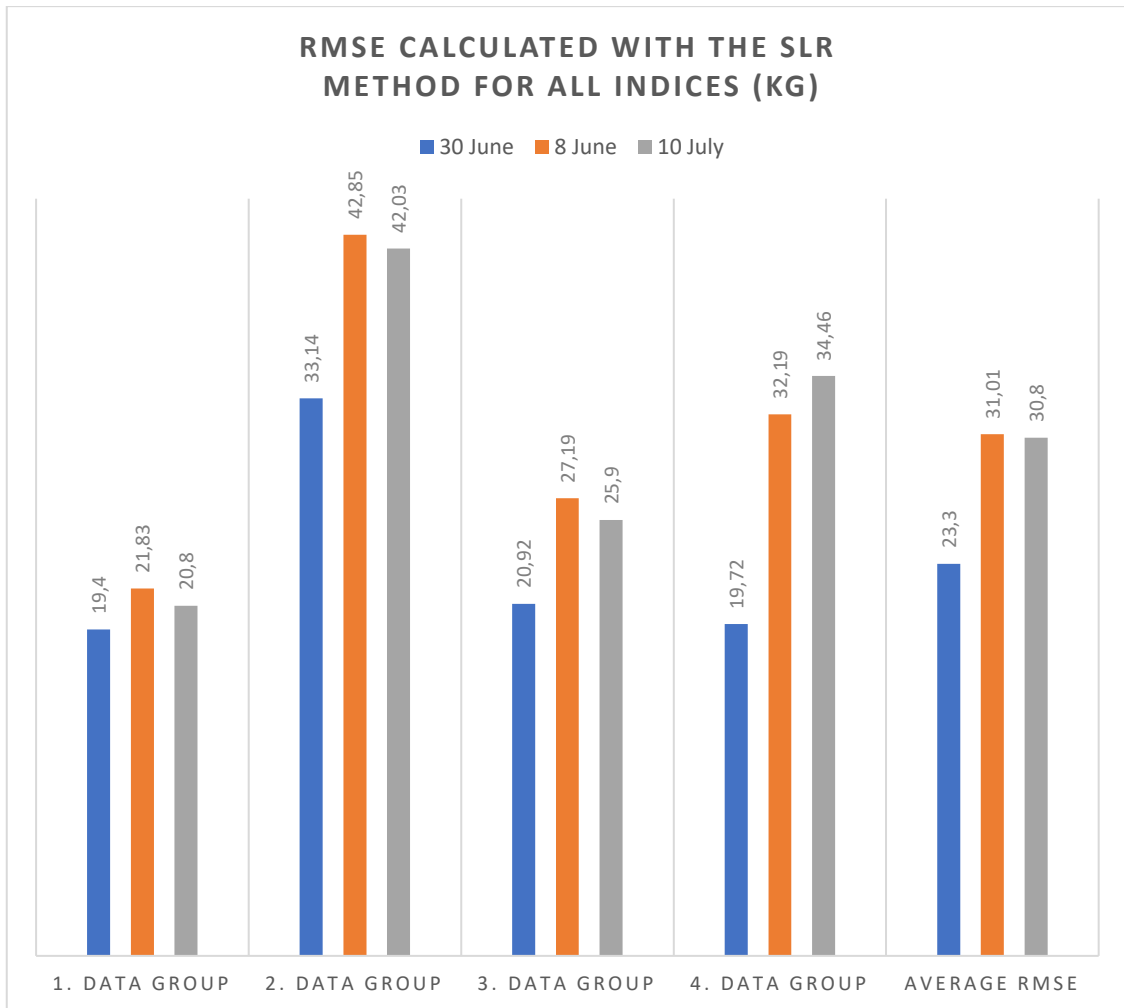
Figure 5.5. RMSE and average RMSE values were calculated using the SLR method.

When all indices were used together as input values, the yield obtained by RMSE, SLR method, and yield values produced by ANN were estimated and analyzed separately for 4 groups for the three dates examined. These results are given in the appendices in detail [Appendix B]. A separate ANN model was created for each examined date. The number of inputs is taken as 4 and the number of outputs as 1. The number of iterations was determined as 1000 without changing it. The number of hidden layers was tried according to the number of entries for each date and the value that gave the best result in different combinations was taken. In Figure 5.6, the ANN model created on June 30, the date that gave the best result in this step, is given as an example.

The number of hidden layers and RMSE selected when used indices are processed together as input are given in Table 5.3. The lowest error values for each date are shown in bold. The results of this experiment are given in Figure 5.7.
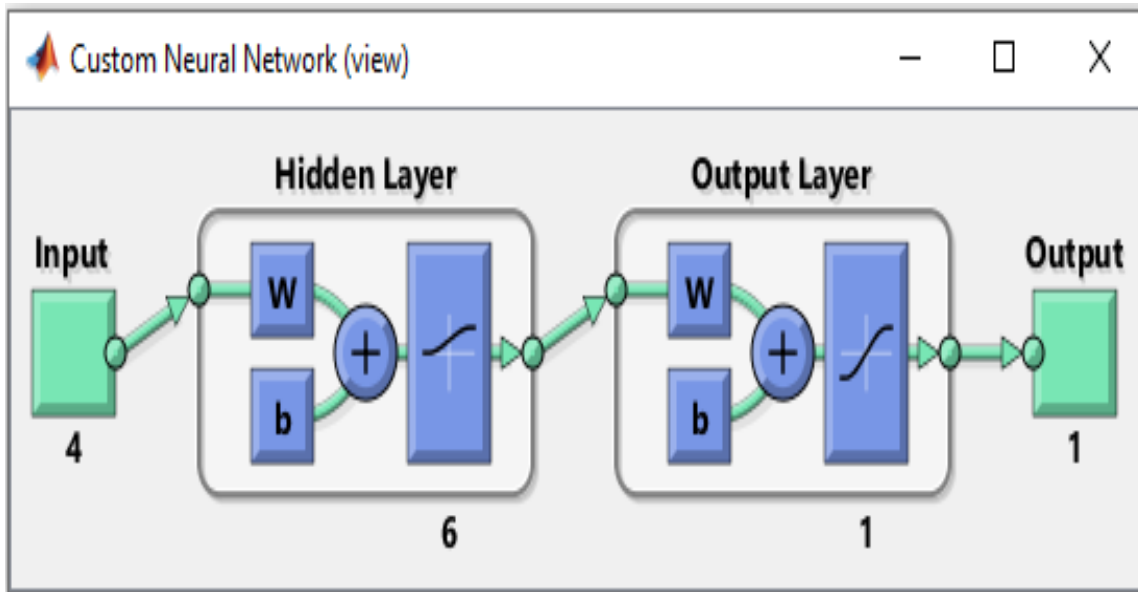
Figure 5.6. ANN model was created by using 4 indices together on 30 June.

Table 5.3: The number of hidden layers and RMSE selected when all indices values are used together as input values

30 June NDVI		8 July NDVI		10 July NDVI	
Hidden Layer Number	Average RMSE	Hidden Layer Number	Average RMSE	Hidden Layer Number	Average RMSE
5	22,13	5	27,81	**5**	**28,63**
6	**21,59**	6	28,64	6	30,55
7	22,36	**7**	**26,93**	7	31,79
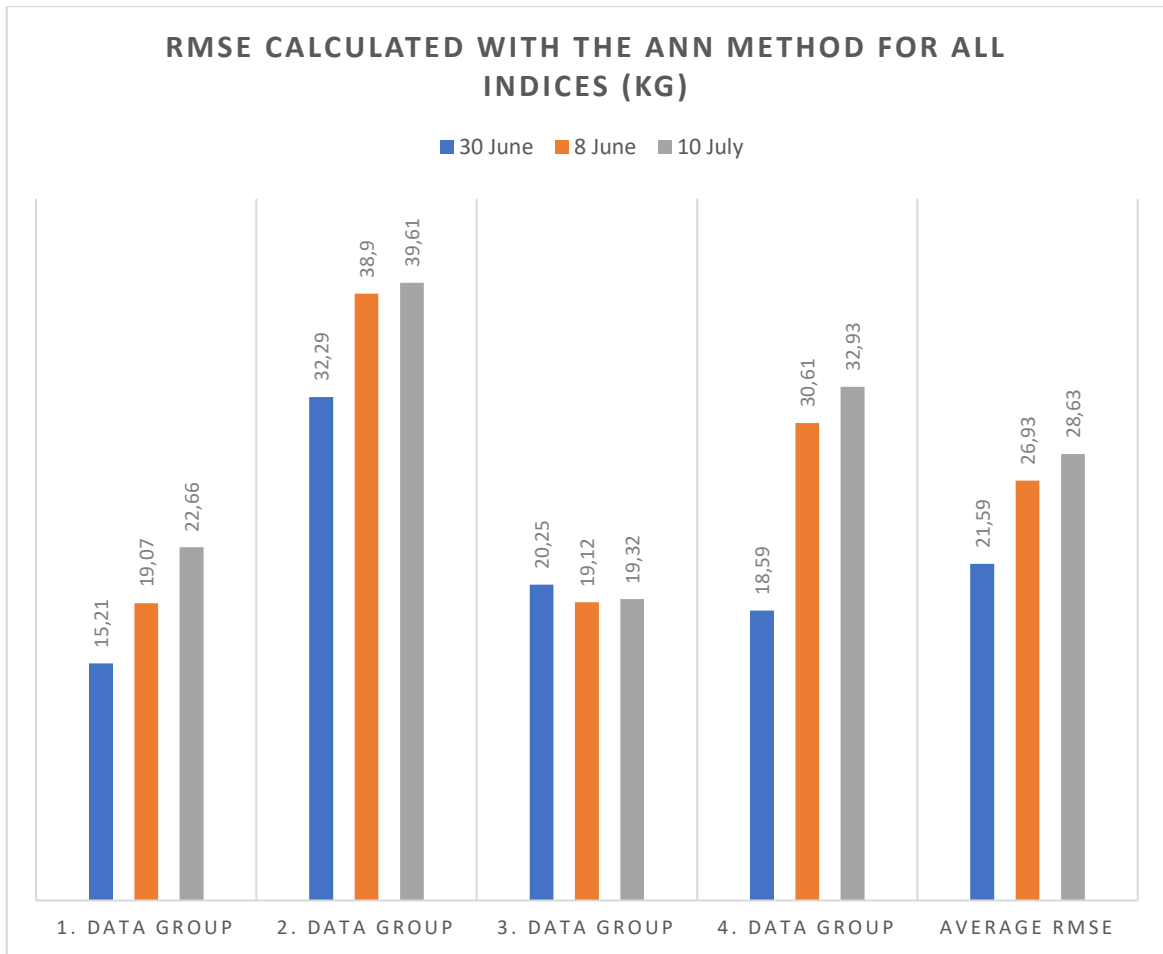
Figure 5.7. RMSE and average RMSE values were calculated using the ANN.

When the graphs in Figure 5.5 and Figure 5.6 were examined, the ANN method gave better results than the SLR in all groups on all 3 dates studied, when all indices were processed together as input values. The best results were obtained during the heading period of the sunflower plant on June 30.

5.2. Results of SAR Data

After, the preprocessing steps the backscatter values of 48 parcels were determined for each date in both VH and VV polarization. As with optical images, the average correlation between reference yield values and backscatter values and RMSE were examined over the produced backscatter values. The average values of the backscatter of 48 parcels for each polarization (VH and VV) are given in Figure 5.8.
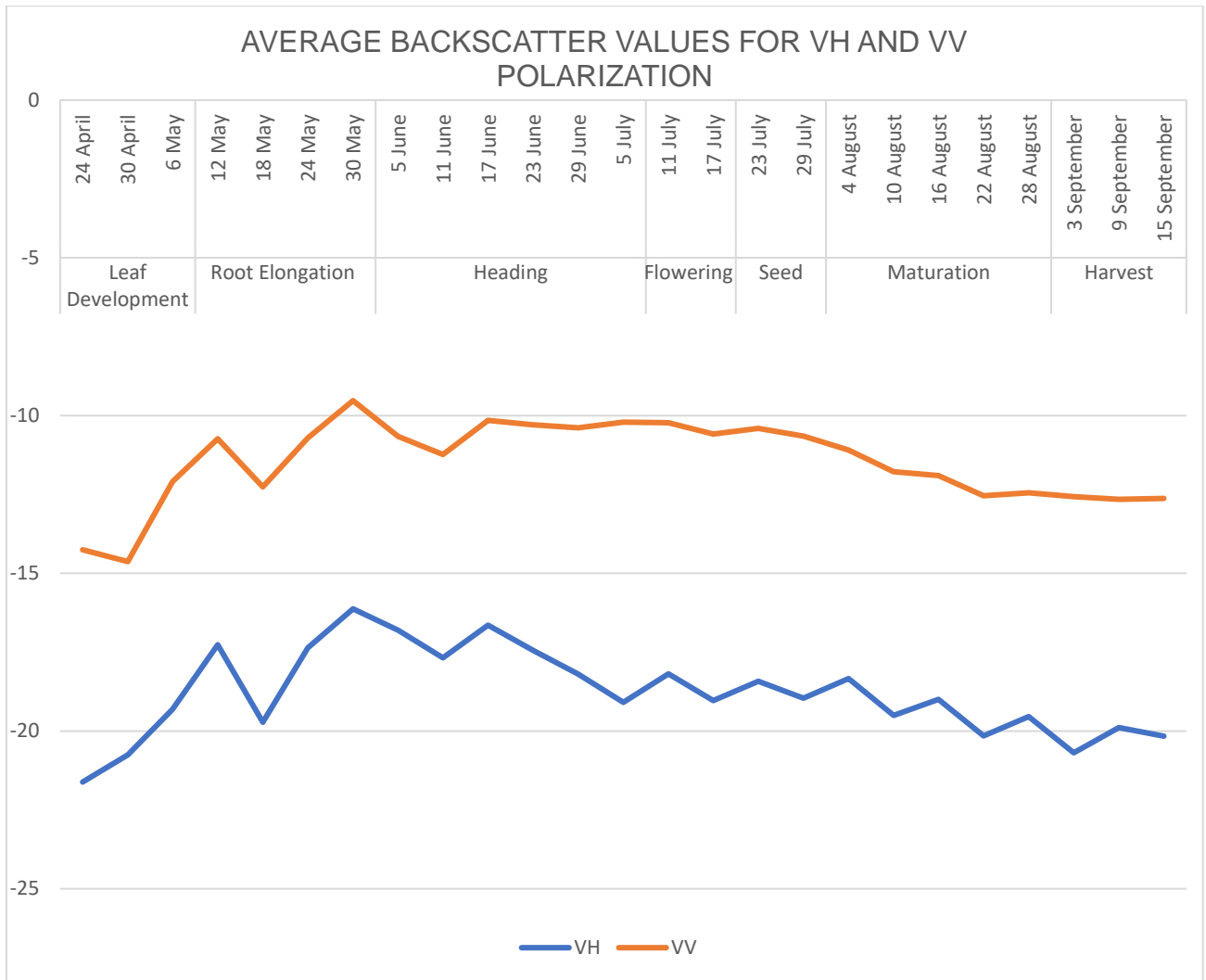
Figure 5.8. Average backscatter values between reference yield and polarization.

Considering the backscatter values, the highest backscatter value was observed in the 30 May root elongation phase in VH and VV polarization. Afterward, a fluctuating decrease and then an increase in the backscatter value were observed in two polarizations, and it was determined that the values remained constant during the harvest period.

In order to compare optical and SAR images in the further step, the SAR image dates closest to 30 June, 8 July, and 10 July, which were determined as the highest correlation dates in optical images, as selected. These image dates are June 29, July 5, and July 11. The correlation between the backscatter values and the predetermined reference yield values was examined for both VH and VV polarization in 48 parcels. Correlation values between reference yield and backscatter values for these dates are given in Table 5.4.

Table 5.4: Correlation values between reference yield values and backscatter values for 29 June, 5 July, and 11 July 2018

	29 June 2018	5 July 2018	11 July 2018
VH	0,039	-0,027	-0,008
VV	0,114	0,030	0,072

It was observed that the correlation values in the VV polarization were higher than the correlation values in the VH polarization within the three dates discussed. It was determined that the date with the highest correlation in both polarizations was June 29 (Table 5.4). The yield was first obtained by backscattering values from the linear regression function. RMSE values were generated on selected dates for each polarization. By the SLR method, 48 plots were divided into 4 groups of 12 for the dates of 29 June, 5 July, and 11 July. Three sets of linear regression functions were used for a test set to generate. The calculated RMSE and average RMSE for each group in both VH and VV polarization are given in Figure 5.9.
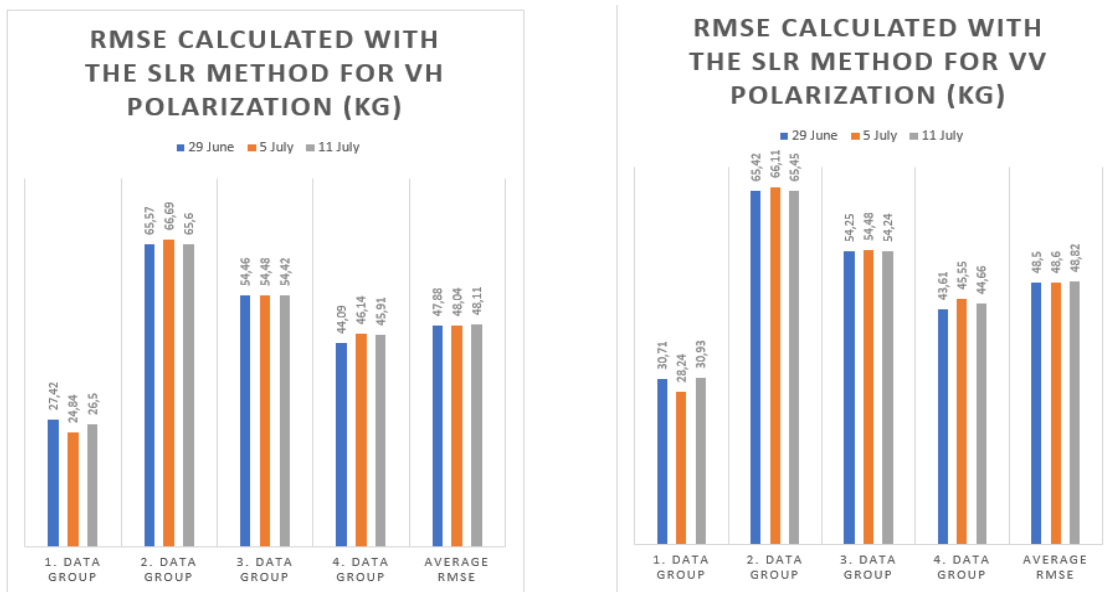
Figure 5.9. RMSE and average RMSE for backscatter values in the SLR method.

Looking at the average RMSE values over the three dates, the SLR method gave better results for VH polarization than for VV polarization (Figure 5.8). ANN method was used as the next step and yield values were obtained with this method. The yield values obtained by these two different methods were compared with the

41

reference yield values. The results are detailed in the appendices [Appendix C]. In the ANN method, firstly, the backscatter values were processed as a single input on the selected dates for each group. The number of inputs is taken as 1 and the number of outputs as 1. The number of iterations was determined as 1000. The number of hidden layers was tried by trial and error method and different combinations were tried and the value that gave the best result was taken as the basis. The number of hidden layers and RMSE selected when used backscatter values are processed as inputs alone are given in Table 5.5. The best result for each date is shown in bold.

Table 5.5: The number of hidden layers and RMSE selected in the VH and VV polarization when the backscatter values alone are used as input values.

29 June Backscatter(VH)		5 July Backscatter (VH)		11 July Backscatter (VH)	
Hidden Layer No	Average RMSE	Hidden Layer No	Average RMSE	Hidden Layer No	Average RMSE
2	**45,6**	**2**	**47,4**	**2**	**48,07**
3	47,61	3	48,49	3	49,9
4	47,54	4	48,88	4	50,05
5	45,98	5	48,73	5	50,55
29 June Backscatter(VV)		5 July Backscatter (VV)		11 July Backscatter (VV)	
2	45,65	**2**	**46,21**	**2**	**48,09**
3	**42,46**	3	48,9	3	49,81
4	44,47	4	48,42	4	51,65
5	43,21	5	49,39	5	51,23

The calculated RMSE and average RMSE for each group in both VH and VV polarization are given in Figure 5.10.
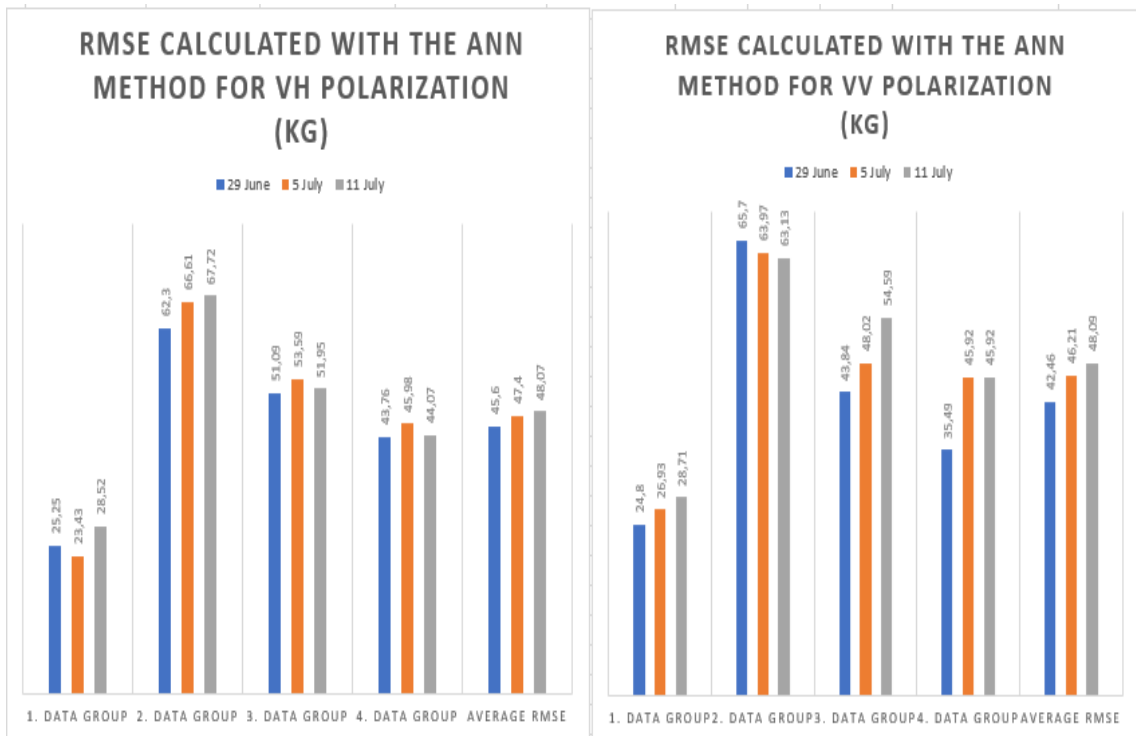
Figure 5.10. RMSE and average RMSE for backscatter values in the ANN method.

Considering the average RMSE values on June 29 and July 5 and using the backscatter values alone as the input value, VV polarization gave better results than VH polarization. On July 10, there is little to no difference between VH and VV polarization (Figure 5.9).

In order to produce coherence values from two different SAR satellite images at two different times, satellite images from 26 different dates were divided into pairs in two polarizations with a 6-day time difference between them. The average coherence value graph obtained from these grouped views is given in Figure 5.11.
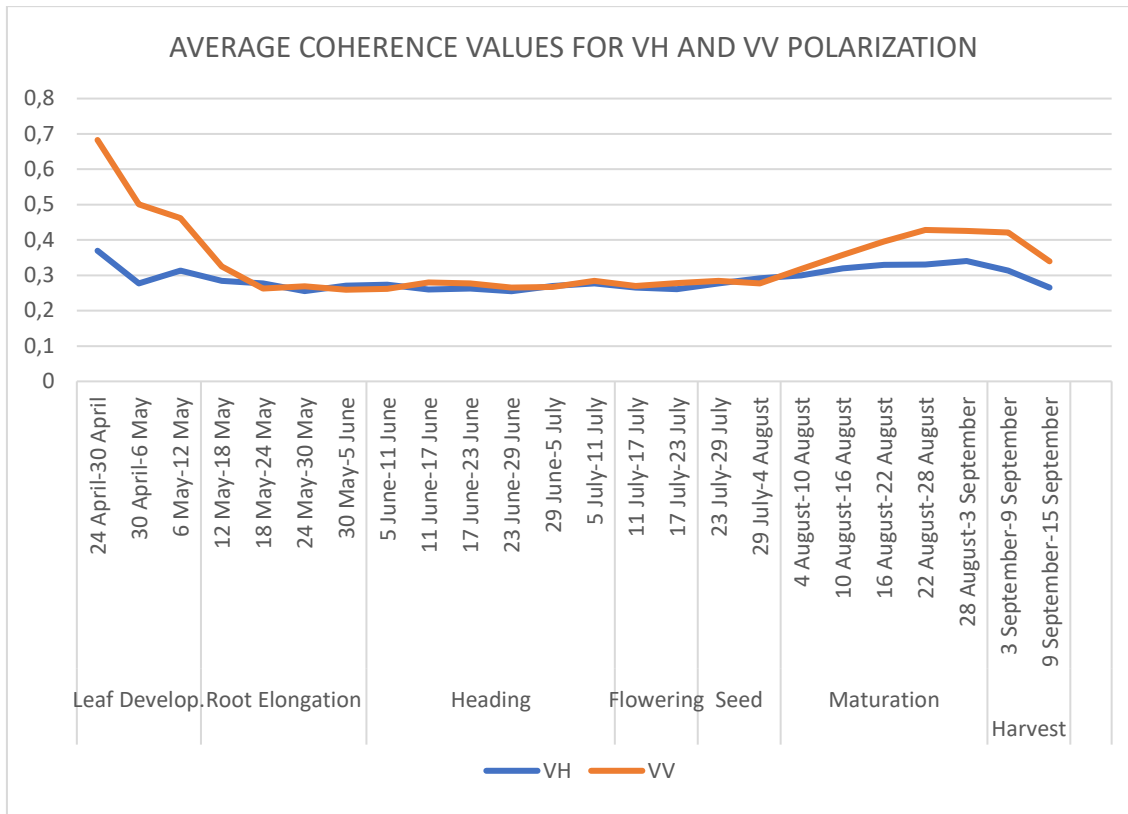
Figure 5.11. Average coherence values of the polarizations.

In both polarizations, the highest coherence value was observed between April 24 and 30, and a significant decrease in coherence values was observed during the leaf development phase. It was observed that the values remained constant in the phase from root elongation to seed maturation, increased during the ripening period, and started to decrease again in the harvest period.

In order to compare the yield values we obtained using optical and SAR images in the further step, the SAR image date ranges closest to 30 June, 8 July, and 10 July, which are determined as the highest correlation date in optical images, are 29 June - 5 July, 5 July - 11 July, and 11 July-17 July were selected and the correlation between the coherence values and the predetermined reference yield values was examined for VH and VV polarization in 48 parcels.

When examining the correlation between the coherence values and the reference yield, it was seen that the correlation in VH polarization was higher on the pair of 29 June - 5 July (Table 5.6). It was seen that the correlation in the VV polarization was higher than the VH polarization in the image dates of 5 July - 11 July and 11

44

July - 17 July. The highest correlation in VH and VV polarization is determined by the image date of July 5th to July 11th (Table 5.6).

Table 5.6: Correlations between reference yield and coherence values on 29 June-5 July, 5 July-11 July, and 11 July - 17 July 2018

	29 June- 5 July 2018	5 July-11 July 2018	11 July-17 July 2018
VH	0,082	-0,128	0,081
VV	0,011	-0,278	0,099

The yield was obtained from coherence values by the SLR method using linear functions. RMSE values were produced at the selected dates for each polarization. For the dates 29 June - 5 July, 5 July - 11 July, and 11 July - 17 July, as applied previously, 48 parcels were divided into four groups of 12 each. It was used for one set of tests to generate three sets of linear functions. The calculated RMSE and average RMSE for each group in both VH and VV polarization are given in Figure 5.12.
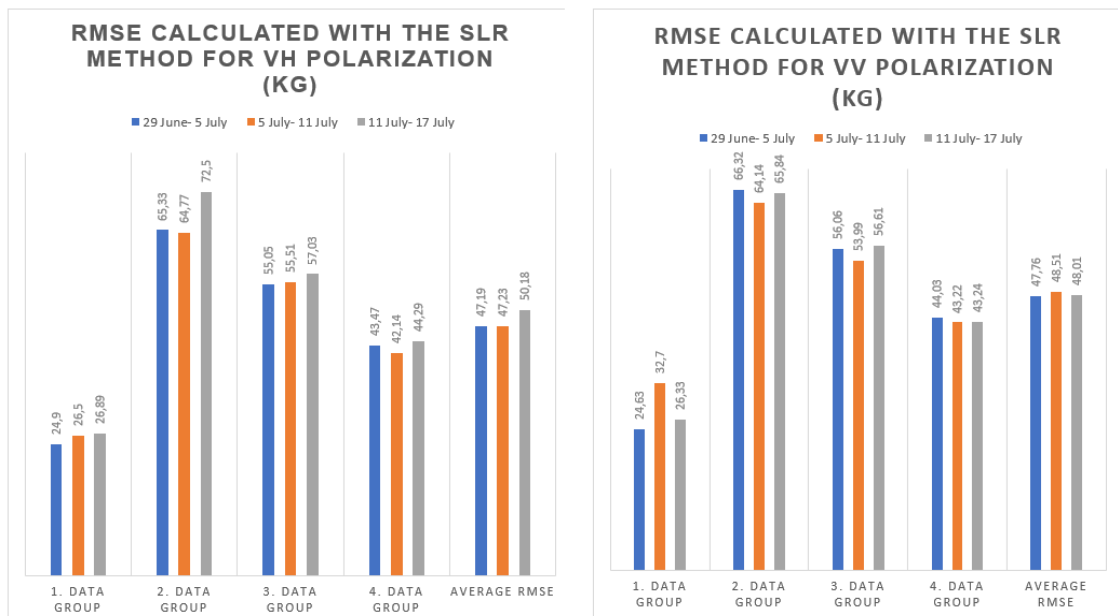
Figure 5.12. RMSE and average RMSE for coherence values in the SLR method.

Considering the average RMSE values, VH polarization on 29 June - 5 July and 5 July - 11 July gave better results in the SLR method than VV polarization (Figure

5.11). On July 11-17, VV polarization gave better results in the SLR method than VH polarization.

While the yield was obtained with the ANN method, the coherence values were first processed separately for each group as a single input for three dates. The number of entries is taken as 1. The output number is taken as 1 again. The number of iterations is set to 1000 without changing it. The number of hidden layers was tried with different combinations by trial and error method and the value that gave the best result was taken. The number of hidden layers and RMSE selected when used coherence values are processed as inputs alone are given in Table 5.7. The best result for each date is shown in bold.

Table 5.7: The number of hidden layers and RMSE selected in the VH and VV polarization when the coherence values alone are used as input values.

29 June-5 July Coherence (VH)		5 July-11 July Coherence (VH)		11 July-17 July Coherence (VH)	
Hidden Layer No	Average RMSE	Hidden Layer No	Average RMSE	Hidden Layer No	Average RMSE
2	49,03	2	48,19	2	51,32
3	**47,17**	3	50,4	**3**	**50,16**
4	54,65	**4**	**47,22**	4	53,76
5	52,86	5	48,02	5	51,59
29 June-5 July Coherence (VV)		5 July-11 July Coherence (VV)		11 July-17 July Coherence (VV)	
Hidden Layer Number	Average RMSE	Hidden Layer Number	Average RMSE	Hidden Layer Number	Average RMSE
2	48,76	**2**	**46,24**	**2**	**46,51**
3	53,01	3	47,28	3	48,87
4	**47,62**	4	47,96	4	50,03

RMSE values were calculated from the yield values estimated by the ANN method. The estimated yield values and reference yield values were compared for both polarizations by SLR and ANN methods and examined. Details are given in the appendices [Appendix D]. Calculated RMSE and mean RMSE for each group in both VH and VV polarization are given in Figure 5.13.
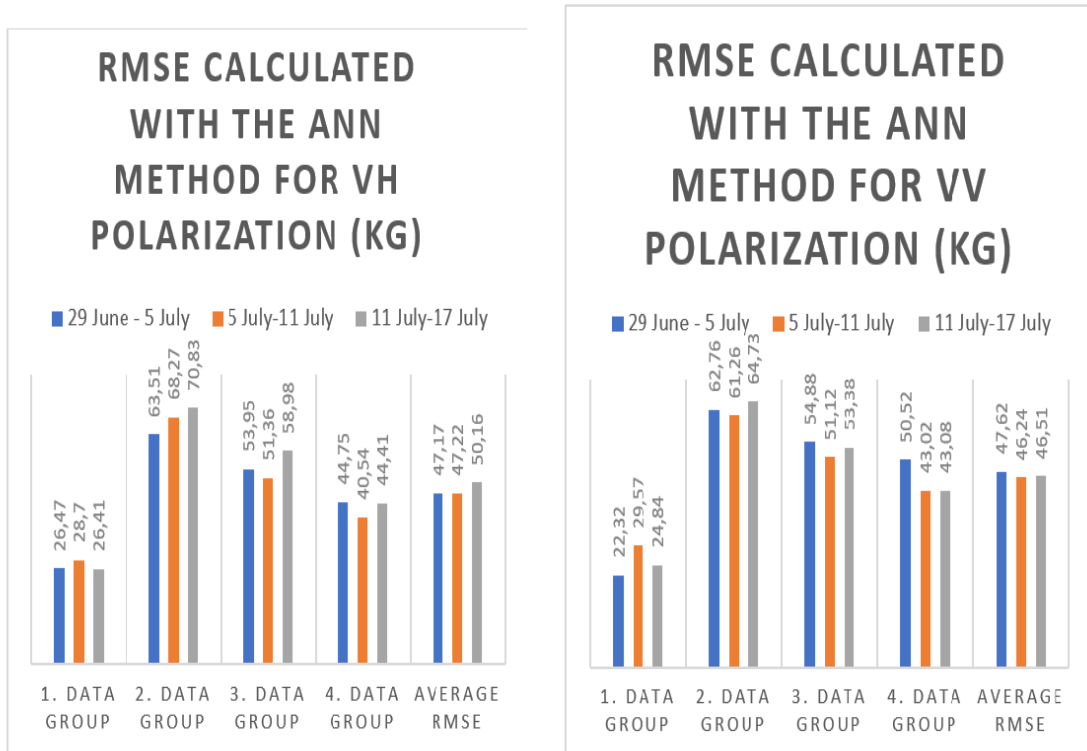
Figure 5.13. RMSE and average RMSE for coherence values in the ANN method.

Considering July 5-11 and July 11-17 coherence data as input values alone, the VV polarization in the ANN method has given better results than the VH polarization comparing the average error (Figure 5.12).

When the backscatter and coherence values are used as input values alone, better values have been obtained from VV polarization compared to VH polarization in the ANN method for the most part. For this reason, when backscatter and coherence values are used together as input values in the ANN method, VV polarization is taken into account after this stage. As an introduction, only VV polarization was used for both backscatter and coherence values. The number of inputs is taken as 2 and the number of outputs as 1. The number of iterations was

taken as 1000 without changing, yield and RMSE was calculated. Details are given in the appendices [Appendix E].

According to the number of entries for each date, the number of hidden layers was tested with different combinations, and the value that gave the best results was taken. When backscatter and coherence are processed together as input, the number of hidden layers and the selected RMSE is given in Table 5.8. The best result for each date is shown in bold.

Table 5.8: When the backscatter and coherence values are used together as the input value, the selected hidden layer number and RMSE

29 June-5 July (VV)		5 July-11 July (VV)		11 July-17 July (VV)	
Hidden Layer Number	Average RMSE	Hidden Layer Number	Average RMSE	Hidden Layer Number	Average RMSE
3	47,81	3	47,56	3	50,54
4	**44,56**	**4**	**47,22**	**4**	**48,52**
5	46,73	5	48,12	5	50,66
6	45,37	6	48,76	6	49,9

When backscatter and coherence are examined together, the calculated RMSE and mean RMSE for each group in both SLR and ANN methods are given in Figure 5.14.
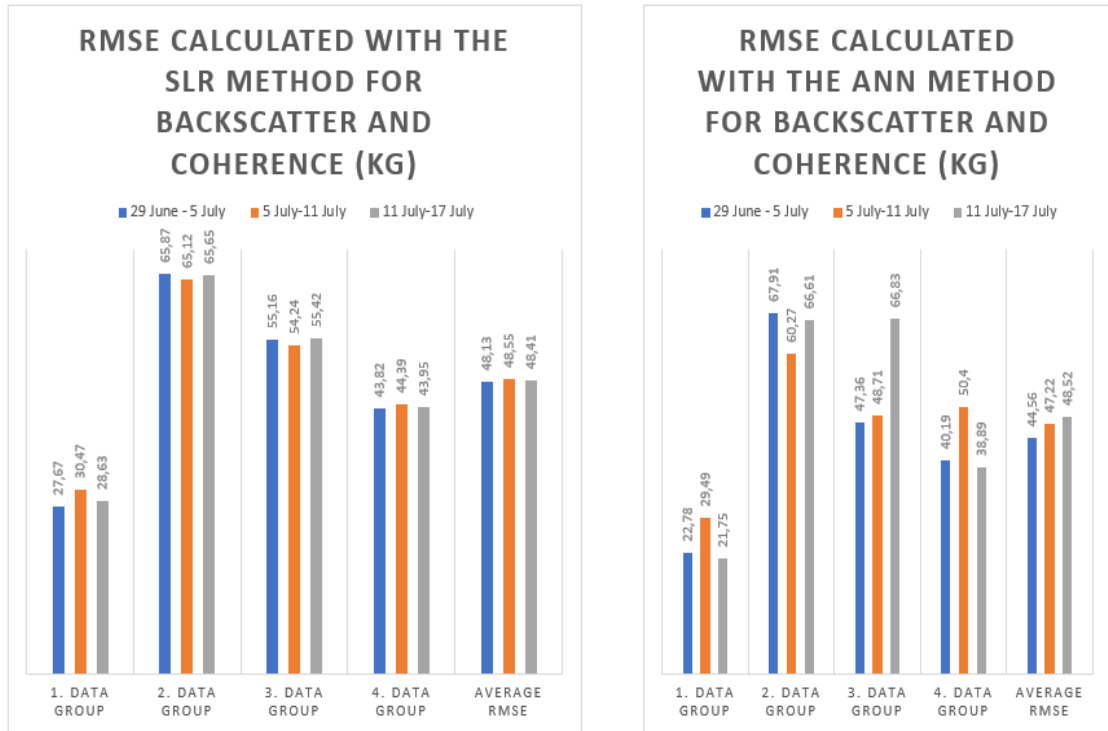
Figure 5.14. RMSE and Average RMSE for coherence and backscatter for VV.

5.3 Results of Optical and SAR Data

In this process step, NDVI, NDVIR1, OSAVI, and IRECI vegetation indices produced from optical satellite images and backscatter and coherence of VV polarized SAR images were used together as input values in the ANN method. The dates were analyzed as 29 June-5 July, 5-11 July, and 10-17 July to include both optical image dates and SAR satellite image dates. The number of iterations is taken as 1000, unchanged. The number of inputs is taken as 6 and the number of outputs as 1. The number of hidden layers, again according to the number of inputs, many different combinations were tried and the value that gave the best result was taken into consideration. When NDVI, NDVIR1, OSAVI, and IRECI, backscatter, and coherence values are used together as inputs, the number of hidden layers and the selected RMSE are given in Table 5.9. The best result for each date is shown in bold.

Table 5.9: The RMSE of the selected number of the hidden layer when SAR and optical image values are used together.

29 June-5 July (VV)	5 July-11 July (VV)	10 July-17 July (VV)

Hidden Layer Number	Average RMSE	Hidden Layer Number	Average RMSE	Hidden Layer Number	Average RMSE
7	28,87	7	35,21	7	32,44
8	**26,83**	**8**	**33,49**	**8**	**31,04**
9	29,9	9	35,36	9	33,56
10	28,54	10	34,75	10	33,98

When the data produced from optical and SAR satellites are examined together, the calculated RMSE and average RMSE for each group in both SLR and ANN methods are given in Figure 5.15. Details are given in the appendices [Appendix F].
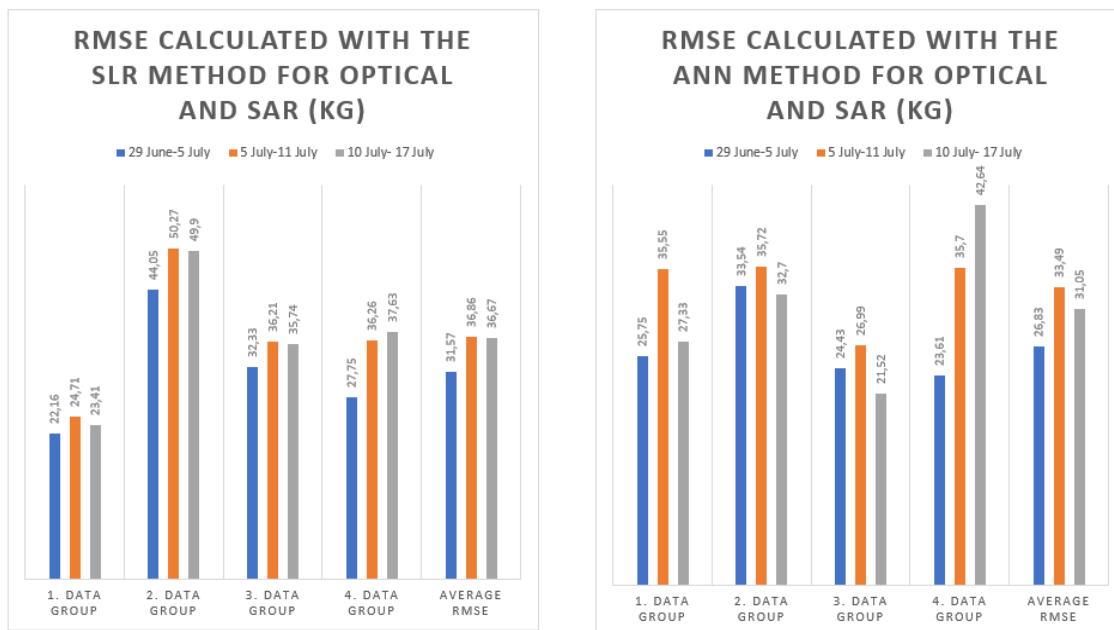
Figure 5.15. RMSE and Average RMSE for optical and SAR.

6. DISCUSSIONS

In the study, first of all, using the index reflectance values obtained from the optical images, the yield estimation study was carried out by SLR and ANN methods and the RMSE was calculated. When the indices are used separately as a single input value, it was noticed that the ANN method gave better results than the SLR method in all three dates examined. Estimated values are given in Table 6.1 for the three dates examined. In the ANN method, NDVI gave the best result on June 30. NDVIR1 gave the best results on 8 and 10 July. However, in the SLR method, the index that gave the best result on June 30 was OSAVI. It was seen that OSAVI produced a better value than NDVI in the SLR method, but NDVI contributed more than OSAVI in the ANN method. As a result, it was concluded that the contribution of the indices may vary according to the method used in yield estimation studies, and in this study, the best estimation study was made in the ANN in the NDVI and NDVIR1 indices.

Table 6.1: The Average RMSE of the indices calculated by SLR and ANN methods.

	NDVI	NDVIR1	OSAVI	IRECI
30 June Average Linear RMSE	22,64	23,67	22,47	24,40
30 June Average ANN RMSE	22,07	22,71	22,32	23,86
8 July Average Linear RMSE	32,33	30,44	30,75	30,54
8 July Average ANN RMSE	29,17	27,53	30,28	27,59
10 July Average Linear RMSE	31,13	29,33	30,74	31,99
10 July Average ANN RMSE	30,95	24,31	28,41	28,67

Similar to this study, G. Narin et al. (2021) investigated the relationship between the NDVI and NDVIR1 indices produced from the Sentinel-2 data. They examined SLR, CNN, and ANN methods together with the use of indices and estimated the yield of the sunflower plant. They stated that they obtained the best estimation results in the NDVI and the CNN technique with the RMSE of 20,87 Kg/da on 30th June 2018. They stated that there was not much superiority between the NDVI and NDVIR1 indices. Likewise, in this study, NDVI gave the best result with 22.07 Kg/da on 30 June in the ANN method. On June 30, it was observed that there was not much superiority between the NDVI and NDVIR1 indices. In addition, combining multispectral and SAR features did not improve the result. In another study, Abdikan et al. (2022) used SLR and ANN methods while determining the crop height of sunflowers utilizing both Sentinel-1 SAR and Sentinel-2 satellite images. In conclusion, they stated that NDVIre1 provided more contribution than the image of NDVI from their previous studies. This shows the result that not only the method but also the contribution of the indices can change according to the subject studied.

When 4 indices are processed together as input values, the ANN method again gave better results than the SLR method. The best yield estimate was made on June 30, when all indices were used together as input values, In Figure 6.1, the difference between the reference yield values of 48 parcels and the estimated yield values is shown by Decolorizing from light to dark. The best performing parcels are shown in the darkest color, while the worst performing parcels are shown in the lightest color. There may be many different reasons why some parcels in the same area produce good value and some parcels produce bad value. The reason for this may be that the soil type is different, the necessary nutrients and needs are not met, less irrigation is performed, or the October area is kept narrow.

When Figure 6.1 is examined, for example, small parcels such as 23 and 24 produced poor yield values, but large parcels such as 21 and 29 produced better values. However, not all small-sized parcels produced bad values, and not all large-sized parcels produced good values. For this reason, a relationship could not be established between the parcel size and the difference yield values obtained from the parcel.
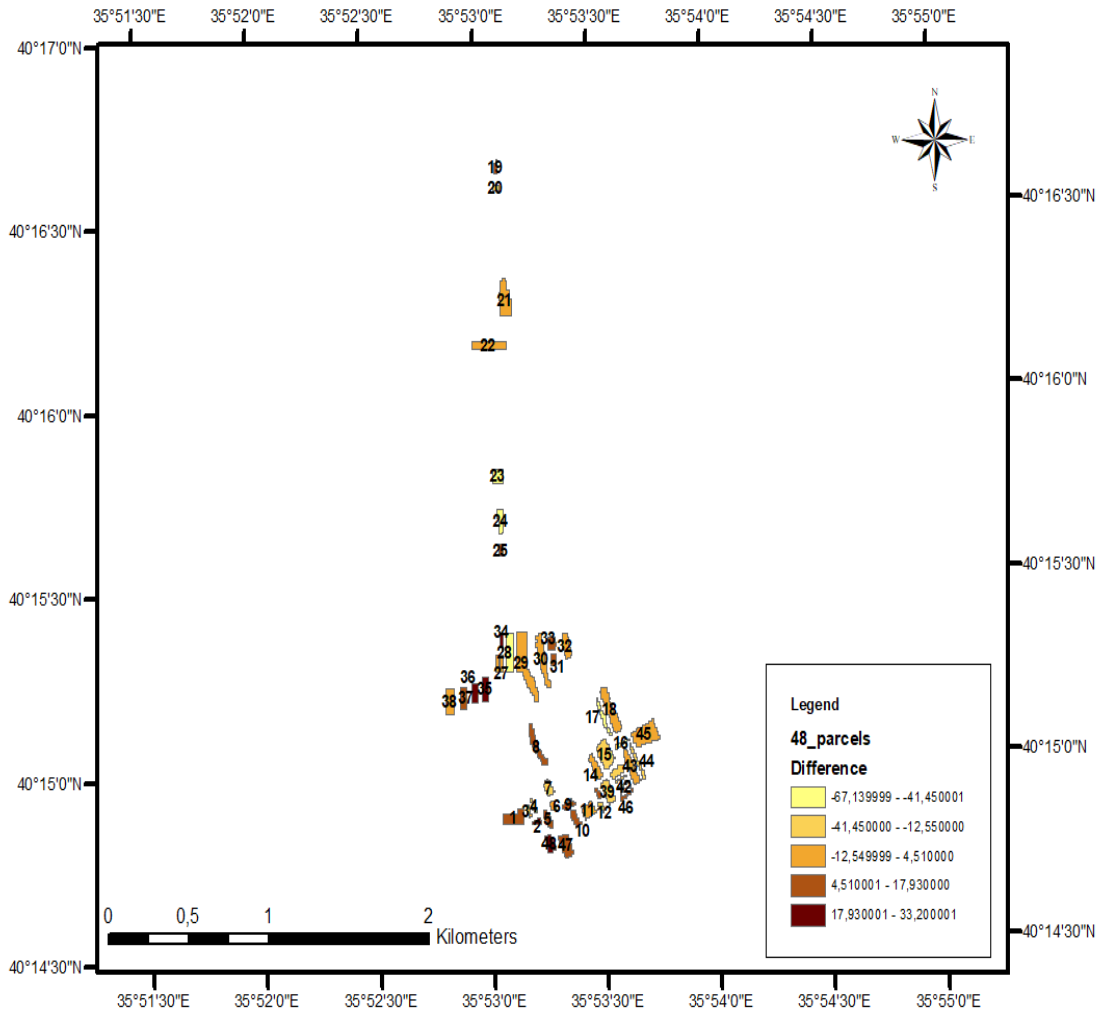
Figure 6.1. Difference (kg) between reference yield values and estimated yield values on 30 June.

It was concluded that using indices together as input in the ANN method reduces the error rate. The results obtained are given in Table 6.2. However, while estimating the yield with the ANN method and determining the number of hidden layers, many different combinations were tried and the number of hidden layers that gave the best results was taken as a basis. The process was repeated many times until the best value was found. Although this situation causes the ANN to memorize the data and work with the learned accuracy, it has been concluded that it is a method that can be used in determining the yield.

Table 6.2: The Average RMSE calculated by SLR and ANN method, when 4 indices are processed together as input value.

	Linear Average RMSE	ANN Average RMSE
30 June	23,30	21,59
8 July	31,01	26,93
10 July	30,80	28,63

Saranya and Nagarajan (2020) compared linear regression and the ANN model in their crop yield estimation study and as a result, they stated that corn and soybean have a higher correlation with the ANN model and give better results than linear regression. However, since the study focused on the estimation of agricultural crop yields using ANNs with good predictive results, they emphasized that research on processing noise in images requires to be explored, and optimization of models needs further investigation [66].

When the yield estimation is made using the backscatter values obtained from the SAR images, it is seen that the ANN method gives better results than the SLR method in both polarizations (VH, VV). The results are given in Table 6.3. However, when the indices were used, the sunflower plant made a better yield estimation. Backscatter values were not sufficiently effective when used alone in yield estimation.

Table 6.3: The Average RMSE of the backscatter calculated by SLR and ANN methods.

	Backscatter (VH)	Backscatter (VV)
29 June Average Linear RMSE	47,88	48,50
29 June Average ANN RMSE	45,60	42,46
5 July Average Linear RMSE	48,04	48,60
5 July Average ANN RMSE	47,40	46,21
11 July Average Linear RMSE	48,11	48,82
11 July Average ANN RMSE	48,07	48,09

Similarly, Fieusal et al. (2016) estimated the yield of maize crops by using the ANN method using Spot-4/5 and Formosat-2 optical and Radarsat-2 and TerraSAR-X microwave satellite images. They determined that the maize crop gave the best estimation result in the red wavelength, and the adaptation of the backscatter values remained lower in the yield estimation. However, they observed that the combination of backscatter and red reflection provided the accuracy of the yield estimation with RMSE=7.0 q ha^{-1} and R^2= 0.69. The combination of backscatter and red wavelength did not give the best results but gave acceptable accuracy.

In this study, the inability to obtain the desired yield estimation contribution from the backscatter values may be related to the angle between the normal surface and the reflected signal. This situation may have caused the desired values not to be produced from the backscatter values. The crop type, size, and shape of the plant may contribute to the backscatter value. Additionally, the water content and biomass of the crops with broad leaves also influence the response of energy [67]. The behavior of the backscatter values does not show a trend as indices derived from optical data. The backscatter has an increasing trend, with an up-and-down behavior from leaf development to the heading period. the backscatter of VV is stable to the end of seed phenology and then decreases to the harvest. The backscatter of VH decreases slowly from the end of root elongation to the harvest time (Figure 5.8).

The coherence also showed stable behavior from the root elongation to the end of seed phenology In both VV and VH polarimetry which indicated the contribution of polarimetry is limited and for the four phenology coherence is almost stable, and it is difficult to discriminate the phenology. Only in the maturation period, there is a difference and VV provided higher coherence than VH data (Figure 5.11). When estimating the yield using the coherence values obtained from the SAR images, it was concluded that the ANN method provided better results than the SLR method in both polarizations (VH, VV). It has been determined that the coherence values cannot be used alone in the estimation of yield, the accuracy of the results is below 70% and the error rates are high. The results are given in Table 6.4.

Table 6.4: The Average RMSE of the coherence calculated by SLR and ANN method.

	Coherence (VH)	Coherence (VV)
29 June - 5 July Average Linear RMSE	47,19	47,76
29 June - 5 July Average ANN RMSE	47,17	47,62
5 July- 11 July Average Linear RMSE	47,23	48,51
5 July- 11 July Average ANN RMSE	47,22	46,24
11 July- 17 July Average Linear RMSE	50,18	48,01
11 July- 17 July Average ANN RMSE	50,16	46,51

While yield was estimated by the ANN method using backscatter values and coherence values, VV polarization gave better results than VH polarization in most of the studied dates. Therefore, when backscattering and coherence values were used together, only VV polarization was considered at this stage. Similarly, Amherdt et al. (2022) investigated the contribution of backscatter and coherence values produced by the Sentinel-1 satellite to the mapping of corn and soybean. As a result, it was determined that VV polarization gave better results than VH polarization.

When the backscatter and coherence values are processed together as input values, ANN gave better results than the SLR method on 29 June-5 July and 5 July-11 July. However, on 11-17 July, the SLR method gave better results than the ANN method. The results are given in Table 6.5. While the use of backscatter and coherence values together reduced the error rate on 29 June-5 July, it did not affect the error rate much on other dates. The use of backscatter and coherence values together did not have a positive effect on yield estimation. It was concluded that adding coherence to the backscatter information in the VV polarization of the sunflower plant did not contribute to the yield estimation study.

Tablo 6.5: The Average RMSE calculated by SLR and ANN method, when backscatter and coherence values are processed together as an input value.

	Linear Average RMSE	ANN Average RMSE
29 June - 5 July (VV)	48,13	44,56
5 July-11 July (VV)	48,55	47,22
11 July-17 July (VV)	48,41	48,52

However, Amherdt et al. (2022) used 605 polygons (samples) from 49 Sentinel-1 satellite images for soybean and corn mapping and investigated the contribution of coherence value to backscatter value using the Random Forest method. They concluded that it might be a suitable tool. This may be due to the method they use and the large number of samples. This has shown that although the use of backscatter and coherence values together contributes in some cases, it does not contribute to the ANN method when estimating the yield and decreases the accuracy and increases the error rate. The reason for this may be the small number of parcels examined in the studied area, the different reactions of the examined plant species in different seasons, the method used, or the study area.

As a final step, the yield was estimated by using the indices, backscatter, and coherence values obtained from the optical and SAR satellite images together. The dates were set as 29 June - 5 July, 5 July - 11 July, and 10 July - 17 July, to cover both optical images and SAR satellite images. For all three dates, the ANN method gave better results than the SLR method. The results are given in Table 6.6.

Table 6.6: The Average RMSE calculated by SLR and ANN method, when indices, backscatter, and coherence values are processed together as input value.

	Linear Average RMSE	ANN Average RMSE
29 June - 5 July (VV)	31,57	26,83
5 July- 11 July (VV)	36,86	33,49
10 July- 17 July (VV)	36,67	31,05

The results show that using the Sentinel-2 optical satellite image and Sentinel-1 SAR satellite image together in the ANN method did not improve the yield

estimation (Table 6.6.). The use of backscatter and coherence values with indices did not reduce the error rate. However, an acceptable result was obtained. The yield estimated using only indices gave much better results. Similar to this study, Ameline et al. (2018) estimated the yield of maize plants using an agro-meteorological model with Landsat-8 optical satellite image and the Sentinel-1 SAR satellite image. As a result, they stated that the efficiency estimation was lower with the use of these two satellites together, but it could be considered an acceptable result. They commented that the use of SAR or optical data alone to enable maize monitoring is not sufficient due to the low sensitivity of the SAR signal to crop growth and the inability to obtain sufficient optical data due to the risk of cloud cover. They also argued that a new model should be included to simulate dry masses and yield.

The average RMSE calculated when optical images, radar images, and optical and radar images are processed together in the ANN method is given in Figure 6.1.
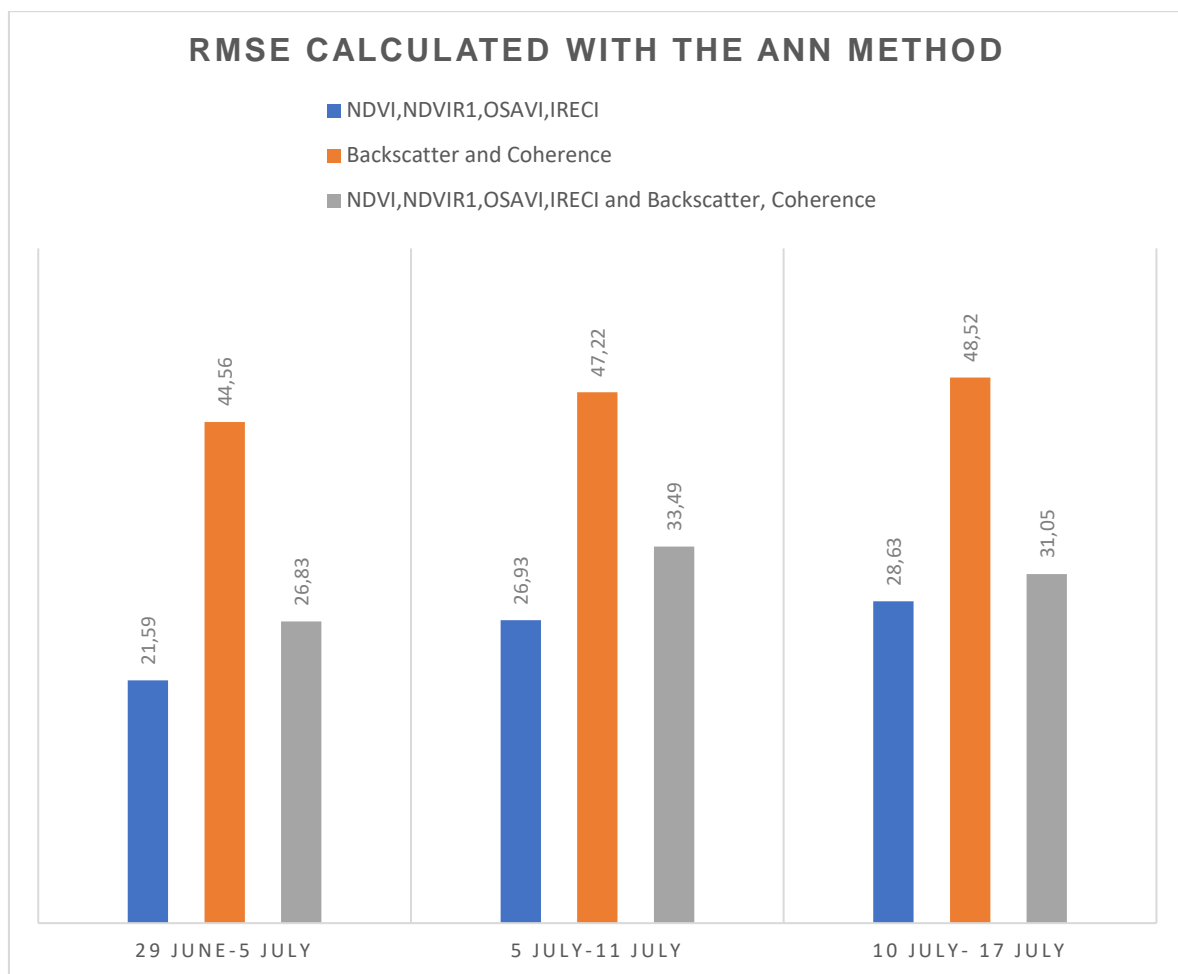
Figure 6.2. Average RMSE for optical, radar, optical, and radar.

7. CONCLUSIONS AND FUTURE WORK

In this thesis, a yield estimation study of 48 sunflower parcels taken from the Zile district of Tokat was conducted. The contribution of different combinations was investigated using optical and SAR satellite images, yield estimation was made with SLR and ANN methods, RMSE ve R^2 values were calculated and reference yield values and estimated yield values were compared. The results found are given below.

The following results were obtained when the yield was estimated using Sentinel-2 optical satellite images.

- When the yield estimation is made from NDVI, NDVIR1, OSAVI, and IRECI indices using the SLR method, the best result for June 30 was obtained from OSAVI (R^2 = 0.77 RMSE = 22.47 kg). NDVIR1 (R^2 = 0.63 RMSE= 30.44 kg) gave the best result for July 8. The index that gave the best result for July 10 was again NDVIR1 (R^2 = 0.63 RMSE= 29.33 kg).

- In the ANN method, when the indices are processed separately as input values, NDVI (R^2=0.76 RMSE= 22.07 kg) gave the best result on 30 June. NDVIR1 (R^2= 0.64 RMSE= 27.53 kg) gave the best result on July 8th. On July 10, NDVIR1 (R^2= 0.71 RMSE= 24.31 kg) gave the best result again.

- When the ANN method is compared with the SLR method, the ANN method gave better results than the SLR method in the three dates considered. As a result, it was concluded that the best estimation study was made in the ANN method in the NDVI and NDVIR1 indices.

- In the ANN method, when the four indices are processed together as input values, ANN gave better results than the SLR method on all three dates. The best result was obtained in the heading period on June 30 (R^2=0.78 RMSE= 21.59 kg). It has been concluded that using the indices together as input in the ANN method reduces the error rate in yield estimation.

- It was determined that it is possible to obtain the sunflowers' phenological stages and estimate yield in advance with higher accuracy by the ANN method using optical images.

The following results were obtained when the yield was estimated using Sentinel-1 SAR satellite images.

- When the yield was estimated using the backscatter values alone, the best result in the SLR method was obtained from the VH polarization on June 29 (R^2= 0.14 RMSE= 47.88 kg).

- When the yield was estimated using the backscatter values alone, the best result in the ANN method was obtained on 29 June VV polarization (R^2=0,09 RMSE= 42,46 kg).

- In the SLR method, backscatter values gave better results in VH polarization compared to VV polarization on all three dates. However, in ANN, VV polarization gave better results than VH polarization.

- The ANN method gave better results than the SLR method, but the backscatter values did not contribute enough. When the R^2 value and the average RMSE are compared with the values obtained in the index values, it is seen that the contribution of the backscatter values to the yield estimation is very small. It has been concluded that using the backscatter values alone in the yield estimation is not sufficient.

- When the yield was estimated using the coherence values, the best result in the SLR method was obtained in VH polarization between 29 June and 5 July (R^2= 0.06 RMSE= 47.17 kg).

- In the ANN method, the best result was obtained on July 5-11 in VV polarization (R^2= 0.01 RMSE= 46.24 kg).

- In the SLR method, VH polarization produced better values compared to VV polarization, but in the ANN method, VV polarization produced better values than VH polarization.

- In both polarizations (VH, VV), the ANN method gave better results than the SLR method but results with sufficient accuracy were not produced.

- It has been concluded that the use of coherence values alone in the yield estimation is not sufficient.

- When backscatter and coherence values are used together, although the error rate decreased on 29 June-5 July, it did not affect the error rate much on other dates. The combined use of backscatter and coherence values had little or no effect on the yield estimate.

- When backscatter and coherence values are used together, the error rate decreased (RMSE= 44,56 kg) on 29 June-5 July, while it increased the error rate on other dates. The combined use of backscatter and coherence values had little or no effect on the yield estimate.

The following results were obtained when the yield was estimated using backscatter and features of SAR (Sentinel-1) data and features of multi-spectral data (Sentinel-2).

- In the ANN method, when the indices, backscatter, and coherence values we obtained from the optical and SAR satellite images were processed as input values together, the ANN gave better results for all three dates than the SLR method. The best result was obtained in the heading period between 29 June - 5 July (R^2=0.67 RMSE= 26.83 kg).
- The estimated yield values were found with acceptable accuracy. However, the values did not improve.

The following are suggested for further studies:

- Yield estimation can be made with the ANN method by using more plant indices in future studies. Because when the 4 vegetation indices used in this study were used together as input in the ANN method, an improvement was observed in the yield estimation.
- In future studies, yield estimation can be made again by increasing the number of data because only 48 sunflower parcels were used in this study.
- The contribution could not be obtained from the backscatter and coherence values obtained from the SAR data using the ANN method and the SLR method for the yield estimation of the sunflower crop. This data should be re-examined by trying different machine learning and deep learning approaches such as Random Forest, SVM, and CNN.
- In this study, annual data for 2018 were used. It is recommended for future studies to re-examine and interpret yield estimation for longer periods using optical and SAR satellite imagery other.

REFERENCES

[1]   J. G. Wesseling ve R. A. Fedes, Assessing crop water productivity from field
to regional scale, Agricultural Water Management, cilt 86, no. 1, pp. 30-39, **2006.**

[2]   Ayçiçeği Report 2018,

https://www.zmo.org.tr/genel/bizden_detay.php?kod=30602&tipi=17&sub
e=0, (Accessed**: April 19, 2023**).

[3]   B. Aydinoglu, A. Shabani, S M. Safavi, Impact Of Priming On Seed Germination, Seedling Growth And Gene Expression In Common Vetch Under Salinity Stress. Cellular Molecular Biology, 65, 18–24, **2019**.

[4]   S. Tewari, N K Arora, Multifunctional Exopolysaccharides from Pseudomonas Aeruginosa PF23 Involved in Plant Growth Stimulation, Biocontrol and Stress Amelioration in Sunflower under Saline Conditions. Current Microbiol 69:487-494 **2014**.

[5]   Y. Sarwar, M. Shahbaz, Modulation in Growth, Photosynthetic Pigments, Gas Exchange Attributes and Inorganic Ions in Sunfower (Helianthus annuus l) by Strigolactones (GR24) Achene Priming Under Saline Conditions. Pakistan J. Bot**, 2020.**

[6]   Ö.G. Narin, Sentinel-2 Uydu Görüntüleri Kullanarak Ayçiçeği Bitkisi Fenolojik Evresinin İzlenmesi ve Verim Tahmin Çalışması, Master's Thesis, Bülent Ecevit University Institute of Science and Technology, Zonguldak, **2019.**

[7]   N. Musaoğlu, Elektro-optik ve Aktif Mikrodalga Algılayıcılarından Elde Edilen Uydu Verilerinden Orman Alanlarında Meşcere Tiplerinin ve Yetişme Ortamı Birimlerinin Belirlenme Olanakları , PhD Thesis, University of İstanbul Teknik, İstanbul, **1999.**

[8]   W. Rouse, R. H. Haas, J. A. Schell ve D. W. Deering, Monitoring vegetation systems in the Great Plains with ERTS, Proceedings of the Third Earth Resources Technology Satellite- 1 Symposium, NASA, January 1, pp.309-317, **1974.**

[9]   J. Dash, A. Mathur, G. M. Foody, P. J. Curran, J. W. Chipman ve T. M. & Lillesand, Land cover classification using multi-temporal MERIS vegetation indices, International Journal of Remote Sensing, cilt 28, pp. 1137-1159, **2007.**

[10]   Y. Cohen, A. V, B. Campus, I. Hermann, A. Karnieli ve D. J. Bonfil, SWIR-based spectral indices for assessing nitrogen content in potato fields., International Journal of Remote Sensing, cilt 31, pp. 5127-5143, **2010.**

[11]   S. Marino, A. Alvino, Detection of Spatial and Temporal Variability of Wheat Cultivars by High-Resolution Vegetation Indices, Agronomy 9(5):226, **2019**.

[12]   W. J. Frampton, J. Dash, G. Watmough, E. J. Milton, Evaluating The Capabilities Of Sentinel-2 For Quantitative Estimation Of Biophysical Variables In Vegetation, August 2013 ISPRS Journal of Photogrammetry and Remote Sensing 82:83–92, **2013.**

[13]   M. C. Arslanoğlu, Optik ve Radar Uydu Görüntüleri Kullanılarak Zeytinin Farklı Fenolojik Dönemlerindeki Özelliklerinin Araştırılması,PhD. Thesis, Namık Kemal University Institute of Sci. and Technology, Tekirdağ, **2019.**

[14]   F. Balik Sanlı, S. Abdikan, Comparıng A Stereoscopıc Dem Wıth An Interferometrıc Dem Usıng The Same Radarsat Data Paır. ISPRS Commission VII Mid-term Symposium "Remote Sensing: From Pixels to Processes", 69-75, Enschede, the Netherlands, **2006.**

[15]   R. Nasirzadehdizaji, Z. Cakir, F. Balik Sanlı, S. Abdikan, A. Pepe, F. Calò, Sentinel-1 Interferometric Coherence And Backscattering Analysis For Crop Monitoring, Computers And Electronics In Agriculture, 185, 106118, **2021.**

[16]   A. Ferretti, A. Monti-quarnieri, C. Prati, F. Rocca, InSAR Principles: Guidelines For SAR Interferometry Processing And Interpretation, ESA Publ. 1–40, **2007.**

[17]   S. Amherdt, N. Leo, A. Pereira, C. Cornero, M. Pacino, Assessment of Interferometric Coherence Contribution To Corn And Soybean Mapping With Sentinel-1 Data Time Series, Geocarto International, pp. 1–24, **2022.**

[18]   M.T. Esetlı, Sentetik Açıklı Radar(Mikrodalga) Uydu Görüntüleri Kullanılarak, Toprak Özelliklerinin Belirlenebilirliği Üzerine Bir Araştırm, PhD Thesis, Ege University Institute of Sci. and Technology, Izmir, **2008.**

[19]   R. Fieuzal, C. Marais Sicre, F. Baup, Estimation Of Corn Yield Using Multi-Temporal Optical And Radar Satellite Data And Artificial Neural Networks. International Journal of Applied Earth Observation and Geoinformation, 861 57, 14-23, **2017.**

[20]   M. Ameline, R. Fieuzal, J. Betbeder, J. F Berthoumieu, F. Baup, Estimation Of Corn Yield By Assimilating SAR And Optical Time Series Into a Simplified Agro-Meteorological Model: From Diagnostic to Forecast. IEEE Journal Of Selected Topıcs In Applied Earth Observations And Remote Sensing, 11, 4747–4760, **2018.**

[21]   Y. Alebele, W. Wang, W. Yu, X. Zhang, X. Yao, Y. Tian, Y. Zhu, W. Cao, T. Cheng, Estimation Of Crop Yield From Combined Optical And SAR Imagery Using Gaussian Kernel Regression, IEEE Journal Of Selected

Topics In Applied Earth Observations And Remote Sensing,14, 10520–10534, **2021.**

[22]   A.K Ranjan, B. R Parida, Predicting Paddy Yield At Spatial Scale Using Optical And Synthetic Aperture Radar (SAR) Based Satellite Data In Conjunction With Field-Based Crop Cutting Experiment (CCE) Data, International Journal of Remote Sensing, 42, 2046–2071, **2021.**

[23]   P. V Lykhovyd, Prediction Of Sweet Corn Yield Depending On Cultivation Technology Parameters By Using Linear Regression And Artificial Neural Network Methods. Biosystems Diversity 26(1): 11-15, **2018.**

[24]   B. Ji, Y. Sun, S. Yang, J. Wan, "Artificial Neural Networks For Rice Yield Prediction In Mountainous Regions, Journal of Agricultural Science, Vol. 145, No. 3, pp. 249-261, **2007.**

[25]   R. Ballesteros, D.S Intrigliolo, J.F Ortega, J.M Ramírez-Cuesta, I. Buesa, M.A Moreno, Vineyard Yield Estimation By Combining Remote Sensing, Computer Vision And Artificial Neural Network Techniques. Precision Agriculture, *21*, 1242–1262, **2020.**

[26]   A. Ashapure, J. Jung, A. Chang, S. Oh, J. Yeom, M. Maeda, A. Maeda, N. Dube, J. Landivar, S. Hague, et al. Developing a Machine Learning Based Cotton Yield Estimation Framework Using Multi-temporal UAS Data, ISPRS J. of Photogrammetry And Remote Sensing*, 169, 180–194, **2020.**

[27]   R. Fieuzal, F. Baup, Estimation Of Leaf Area Index And Crop Height Of Sunflowers Using Multi-temporal Optical And SAR Satellite Data, International Journal of Remote Sensing, 37 (12): 2780-2809, **2016.**

[28]   Z . Wenzhi, X. Chi, G. Zhao, W. Jingwei, H. Jiesheng, Estimation Of Sunflower Seed Yield Using Partial Least Squares Regression And Artificial Neural Network Models, Pedosphere, 28(5), 764, **2018.**

[29]   O. G Narin, A. Sekertekin, S. Abdikan, F. Balik Sanlı, M. Gullu, Yield Estimation Of Sunflower Plant With CNN And ANN Using Sentinel-2. Int Arch Photogramm Remote Sens Spatial Inf Sci. XLVI-4/W5-2021: 385–389, **2021.**

[30]   O. G Narin, S. Abdikan, Monitoring Of Phenological Stage And Yield Estimation Of Sunflower Plant Using Sentinel-2 Satellite Images, Geocarto International 37(5):1378–1392, **2022.**

[31]   K. Amankulova, N. Farmonov, L. Mucsi, Time-Series Analysis Of Sentinel-2 Satellite Images For Sunflower Yield Estimation, Smart Agricultural Technology, vol. 3, Art. no. 100098, **2023.**

[32]   X. Cui, W. Han, H. Zhang, J. Cui, W. Ma, L. Zhang, G. Li, Estimating Soil Salinity Under Sunflower Cover In The Hetao Irrigation District Based On Unmanned Aerial Vehicle Remote Sensing, Land Degrad. Dev., *34*, 84–97, **2022.**

[33]   S. Khalifani, R. Darvishzadeh, N. Azad, R. Seyed Rahmani, Prediction Of Sunflower Grain Yield Under Normal And Salinity Stress By RBF, MLP And, CNN Models, Industrial Crops & Products, 189, 115762, **2022.**

[34]   P. Bognár, A. Kern, S. Pásztor, P. Steinbach, J. Lichtenberger, Testing the Robust Yield Estimation Method for Winter Wheat, Corn, Rapeseed, and Sunflower with Different Vegetation Indices and Meteorological Data, Remote Sensing, 14, 2860, **2022.**

[35]   M A. Sadenova, N A. Beisekenov, P S. Varbanov, Forecasting Crop Yields Based on Earth Remote Sensing Methods. Chemical Engineering Transactions, 92, 691-696, **2022.**

[36]   S. Abdikan, A. Sekertekin, O G. Narin, A. Delen, F. Balik Sanli, A Comparative Analysis Of SLR, MLR, ANN, XGBoost And CNN For Crop Height Estimation Of Sunflower Using Sentinel-1 and Sentinel-2. Advances in Space Research, Vol. 71(7), 3045- 3059, **2022.**

[37]   Gezipedia. Net ,

        https://www.gezipedia.net/559-zilede-gezilecek-yerler.html,

        (Accessed**: April 14, 2023**).

[38]   Weather Today Zile-Meteoblue,

         https://www.meteoblue.com/en/weather/zile_turkey_737054,(Accessed**: April 14, 2023**).

[39]   Simulated Historical Climate & Weather Data For Zile- Meteoblue, https://www.meteoblue.com/en/weather/historyclimate/climatemodelled/zel e_belgium_2783293, (Accessed**: April 14, 2023**).

[40]   C. Ayla, Azot-Su İlişkileri ve Su Tüketiminin Tarla Parsellerinde Tespiti, Merkez Topraksu Araştırma Enstütüsü Müdürlüğü Yayınları, No: 7, s.62, **1974.**

[41]   Anonymous. (2022, May 12). Sunflower production by country | World Agricultural Production 2021/2022. http://www.worldagriculturalproduction.com/crops/sunflower.aspx. (Accessed**: April 14, 2023**).

[42]   S**.** Tan ,Tarım Ve Köyişleri Bakanlığı Tarımsal Araştırmaları Genel Müdürlüğü, Ege Tarımsal Araştırması Genel Müdürlüğü, Çiftçi Broşürü. No;136 Ankara, **2007.**

[43]   Ayçiçeği Vikipedi,

        https://tr.wikipedia.org/wiki/Ayçiçeği, (Accessed**: April 24, 2023**).

[44]   U. Meier, Growth stages of mono- and dicotyledonous plants - BBCH Monograph. 2nd Edition, Federal Biological Research Centre For Agriculture And Forestry, Basel, Switzerland, P:158, **2001.**

[45]   Sentinel-2 User Handbook**,** European Space Agency (ESA), Paris, France, Tech, Rep**, 2015**

[46]   Y. Kurucu, M T Esetlili, F. Balık Sanlı, Y A. Hussın, Toprağın Değişen Nem Düzeylerinin SAR (Radar) Uydu Görüntüleri İle Belirlenebilirliği Üzerine Bir Araştırma. İzmir, **2008.**

[47]   ESA, About Launch,

https://www.esa.int/Applications/Observing_the_Earth/Copernicus/Sentinel-1/About_the_ launch, (Accessed**: April 15, 2023**).

[48]   Sentinel.ESA.INT,

https://earth.esa.int/web/sentinel/user-guides/sentinel-2- msi/product-types/level-2a, (Accessed**: April 15, 2023**).

[49]   M. Usul, Arazi Kalite Parametrelerinin Buğday Ürün Dekoltesi Üzerine Etkilerinin Uzaktan Algılama ve Coğrafi Bilgi Sistemi Kullanılarak Belirlenmesi, Altınova Tarım İşletme Örneği, PhD Thesis, Ankara University Institute of Science and Technology, Ankara, **2010.**

[50]   M H. Kose, Uydu Radar Görüntülerinden Üç Boyutlu Sayısal Arazi Modelin Üretilmesi, Master's Thesis, Selçuk University Institute of Science and Technology, Konya, **2006.**

[51]   Y. Kurucu, F. Sanlı, M T. Esetlili, M. Bolca, C. Göksel, Contribution Of SAR Images To Define Soil Surface Moisture, 1st Remote Sensing and GIS Symposium, 27-29 November, İstanbul**, 2006**.

[52]   M T Esetlili, Sentetik Açıklıklı Radar (Mikrodalga) Uydu Görüntüleri Kullanılarak Toprak Özelliklerinin Belirlenebilirliği Üzerine Bir Araştırma. PhD Thesis, Ege University Institute of Science and Technology, Izmir**, 2008.**

[53]   S. Abdikan, SAR Görüntülerinden Üretilen İnterferometik ve Stereo Sayısal Yükseklik Modellerinin Kalitesinin İncelenmesi, Master's Thesis, Yıldız Teknik University Institute of Science and Technology, Istanbul, **2007.**

[54]   NİK,

http://nik.com.tr›content_sistem_uydu.asp?id=101, (Accessed**: April 15, 2023**).

[55]   H. B Makineci, H. Karabörek, Research On Accuracy Of Digital Elevation Model Gain From Varied Radar Satellites Data, 6. Remote Sensıng-GIS Symposium, 5- 7 October Adana, **2016.**

[56]   Sentinel-1 Team, Sentinel-1 User Handbook. European Space Agency (ESA), Reference GMES-S1OP-EOPG-TN-13-000, P:80, **2013.**

[57]   Investigation Of Geological Features Of Denizli And Its Surroundings By The Remote Sensing Method, Master's Thesis, Pamukkale University Institute of Science and Technology, Denizli, **2005.**

[58]   M. Loannidou, A. Koukos, V. Sitokonstantinou, I. Papoutsis, C. Kontoes, Assessing The Added Value Of Sentinel-1 PolSAR Data For Crop Classification, Remote Sensing*, 14*, 5739, **2022.**

[59]   S. Kavuret, S. Dereci, O. Cicek, 2021 Ever Given Gemi Kazası Sonrası Süveyş Kanalı Trafik Sıkışıklığının Sentinel-1 Uydu Görüntüleriyle İncelenmesi, Kocaeli University Institute of Science and Technology, Kocaeli, **2021.**

[60]   M S. Ozerdem, E. Acar, Toprak nemi tahmini için Radarsat-2 verisinden çoklu saçılma katsayılarının elde edilmesi, Dicle University Faculty of Engineering Journal of Engineering, Diyarbakır, 8 (4), 759-766, **2017**.

[61]   S. Medasani, G U. Reddy, Analysis And Evaluation Of Speckle Filters For Polarimetric Synthetic Aperture Radar (PolSAR) Data, International Journal Of Applied Engineering Research, Volume 12 Number 15, 4916-4927, **2017**.

[62]   E. Acar, Dicle Nehri Havzasında Toprak Nem Ölçümleri ile SAR İmgeleri Arasındaki İlişkiyi Saptama ve Bu İlişkiye Dayalı Toprak Neminin Tahmini, PhD Thesis, Dicle University Institute of Science and Technology, Diyarbakır, **2017.**

[63]   E. Acar, M S. Özerdem, A Prestudy Over Determination Of The Relationship Between Ground Soil Moistures And RADARSAT-2 Image In Dıcle River Basın, International Engineering, Science and Education Conference, 01-03 December **2016**.

[64]   M. Altun, M. Turker, Agricultural Crop Detection with a Machine Learning Algorithm from Fused Sentinel-1 SAR And Landsat-8 Optical Data, Turkish Journal of Remote Sensing and GIS, 3 (1), 1-19, **2022.**

[65]   M. Kaul, R L. Hill, C. Walthall, Artificial Neural Networks For Corn And Soybean Yield Prediction Agricultural Systems 85, 1–18, **2005.**

[66]   C. Saranya, N. Nagarajan, Efficient Agricultural Yield Prediction Using Metaheuristic Optimized Artificial Neural Network Using Hadoop Framework, Soft Computing., vol. 24, pp. 1–11, January **2020.**

[67]   J. Soria-Ruiz, Y. Fernandez-Ordonez, H. McNairn, Corn Monitoring and Crop Yield Using Optical and Microwave Remote Sensing, Geoscience and Remote Sensing, Pei-Gee Peter Ho (Ed.), ISBN: 978-953-307-003-2, InTech, **2009**.

ADDITIONAL EXPLANATIONS

APPENDIX A: Yield and RMSE values calculated using linear regression and ANN method in NDVI, NDVIR1, OSAVI and IRECI indices for each parcel on 30 June, 8 July and 10 July, and comparison of these values with actual yield values.

Table A.1: Results found for June 30 NDVI index

Parcel Number	Real Yield	Yield Produced With NDVI	30 June Difference	RMSE	Yield Produced With ANN	Difference	RMSE
1	340	320,6801	19,319878	15,9956	317,95	22,05	15,3347
2	340	319,0717	20,928293		317,38	22,62	
3	310	299,8743	10,125745		304,74	5,26	
4	300	313,6225	-13,62249		315,22	-15,22	
5	300	280,9833	19,016654		291,43	8,57	
6	270	267,4991	2,5009055		274,32	-4,32	
7	285	299,5618	-14,56178		304,43	-19,43	
8	330	325,5526	4,4473893		319,9	10,1	
9	340	336,2684	3,7315558		329,29	10,71	
10	330	335,5250	-5,524999		328,24	1,76	
11	340	341,0378	-1,037774		337,77	2,23	
12	300	336,41053	-36,41053		329,5	-29,5	
13	350	346,9811	3,0189336	33,3408	341,2	8,8	33,2916
14	395	366,5974	28,402598		380,95	14,05	
15	230	229,5088	0,4912008		240,09	-10,09	
16	200	213,9092	-13,90919		240,09	-40,09	
17	345	365,2177	-20,21774		380,07	-35,07	
18	300	301,3252	-1,32524		300,89	-0,89	
19	260	257,9809	2,0191269		240,45	19,55	
20	320	340,9152	-20,91517		329,32	-9,32	
21	310	298,3370	11,662998		295,19	14,81	
22	390	376,3986	13,601394		383,48	6,52	
23	260	316,7088	-56,70881		318,33	-58,33	
24	250	339,1112	-89,11125		327,15	-77,15	
25	240	230,0003	9,9997475	21,9899	251,64	-11,64	21,8221
26	320	326,0870	-6,086984		323,59	-3,59	
27	330	329,8219	0,1780748		326,35	3,65	
28	340	365,2424	-25,24244		372,03	-32,03	
29	350	333,0570	16,942982		329,26	20,74	
30	350	331,8520	18,147962		328,14	21,86	
31	410	385,9154	24,08461		403,09	6,91	
32	360	347,0661	12,933938		340,67	19,33	
33	400	369,3315	30,668527		385,32	14,68	
34	380	344,1494	35,85064		338,72	41,29	
35	350	319,7841	30,215937		320,59	29,41	
36	340	317,0690	22,931		319,7	20,3	
37	405	382,1210	22,8790	19,2235	396,25	8,75	17,8196
38	340	345,6486	-5,6486		343,67	-3,67	
39	325	356,1863	-31,1863		347,37	-22,37	
40	385	374,1082	10,8918		373,99	11,01	
41	290	313,9742	-23,9742		308,77	-18,77	
42	270	290,8775	-20,8775		287,17	-17,17	
43	315	317,6169	-2,6169		316,69	-1,69	
44	325	346,9481	-21,9481		344	-19	
45	300	308,3930	-8,3930		298,63	1,37	
46	330	316,3465	13,6535		313,9	16,1	
47	240	230,6816	9,3184		213,01	26,99	
48	320	289,2581	30,7419		286,86	33,14	

Table A.2: Results found for July 8 NDVI index

Parcel Number	Real Yield	Yield Produced With NDVI	8 July Difference	RMSE	Yield Produced With ANN	Difference	RMSE
1	340	331,3038723	8,696128	20,79	326,39	13,61	20,19
2	340	329,6960263	10,30397		324,84	15,16	
3	310	321,2554548	-11,25545		318,19	-8,19	
4	300	290,435219	9,564781		298,78	1,22	
5	300	310,0388523	-10,03885		311,68	-11,68	
6	270	304,3350823	-34,33508		308,59	-38,59	
7	285	327,986737	-42,98674		323,3	-38,3	
8	330	333,0418981	-3,041898		328,18	1,82	
9	340	339,6248714	0,375129		336,27	3,73	
10	330	296,337939	33,66206		303,58	26,42	
11	340	317,533685	22,46631		315,84	24,16	
12	300	296,7093376	3,290662		303,84	-3,84	
13	350	315,5418958	34,4581	44,88	316,14	33,86	42,44
14	395	360,9125154	34,08748		380,73	14,27	
15	230	268,0114293	-38,01143		254,47	-24,47	
16	200	277,3827589	-77,38276		275,26	-75,26	
17	345	362,7103281	-17,71033		385,61	-40,61	
18	300	336,010277	-36,01028		326,7	-26,7	
19	260	304,6787546	-44,67875		312,47	-52,47	
20	320	319,1041129	0,895887		317,24	2,76	
21	310	306,8577651	3,142235		313,35	-3,35	
22	390	356,0310936	33,96891		366,41	23,59	
23	260	328,6487627	-68,64876		321,22	-61,22	
24	250	320,0522005	-70,0522		317,55	-67,55	
25	240	176,1839482	63,81605	29,94	203	37	23,54
26	320	329,5599711	-9,559971		319,38	0,62	
27	330	341,008254	-11,00825		336,62	-6,62	
28	340	357,6258211	-17,62582		377,97	-37,97	
29	350	352,6540482	-2,654048		366,06	-16,06	
30	350	350,8591969	-0,859197		361,3	-11,3	
31	410	368,5646045	41,4354		393,61	16,39	
32	360	357,7561098	2,24389		378,25	-18,25	
33	400	357,6429837	42,35702		378,01	21,99	
34	380	357,2829275	22,71707		377,24	2,76	
35	350	307,440713	42,55929		309,38	40,62	
36	340	322,4341684	17,56583		314,16	25,84	
37	405	360,5924673	44,40753	33,73	379,67	25,33	30,51
38	340	356,1769985	-16,177		371,28	-31,28	
39	325	339,9073892	-14,90739		334,49	-9,49	
40	385	364,1660805	20,83392		385,34	-0,34	
41	290	339,4542335	-49,45423		333,52	-43,52	
42	270	331,4002088	-61,40021		318,47	-48,47	
43	315	281,6719057	33,32809		289,26	25,74	
44	325	294,7464257	30,25357		291,53	33,47	
45	300	285,4459329	14,55407		289,8	10,2	
46	330	327,3476258	2,652374		312,49	17,51	
47	240	252,0323917	-12,03239		284,87	-44,87	
48	320	273,5692537	46,43075		288,25	31,75	

Table A.3: Results found for July 10 NDVI index

Parcel Number	Real Yield	Yield Produced With NDVI	10 July Difference	RMSE	Yield Produced With ANN	Difference	RMSE
1	340	322,2485761	17,7514239	18,378	307,14	32,86	24,379
2	340	319,7971083	20,2028917		306,97	33,03	
3	310	310,0386501	-0,0386501		306,68	3,32	
4	300	290,3358048	9,66419523		306,65	-6,65	
5	300	301,2621121	-1,2621121		306,63	-6,63	
6	270	291,7356925	-21,735692		306,65	-36,65	
7	285	322,661498	-37,661498		307,17	-22,17	
8	330	331,5169406	-1,5169406		308,76	21,24	
9	340	335,0177719	4,98222806		310,21	29,79	
10	330	302,2677387	27,7322613		306,63	23,37	
11	340	317,5282487	22,4717513		306,86	33,14	
12	300	293,4705028	6,52949715		306,64	-6,64	
13	350	314,0736859	35,9263141	42,94	309,29	40,71	40,238
14	395	365,6703388	29,3296612		381,56	13,44	
15	230	254,1742133	-24,174213		247,89	-17,89	
16	200	269,681556	-69,681556		269,16	-69,16	
17	345	366,5800657	-21,580066		384,43	-39,43	
18	300	336,5731501	-36,57315		315,11	-15,11	
19	260	299,6470847	-39,647085		306,53	-46,53	
20	320	318,1778959	1,82210412		309,82	10,18	
21	310	295,0981494	14,9018506		304,72	5,28	
22	390	354,8619739	35,1380261		344,08	45,92	
23	260	328,4558712	-68,455871		311,74	-51,74	
24	250	320,8064	-70,8064		310,19	-60,19	
25	240	241,1028253	-1,1028253	26,275	224,23	15,77	22,923
26	320	334,91627	-14,91627		326,84	-6,84	
27	330	345,8263465	-15,826347		344,38	-14,38	
28	340	361,1772269	-21,177227		380,24	-40,24	
29	350	356,8370456	-6,8370456		371,07	-21,07	
30	350	355,6072046	-5,6072046		368,14	-18,14	
31	410	369,6924266	40,3075734		391,66	18,34	
32	360	359,569093	0,43090703		377,09	-17,09	
33	400	359,8629504	40,1370496		377,69	22,31	
34	380	356,116156	23,883844		369,37	10,63	
35	350	299,2717578	50,7282422		311,1	38,9	
36	340	309,9292997	30,0707003		314,34	25,66	
37	405	370,9617567	34,0382433	36,928	375,7	29,3	36,26
38	340	362,1286674	-22,128667		368,03	-28,03	
39	325	339,3396517	-14,339652		348,87	-23,87	
40	385	362,0885923	22,9114077		367,99	17,01	
41	290	348,6890708	-58,689071		356,72	-66,72	
42	270	332,4525945	-62,452595		342,99	-72,99	
43	315	278,9676908	36,0323092		294,15	20,85	
44	325	291,1756156	33,8243844		305,37	19,63	
45	300	278,6366729	21,3633271		293,85	6,15	
46	330	336,6727543	-6,6727543		346,61	-16,61	
47	240	240,2504717	-0,2504717		262,83	-22,83	
48	320	259,193356	60,806644		277,1	42,9	

Table A.4: Results found for June 30 NDVIR1 index

Parcel Number	Real Yield	Yield Produced With NDVIR1	30 June Difference	RMSE	Yield Produced With ANN	Difference	RMSE
1	340	312,3761623	27,62383772	20,68	318,74	21,26	17,93
2	340	310,3249614	29,67503858		317,18	22,82	
3	310	297,66532	12,33468003		312,09	-2,09	
4	300	301,3021659	-1,302165924		312,93	-12,93	
5	300	267,1269366	32,87306338		304,08	-4,08	
6	270	256,7628092	13,23719081		287,75	-17,75	
7	285	290,3958439	-5,395843912		311,09	-26,09	
8	330	311,3228628	18,6771372		317,91	12,09	
9	340	312,5145678	27,48543217		318,86	21,14	
10	330	317,1519703	12,84802975		323,17	6,83	
11	340	348,2482545	-8,24825447		343,09	-3,09	
12	300	326,6481522	-26,64815223		332,44	-32,44	
13	350	342,4707665	7,52923351	32,27	337,88	12,1	32,23
14	395	384,173205	10,82679501		394,64	0,36	
15	230	234,2843049	-4,284304912		240,96	-10,96	
16	200	225,8707606	-25,87076065		240,91	-40,91	
17	345	381,9191868	-36,91918685		392,2	-47,2	
18	300	297,1763393	2,823660735		292,91	7,09	
19	260	261,8882401	-1,888240136		256,87	3,13	
20	320	337,1936763	-17,1936763		331,76	-11,76	
21	310	317,9403969	-7,940396925		313,04	-3,04	
22	390	395,6104647	-5,610464746		397,53	-7,53	
23	260	319,8977016	-59,89770161		314,13	-54,13	
24	250	329,2394173	-79,23941731		321,43	-71,43	
25	240	240,2291064	-0,229106368	21,67	235,13	4,87	22,8
26	320	310,9560473	9,04395272		316,86	3,14	
27	330	321,0244406	8,975559369		319,84	10,16	
28	340	357,5108695	-17,51086945		357,6	-17,6	
29	350	332,0922321	17,90776787		325,23	24,77	
30	350	331,2551596	18,74484036		324,53	25,47	
31	410	399,1212637	10,87873634		398,65	11,35	
32	360	335,7051005	24,29489951		329,13	30,87	
33	400	365,7270086	34,27299142		362,94	37,06	
34	380	356,3690578	23,63094223		356,87	23,13	
35	350	315,3078228	34,69217716		318,35	31,65	
36	340	310,8863384	29,11366157		316,83	23,17	
37	405	385,8086565	19,19134354	20,08	389,19	15,81	17,87
38	340	358,9450663	-18,94506634		353,49	-13,49	
39	325	346,9474106	-21,94741062		331,12	-6,12	
40	385	389,9337584	-4,933758365		390,32	-5,32	
41	290	305,5995734	-15,59957338		304,02	-14,02	
42	270	319,6864972	-49,68649722		316,37	-46,37	
43	315	316,8656482	-1,865648243		313,9	1,1	
44	325	330,9788231	-5,978823082		322,75	2,25	
45	300	314,5180871	-14,51808706		311,68	-11,68	
46	330	310,4907443	19,50925575		307,89	22,11	
47	240	249,0967157	-9,096715715		251,09	-11,09	
48	320	306,5532741	13,44672588		304,69	15,31	

Table A.5: Results found for July 8 NDVIR1 index

		8 July					
Parcel Number	Real Yield	Yield Produced With NDVIR1	Difference	RMSE	Yield Produced With ANN	Difference	RMSE
1	340	324,7513122	15,24868783	19,57	327,02	12,98	19,92
2	340	322,4770631	17,52293688		325,42	14,58	
3	310	317,1997517	-7,199751712		321,78	-11,78	
4	300	291,5237629	8,476237076		299,51	0,49	
5	300	296,837259	3,16274095		305,31	-5,31	
6	270	293,6056704	-23,60567036		301,88	-31,88	
7	285	317,3675751	-32,36757509		321,89	-36,89	
8	330	328,3027353	1,697264745		329,63	0,37	
9	340	326,6569854	13,34301461		328,4	11,6	
10	330	284,842411	45,157589		290,99	39,01	
11	340	330,3062537	9,693746318		331,19	8,81	
12	300	301,7951864	-1,795186373		310,02	-10,02	
13	350	318,058179	31,941821	41,28	310,48	39,52	34,68
14	395	366,4551271	28,54487286		373,91	21,09	
15	230	263,0895658	-33,08956583		244,06	-14,06	
16	200	274,4332621	-74,43326206		256,69	-56,69	
17	345	364,2954543	-19,29545432		369,06	-24,06	
18	300	326,523986	-26,52398599		314,9	-14,9	
19	260	298,0985475	-38,09854753		297,76	-37,76	
20	320	323,0718585	-3,071858515		312,98	7,02	
21	310	311,5575136	-1,557513569		307,29	2,71	
22	390	375,0493284	14,95067158		390,89	-0,89	
23	260	325,7412549	-65,74125492		314,44	-54,44	
24	250	319,9737287	-69,9737287		311,4	-61,4	
25	240	178,8626584	61,13734161	27,61	203,45	36,55	23,81
26	320	311,372862	8,627138034		313,39	6,61	
27	330	328,6428932	1,357106811		317,6	12,4	
28	340	350,643823	-10,64382302		337,88	2,12	
29	350	341,9500592	8,049940848		326,24	23,76	
30	350	341,193	8,80699996		325,5	24,5	
31	410	382,4417121	27,55828789		399,83	10,17	
32	360	349,7629196	10,23708039		336,4	23,6	
33	400	362,2213501	37,77864991		363,41	36,59	
34	380	368,2631671	11,73683286		378,51	1,49	
35	350	304,7641425	45,23585753		312,21	37,79	
36	340	315,448429	24,55157105		314,11	25,89	
37	405	374,2499355	30,75006454	33,3	385,67	19,33	31,72
38	340	363,9244667	-23,92446671		373,56	-33,56	
39	325	350,2506579	-25,25065791		353,99	-28,99	
40	385	382,0916819	2,908318132		392,24	-7,24	
41	290	335,4879443	-45,48794433		335,08	-45,08	
42	270	348,799619	-78,79961899		351,92	-81,92	
43	315	295,3046379	19,69536211		306,93	8,07	
44	325	295,7470051	29,25299489		307,22	17,78	
45	300	290,5514219	9,448578096		303,58	-3,58	
46	330	318,6523405	11,34765947		320,71	9,29	
47	240	255,1567506	-15,15675063		246,13	-6,13	
48	320	285,7750755	34,22492453		299,55	20,45	

Table A.6: Results found for July 10 NDVIR1 index

		10 July					
Parcel Number	Real Yield	Yield Produced With NDVIR1	Difference	RMSE	Yield Produced With ANN	FARK	RMSE
1	340	317,4688462	22,53115384	19,158	320,05	19,95	18,0895557
2	340	316,062903	23,93709704		319,56	20,44	
3	310	305,4726029	4,527397111		315,25	-5,25	
4	300	289,7149688	10,28503123		303,25	-3,25	
5	300	288,1344611	11,86553891		301,47	-1,47	
6	270	281,0118996	-11,0118996		291,99	-21,99	
7	285	313,2755448	-28,2755448		318,56	-33,56	
8	330	328,6647542	1,335245848		324,15	5,85	
9	340	322,9344634	17,06553656		321,94	18,06	
10	330	288,5070307	41,4929693		301,9	28,1	
11	340	329,9522311	10,04776893		324,71	15,29	
12	300	295,496441	4,503559001		308,78	-8,78	
13	350	317,0613767	32,93862329	39,474	320,84	29,16	36,7081176
14	395	371,5269265	23,4730735		390,64	4,36	
15	230	251,5261673	-21,5261673		241,79	-11,79	
16	200	266,306296	-66,306296		245,16	-45,16	
17	345	370,1314122	-25,1314122		386,89	-41,89	
18	300	328,1891739	-28,1891739		322,99	-22,99	
19	260	294,5114927	-34,5114927		302,37	-42,37	
20	320	321,7881738	-1,78817377		321,85	-1,85	
21	310	299,105482	10,89451802		309,58	0,42	
22	390	373,25746	16,74254003		394,69	-4,69	
23	260	325,6173637	-65,6173637		322,53	-62,53	
24	250	319,8379561	-69,8379561		321,47	-71,47	
25	240	241,8990058	-1,89900580	23,183	229,26	10,74	18,9352709
26	320	318,1257088	1,874291214		229,26	4,92	
27	330	339,42744	-9,42743999		229,26	5,22	
28	340	358,3354512	-18,3354512		229,26	-16,31	
29	350	349,165693	0,834306987		229,26	12,65	
30	350	347,5518085	2,448191539		229,26	15,29	
31	410	382,5733005	27,42669948		395,5	14,5	
32	360	355,9904688	4,009531158		350,95	9,05	
33	400	363,2856035	36,7143965		367,88	32,12	
34	380	367,5359218	12,46407825		377,03	2,97	
35	350	297,9336822	52,06631784		311,97	38,03	
36	340	307,9326504	32,06734961		313,6	26,4	
37	405	378,3047264	26,69527363	35,512	378,69	26,31	23,5016991
38	340	368,2543362	-28,2543362		353,94	-13,94	
39	325	348,2830836	-23,2830836		317,71	7,29	
40	385	379,1944242	5,805575761		380,65	4,35	
41	290	344,8271929	-54,8271929		314,34	-24,34	
42	270	345,7028298	-75,7028298		315,13	-45,13	
43	315	286,9608344	28,03916564		298,83	16,17	
44	325	295,5029955	29,49700453		300,14	24,86	
45	300	282,1522628	17,84773723		297,81	2,19	
46	330	325,2682529	4,731747054		304,46	25,54	
47	240	244,7513979	-4,75139788		269,23	-29,23	
48	320	272,147457	47,852543		294,52	25,48	

Table A.7: Results found for June 30 OSAVI index

Parcel Number	Real Yield	30 June Yield Produced With OSAVI	Difference	RMSE	Yield Produced With ANN	Difference	RMSE
1	340	321,443675	18,556325	16,36133	321,7	18,69	15,6635
2	340	317,326156	22,673844		317,45	25,54	
3	310	286,486779	23,513221		297,04	13,42	
4	300	305,645847	-5,645847		304,18	-1,07	
5	300	276,739183	23,260817		295,54	5,12	
6	270	266,319339	3,680661		290,27	-18,18	
7	285	296,906623	-11,906623		299,09	-12,87	
8	330	318,754683	11,245317		319,02	13,18	
9	340	336,317162	3,682838		334,72	3,14	
10	330	328,334217	1,665783		327,25	-0,87	
11	340	331,695457	8,304543		329,95	6,03	
12	300	329,342589	-29,342589		328,03	-31,91	
13	350	343	7,45931	32,49312	334,84	15,16	32,0035
14	395	369,61693	25,38307		381,56	13,44	
15	230	235,18025	-5,18025		242,25	-12,25	
16	200	225,81376	-25,81376		240,64	-40,64	
17	345	367,64918	-22,64918		380,53	-35,53	
18	300	297,83341	2,16659		295,72	4,28	
19	260	262,25649	-2,25649		265,52	-5,52	
20	320	337,97551	-17,97551		329,63	-9,63	
21	310	294,37017	15,62983		294,48	15,52	
22	390	369,77435	20,22565		381,63	8,37	
23	260	314,67735	-54,67735		310,72	-50,72	
24	250	332,3871	-82,3871		326,1	-76,1	
25	240	230,206	9,794	20,49868	236,6	6,73	20,3397
26	320	334,569785	-14,569785		327,59	-7,35	
27	330	334,48969	-4,48969		327,47	2,83	
28	340	368,77035	-28,77035		372,57	-33,37	
29	350	342,01862	7,98138		340,01	3,55	
30	350	341,53805	8,46195		339,22	4,77	
31	410	388,393625	21,606375		402,18	12,52	
32	360	352,91154	7,08846		352,54	-4,49	
33	400	368,850445	31,149555		372,75	26,57	
34	380	347,865555	32,134445		348,01	21,44	
35	350	322,235155	27,764845		316,66	38,37	
36	340	318,550785	21,449215		315,18	29,89	
37	405	387,277184	17,722816	20,53813	381,53	23,47	21,2811
38	340	348,67712	-8,67712		346,73	-6,73	
39	325	349,433984	-24,433984		348,6	-23,6	
40	385	371,80352	13,19648		373,43	11,57	
41	290	305,872256	-15,872256		305,04	-15,04	
42	270	296,369408	-26,369408		299,6	-29,6	
43	315	330,260096	-15,260096		316,29	-1,29	
44	325	358,600448	-33,600448		365,64	-40,64	
45	300	310,665728	-10,665728		308,09	-8,09	
46	330	319,579904	10,420096		312,14	17,86	
47	240	228,167552	11,832448		220,3	19,7	
48	320	284,932352	35,067648		295,11	24,89	

Table A.8: Results found for July 8 OSAVI index

Parcel Number	Real Yield	Yield Produced With OSAVI	8 July Difference	RMSE	Yield Produced With ANN	Difference	RMSE
1	340	326,292548	13,70745	20,47866	315,78	24,22	21,0263
2	340	323,26234	16,73766		314,16	25,84	
3	310	305,696603	4,303397		310,23	-0,23	
4	300	285,195352	14,80465		293,77	6,23	
5	300	301,340679	-1,34068		308,94	-8,94	
6	270	295,564345	-25,5643		305,74	-35,74	
7	285	323,072952	-38,073		314,07	-29,07	
8	330	327,570917	2,429083		316,67	13,33	
9	340	336,850929	3,149071		329,06	10,94	
10	330	293,43373	36,56627		303,93	26,07	
11	340	311,520284	28,47972		311,29	28,71	
12	300	292,392096	7,607904		302,91	-2,91	
13	350	313,453624	36,54638	42,86491	315,89	34,11	41,8674
14	395	367,770002	27,23		370,4	24,6	
15	230	264,14373	-34,1437		244,91	-14,91	
16	200	274,514304	-74,5143		277,29	-77,29	
17	345	369,597766	-24,5978		370,02	-25,02	
18	300	332,247806	-32,2478		317,78	-17,78	
19	260	301,573158	-41,5732		311,93	-51,93	
20	320	317,705162	2,294838		316,34	3,66	
21	310	300,142734	9,857266		311,12	-1,12	
22	390	354,459112	35,54089		347,45	42,55	
23	260	325,254622	-65,2546		316,88	-56,88	
24	250	315,241654	-65,2417		316,11	-66,11	
25	240	189,631728	50,36827	28,00417	239,49	0,51	26,2076
26	320	338,788532	-18,7885		333,32	-13,32	
27	330	346,761054	-16,7611		358,13	-28,13	
28	340	366,742818	-26,7428		387,41	-47,41	
29	350	359,981312	-9,98131		374,4	-24,4	
30	350	355,995051	-5,99505		369,64	-19,64	
31	410	376,279569	33,72043		400,78	9,22	
32	360	364,825376	-4,82538		383,23	-23,23	
33	400	365,178589	34,82141		383,99	16,01	
34	380	362,807016	17,19298		379,13	0,87	
35	350	303,517691	46,48231		309,6	40,4	
36	340	316,334277	23,66572		300,88	39,12	
37	405	363,723995	41,27601	31,64779	376,92	28,08	32,0014
38	340	359,783321	-19,7833		373,52	-33,52	
39	325	337,773215	-12,7732		322,15	2,85	
40	385	360,215834	24,78417		374,16	10,84	
41	290	336,427619	-46,4276		321,52	-31,52	
42	270	331,910261	-61,9103		319,9	-49,9	
43	315	301,00961	13,99039		316,2	-1	
44	325	313,02386	11,97614		321,65	3,35	
45	300	291,157925	8,842075		304,22	-4,22	
46	330	328,209872	1,790128		319,5	10,5	
47	240	249,876962	-9,87696		296,91	-56,91	
48	320	268,619192	51,38081		261,79	58,21	

Table A.9: Results found for July 10 OSAVI index

Parcel Number	Real Yield	Yield Produced With OSAVI	10 July Difference	RMSE	Yield Produced With ANN	Difference	RMSE
1	340	317,66245	22,3376	19,4929	315,81	24,19	19,35691
2	340	314,689082	25,3109		315,73	24,27	
3	310	300,740488	9,25951		313,68	-3,68	
4	300	286,529538	13,4705		275,42	24,58	
5	300	294,225314	5,77469		307,44	-7,44	
6	270	285,174032	-15,174		263,88	6,12	
7	285	317,706176	-32,7062		315,81	-30,81	
8	330	327,457074	2,54293		316,08	13,92	
9	340	331,042606	8,95739		316,29	23,71	
10	330	298,291832	31,7082		312,24	17,76	
11	340	314,383	25,617		315,72	24,28	
12	300	291,558028	8,44197		301,2	-1,2	
13	350	312,968988	37,031	42,336	325,01	24,99	39,60943
14	395	369,784692	25,2153		376,19	18,81	
15	230	255,66672	-25,6667		269,16	-39,16	
16	200	271,798188	-71,7982		249,21	-49,21	
17	345	370,608108	-25,6081		375,74	-30,74	
18	300	332,431548	-32,4315		317,58	-17,58	
19	260	297,735792	-37,7358		303,46	-43,46	
20	320	316,936356	3,06364		323,17	-3,17	
21	310	292,196448	17,8036		273,22	36,78	
22	390	353,653224	36,3468		362,91	27,09	
23	260	325,46994	-65,4699		318,29	-58,29	
24	250	317,98434	-67,9843		322,5	-72,5	
25	240	245,941	-5,941	26,9445	237,47	2,53	22,55839
26	320	340,62154	-20,6215		323,84	-3,84	
27	330	349,287655	-19,2877		329,73	0,28	
28	340	366,14562	-26,1456		380	-40	
29	350	361,532315	-11,5323		357,66	-7,66	
30	350	358,98853	-8,98853		347,34	2,66	
31	410	377,053715	32,9463		401,52	8,48	
32	360	363,256915	-3,25691		365,95	-5,95	
33	400	364,722825	35,2772		373,25	26,75	
34	380	359,7646	20,2354		350,19	29,81	
35	350	295,35079	54,6492		307,38	42,62	
36	340	304,706745	35,2933		310,13	29,86	
37	405	373,297606	31,7024	34,1947	380,86	24,14	32,10655
38	340	362,981849	-22,9818		369,75	-29,75	
39	325	338,88091	-13,8809		314,62	10,38	
40	385	357,014438	27,9856		365,1	19,9	
41	290	344,43199	-54,432		334,87	-44,87	
42	270	334,069974	-64,07		303,12	-33,12	
43	315	294,47227	20,5277		309,48	5,52	
44	325	305,11184	19,8882		308,17	16,83	
45	300	286,654499	13,3455		306,4	-6,4	
46	330	336,429183	-6,42918		307,89	22,11	
47	240	244,651327	-4,65133		229,21	10,79	
48	320	261,720898	58,2791		240,45	79,55	

Table A.10: Results found for June 30 IRECI index

Parcel Number	Real Yield	Yield Produced With IRECI	Difference	RMSE	Yield Produced With ANN	Difference	RMSE
			30 June				
1	340	317,399167	22,600833	24,5759	320,82	19,18	22,829
2	340	313,623484	26,376516		317,73	22,27	
3	310	275,305909	34,694091		278,51	31,49	
4	300	292,178103	7,821897		307,87	-7,87	
5	300	263,929016	36,070984		252,91	47,09	
6	270	264,091009	5,908991		253,16	16,84	
7	285	289,100236	-4,100236		305,16	-20,16	
8	330	293,710806	36,289194		308,92	21,08	
9	340	326,059562	13,940438		332,05	7,95	
10	330	291,056613	38,943387		306,99	23,01	
11	340	325,299441	14,700559		330,89	9,11	
12	300	313,399186	-13,399186		317,58	-17,58	
13	350	338,723281	11,276719	34,4641	343,4	6,6	34,2013
14	395	381,01067	13,98933		386,62	8,38	
15	230	265,417366	-35,417366		258,87	-28,87	
16	200	256,830556	-56,830556		251,82	-51,82	
17	345	377,72436	-32,72436		382,19	-37,19	
18	300	296,828129	3,171871		299,39	0,61	
19	260	276,103174	-16,103174		264,61	-4,61	
20	320	339,497154	-19,497154		344,58	-24,58	
21	310	298,524289	11,475711		303,02	6,98	
22	390	381,000069	8,999931		386,61	3,39	
23	260	315,655505	-55,655505		319,19	-59,19	
24	250	316,45058	-66,45058		319,51	-69,51	
25	240	235,736376	4,263624	19,5156	223,28	16,72	19,4755
26	320	312,19224	7,80776		311,19	8,81	
27	330	339,695484	-9,695484		339,93	-9,93	
28	340	378,056868	-38,056868		377,45	-37,45	
29	350	351,572712	-1,572712		350,14	-0,14	
30	350	354,16896	-4,16896		354,26	-4,26	
31	410	425,590044	-15,590044		398,17	11,83	
32	360	358,803384	1,196616		361,55	-1,55	
33	400	382,873272	17,126728		383,1	16,9	
34	380	351,475656	28,524344		349,99	30,01	
35	350	317,433264	32,566768		319,66	30,34	
36	340	317,263416	22,736584		319,36	20,64	
37	405	385,9603	19,0397	19,0431	385,88	19,12	18,9388
38	340	347,27065	-7,27065		350,08	-10,08	
39	325	346,59495	-21,59495		349,94	-24,94	
40	385	370,9318	14,0682		360,12	24,88	
41	290	283,28885	6,71115		294,63	-4,63	
42	270	306,77525	-36,77525		304,25	-34,25	
43	315	320,10285	-5,10285		322,13	-7,13	
44	325	345,19695	-20,19695		349,63	-24,63	
45	300	314,4992	-14,4992		312,35	-12,35	
46	330	323,50465	6,49535		328,82	1,18	
47	240	249,0029	-9,0029		233,27	6,73	
48	320	286,7256	33,2744		296,66	23,34	

Table A.11: Results found for July 8 IRECI index

Parcel Number	Real Yield	Yield Produced With IRECI	Difference	RMSE	Yield Produced With ANN	Difference	RMSE
			8 July				
1	340	318,260308	21,7397	26,4869	313,86	26,14	24,4496
2	340	315,689726	24,3103		314,39	25,61	
3	310	287,638398	22,3616		307,61	2,39	
4	300	277,735142	22,2649		287,07	12,93	
5	300	282,248468	17,7515		298,39	1,61	
6	270	281,632476	-11,6325		297,01	-27,01	
7	285	307,823982	-22,824		315,21	-30,21	
8	330	307,634446	22,3656		315,21	14,79	
9	340	324,408382	15,5916		312,36	27,64	
10	330	275,484402	54,5156		280,91	49,09	
11	340	302,52882	37,4712		315,05	24,95	
12	300	283,610758	16,3892		301,22	-1,22	
13	350	308,75595252	41,2405	42,3513	295,59	54,41	35,6256
14	395	383,8477104	11,1523		405,43	-10,43	
15	230	278,1393496	-48,1393		242,47	-12,47	
16	200	280,6087186	-80,6087		242,68	-42,68	
17	345	381,494547	-36,4945		405,48	-60,48	
18	300	323,7984666	-23,7985		306,51	-6,51	
19	260	298,4656458	-38,4656		268,44	-8,44	
20	320	315,112098	4,8879		300,87	19,13	
21	310	296,0543796	13,9456		259,89	50,11	
22	390	362,6208208	27,3792		389,04	0,96	
23	260	318,210914	-58,2109		302,62	-42,62	
24	250	306,1158478	-56,1158		291,45	-41,45	
25	240	241,75866	-1,75866	23,2222	226,52	13,48	22,2214
26	320	326,704736	-6,70474		306,56	13,44	
27	330	351,006559	-21,0066		324,96	5,04	
28	340	374,484001	-34,484		375,03	-35,03	
29	350	363,697382	-13,6974		366,59	-16,59	
30	350	358,832373	-8,83237		354,81	-4,81	
31	410	403,49989	6,50011		403,03	6,97	
32	360	372,347577	-12,3476		374,05	-14,05	
33	400	380,359167	19,6408		378,65	21,35	
34	380	368,063118	11,9369		371,56	8,44	
35	350	296,632246	53,3678		302,05	47,95	
36	340	309,079238	30,9208		309,34	30,66	
37	405	364,862018	40,138	30,0853	396,32	8,68	28,0611
38	340	362,445072	-22,4451		390,7	-50,7	
39	325	339,411688	-14,4117		308,58	16,42	
40	385	359,05912	25,9409		377,88	7,12	
41	290	316,266924	-26,2669		313,29	-23,29	
42	270	335,034454	-65,0345		306,86	-36,86	
43	315	306,04224	8,95776		314,19	0,81	
44	325	317,325034	7,67497		312,93	12,07	
45	300	295,539106	4,46089		308,13	-8,13	
46	330	323,105656	6,89434		310,29	19,71	
47	240	263,261182	-23,2612		256,46	-16,46	
48	320	273,107174	46,8928		259,09	60,91	

Table A. 12: Results found for July 10 IRECI index

Parcel Number	Real Yield	Yield Produced With IRECI	10 July Difference	RMSE	Yield Produced With ANN	Difference	RMSE
1	340	310,103816	29,8962	26,1907	310,99	29,01	22,68829
2	340	308,548836	31,4512		310,51	29,49	
3	310	286,907804	23,0922		298,1	11,9	
4	300	281,771008	18,229		295,77	4,24	
5	300	279,744172	20,2558		294,49	5,51	
6	270	277,492132	-7,49213		292,55	-22,55	
7	285	303,905344	-18,9053		308,48	-23,48	
8	330	307,851776	22,1482		310,26	19,74	
9	340	317,589168	22,4108		312,9	27,1	
10	330	281,8568	48,1432		295,81	34,19	
11	340	306,500552	33,4994		309,74	30,26	
12	300	284,956036	15,044		297,28	2,72	
13	350	309,8176242	40,1824	43,3583	319,89	30,11	40,62285
14	395	380,868657	14,1313		384,02	10,98	
15	230	278,1207375	-48,1207		252,82	-22,82	
16	200	283,3644843	-83,3645		265,89	-65,89	
17	345	379,6792641	-34,6793		382,7	-37,7	
18	300	323,8906599	-23,8907		321,77	-21,77	
19	260	297,5851089	-37,5851		306,64	-46,64	
20	320	314,3321082	5,66789		320,83	-0,83	
21	310	294,6680577	15,3319		298,97	11,03	
22	390	358,0531494	31,9469		356,96	33,04	
23	260	318,794502	-58,7945		321,28	-61,28	
24	250	309,5745366	-59,5745		319,81	-69,81	
25	240	264,275474	-24,2755	27,1961	233,05	6,95	23,14902
26	320	329,070407	-9,07041		318,6	1,4	
27	330	352,545449	-22,5454		339,64	-9,64	
28	340	374,56788	-34,5679		379,77	-39,77	
29	350	366,552012	-16,552		372,32	-22,32	
30	350	363,053022	-13,053		367,07	-17,07	
31	410	407,522004	2,478		403,03	6,97	
32	360	369,47844	-9,47844		375,27	-15,27	
33	400	378,533402	21,4666		384,68	15,32	
34	380	365,353873	14,6461		370,79	9,21	
35	350	290,125588	59,8744		304,27	45,73	
36	340	298,767033	41,233		305,02	34,98	
37	405	264,275474	-24,2755	31,2198	397,73	7,27	28,23564
38	340	329,070407	-9,07041		374,69	-34,69	
39	325	352,545449	-22,5454		346,4	-21,4	
40	385	374,56788	-34,5679		359,02	25,98	
41	290	366,552012	-16,552		317,05	-27,05	
42	270	363,053022	-13,053		338,44	-68,44	
43	315	407,522004	2,478		313,13	1,87	
44	325	369,47844	-9,47844		310,89	14,11	
45	300	378,533402	21,4666		317,49	-17,49	
46	330	365,353873	14,6461		322,7	7,3	
47	240	290,125588	59,8744		228,61	11,39	
48	320	298,767033	41,233		287,28	32,72	

APPENDIX B: Yield and RMSE values calculated using linear regression and ANN method on 30 June, 8 July and 10 July, when all index values are used together, and comparison of these values with actual yield values.

Table B.1: Results for June 30, when all indices are traded together

Parcel Number	Real Yield	30 June Yield Produced With ANN	Difference	RMSE Produced With ANN	Linear RMSE Values NDVI	NDVR1	OSAVI	IRECI	Linear Average RMSE
1	340	322,07	17,93	15,21286736	15,996	20,6761	16,361	24,5759	19,40223856
2	340	320,02	19,98						
3	310	305,49	4,51						
4	300	314,37	-14,37						
5	300	293,2	6,8						
6	270	281,19	-11,19						
7	285	305,77	-20,77						
8	330	318,69	11,31						
9	340	333,14	6,86						
10	330	315,75	14,25						
11	340	339,11	0,89						
12	300	329,12	-29,12						
13	350	334,51	15,49	32,28829548	33,341	32,26569	32,493	34,4641	33,14091432
14	395	391,35	3,65						
15	230	242,55	-12,55						
16	200	241,45	-41,45						
17	345	388,19	-43,19						
18	300	304,44	-4,44						
19	260	253,95	6,05						
20	320	334,94	-14,94						
21	310	310,1	-0,1						
22	390	396,11	-6,11						
23	260	320,78	-60,78						
24	250	317,12	-67,12						
25	240	223,56	16,44	20,24704073	21,99	21,66775	20,499	19,5156	20,9179952
26	320	317,74	2,26						
27	330	335,23	-5,23						
28	340	382,21	-42,21						
29	350	345,98	4,02						
30	350	347,2	2,8						
31	410	398,47	11,53						
32	360	358,53	1,47						
33	400	386,15	13,85						
34	380	352,61	27,39						
35	350	316,8	33,2						
36	340	314,87	25,13						
37	405	392,79	12,21	18,59463744	19,224	20,08218	20,538	19,0431	19,72174462
38	340	349,5	-9,5						
39	325	357,86	-32,86						
40	385	386,78	-1,78						
41	290	313,64	-23,64						
42	270	293,02	-23,02						
43	315	317,48	-2,48						
44	325	354,14	-29,14						
45	300	306,75	-6,75						
46	330	317,81	12,19						
47	240	231,93	8,07						
48	320	295,03	24,97						

Table B.2: Results for July 8, when all indices are traded together

		8 July				Linear RMSE Values				
Parcel Number	Real Yield	Yield Produced With ANN	Difference	RMSE Produced With ANN	NDVI	NDVR1	OSAVI	IRECI	Linear Average RMSE
1	340	319	21	19,06968165	20,788	19,569	20,479	26,487	21,83066357
2	340	315,11	24,89						
3	310	306,88	3,12						
4	300	294,93	5,07						
5	300	297,01	2,99						
6	270	293,81	-23,81						
7	285	313,45	-28,45						
8	330	323,84	6,16						
9	340	324,14	15,86						
10	330	293,04	36,96						
11	340	325,59	14,41						
12	300	304,41	-4,41						
13	350	317,06	32,94	38,90187785	44,883	41,283	42,865	42,351	42,84542683
14	395	399,26	-4,26						
15	230	246,94	-16,94						
16	200	255,65	-55,65						
17	345	396,81	-51,81						
18	300	320,92	-20,92						
19	260	308,78	-48,78						
20	320	318,88	1,12						
21	310	312,17	-2,17						
22	390	380,66	9,34						
23	260	319,7	-59,7						
24	250	317,19	-67,19						
25	240	231,16	8,84	19,12173719	29,938	27,61	28,004	23,222	27,19372438
26	320	310,12	9,88						
27	330	328,33	1,67						
28	340	363,69	-23,69						
29	350	350,28	-0,28						
30	350	347,08	2,92						
31	410	389,26	20,74						
32	360	363,32	-3,32						
33	400	371,89	28,11						
34	380	374,15	5,85						
35	350	310,6	39,4						
36	340	311,34	28,66						
37	405	374,91	30,09	30,60878401	33,728	33,298	31,648	30,085	32,18991851
38	340	365,63	-25,63						
39	325	347,34	-22,34						
40	385	381,84	3,16						
41	290	327,88	-37,88						
42	270	342,98	-72,98						
43	315	308,57	6,43						
44	325	313,39	11,61						
45	300	301,39	-1,39						
46	330	323,2	6,8						
47	240	243,43	-3,43						
48	320	273,37	46,63						

Table B.3: Results for July 10, when all indices are traded together

		10 july				Linear RMSE Values				
Parcel Number	Real Yield	Yield Produced With ANN	Difference	RMSE Produced With ANN	NDVI	NDVR1	OSAVI	IRECI	Linear Average RMSE
1	340	313,73	26,27	22,65977015	18,378	19,158	19,493	26,191	20,80488086
2	340	313,55	26,45						
3	310	314,17	-4,17						
4	300	309,96	-9,96						
5	300	313,75	-13,75						
6	270	311,62	-41,62						
7	285	313,42	-28,42						
8	330	314,36	15,64						
9	340	314,88	25,12						
10	330	313,24	16,76						
11	340	314,25	25,75						
12	300	310,33	-10,33						
13	350	319,44	30,56	39,60945058	42,94	39,474	42,336	43,358	42,02699666
14	395	399,88	-4,88						
15	230	243,33	-13,33						
16	200	259,27	-59,27						
17	345	397,98	-52,98						
18	300	317,72	-17,72						
19	260	311,88	-51,88						
20	320	318,89	1,11						
21	310	312,64	-2,64						
22	390	374,42	15,58						
23	260	318,07	-58,07						
24	250	318,87	-68,87						
25	240	230,89	9,11	19,32246814	26,275	23,183	26,945	27,196	25,89989421
26	320	324,08	-4,08						
27	330	340,32	-10,32						
28	340	365,93	-25,93						
29	350	353,13	-3,13						
30	350	351,22	-1,22						
31	410	391,84	18,16						
32	360	362,36	-2,36						
33	400	372,17	27,83						
34	380	372,13	7,87						
35	350	306,94	43,06						
36	340	316,24	23,76						
37	405	369,74	35,26	32,93257556	36,928	35,512	34,195	31,22	34,46372838
38	340	359,87	-19,87						
39	325	341,91	-16,91						
40	385	363,25	21,75						
41	290	320,81	-30,81						
42	270	341,98	-71,98						
43	315	316,55	-1,55						
44	325	331,35	-6,35						
45	300	307,1	-7,1						
46	330	325,73	4,27						
47	240	237,43	2,57						
48	320	253,9	66,1						

APPENDIX C: Yield and RMSE values calculated by linear regression and ANN method using backscatter values for each parcel in VH and VV polarization on 29 June, 5 July and 11 July, and comparison of these values with actual yield values.

Table C.1: Results for June 29 for VH polarızatıon

Parcel Number	Real Yield	Yield Produced With Backscatter	29 June Difference	RMSE	Yield Produced With ANN	Difference	RMSE
1	340	314,8986648	25,10134	27,416	334,29	5,71	25,249
2	340	318,4725894	21,52741		322,13	17,87	
3	310	328,3209224	-18,32092		321,14	-11,14	
4	300	331,1169745	-31,11697		321,12	-21,12	
5	300	328,1316595	-28,13166		321,14	-21,14	
6	270	326,0984889	-56,09849		321,15	-51,15	
7	285	327,9642587	-42,96426		321,14	-36,14	
8	330	326,5825771	3,417423		321,15	8,85	
9	340	328,6428151	11,35718		321,14	18,86	
10	330	330,1910647	-0,191065		321,13	8,87	
11	340	317,8462938	22,15371		322,73	17,27	
12	300	314,3646061	-14,36461		339,34	-39,34	
13	350	322,2404359	27,75956	65,569	326,03	23,97	62,3
14	395	322,8555254	72,14447		316,37	78,63	
15	230	323,0999236	-93,09992		313,66	-83,66	
16	200	324,7551321	-124,7551		305,07	-105,07	
17	345	322,0738234	22,92618		329,45	15,55	
18	300	324,5309557	-24,53096		305,62	-5,62	
19	260	327,7505608	-67,75056		303,82	-43,82	
20	320	328,9842135	-8,984213		306,03	13,97	
21	310	326,923825	-16,92383		303,43	6,57	
22	390	331,026117	58,97388		325,05	64,95	
23	260	331,8679882	-71,86799		345,77	-85,77	
24	250	331,5956765	-81,59568		338,16	-88,16	
25	240	313,3997026	-73,3997	54,463	313,57	-73,57	51,087
26	320	310,7097875	9,290213		313,74	6,26	
27	330	312,2343699	17,76563		313,1	16,9	
28	340	310,5006451	29,49935		314,14	25,86	
29	350	310,5725983	39,4274		313,98	36,02	
30	350	312,018058	37,98194		313,09	36,91	
31	410	314,4536177	95,54638		316,97	93,03	
32	360	313,8798001	46,1202		314,39	45,61	
33	400	314,68246	85,31754		318,92	81,08	
34	380	310,870875	69,12913		313,53	66,47	
35	350	308,9387297	41,06127		334,21	15,79	
36	340	309,3844007	30,6156		323,37	16,63	
37	405	318,3369021	86,6631	44,092	324,48	80,52	43,758
38	340	320,2629727	19,73703		324,75	15,25	
39	325	323,1096273	1,890373		326,66	-1,66	
40	385	318,2188314	66,78117		324,45	60,55	
41	290	319,5324042	-29,5324		324,66	-34,66	
42	270	320,031763	-50,03176		324,72	-54,72	
43	315	319,266866	-4,266866		324,63	-9,63	
44	325	318,013634	6,986366		324,4	0,6	
45	300	323,0451284	-23,04513		326,52	-26,52	
46	330	321,9613148	8,038685		325,21	4,79	
47	240	323,2182214	-83,21822		326,93	-86,93	
48	320	318,4854333	1,514567		324,51	-4,51	

Table C.2: Results for July 5 for VH polarızatıon

Parcel Number	Real Yield	Yield Produced With Backscatter	5 July Difference	RMSE	Yield Produced With ANN	Difference	RMSE
1	340	322,020357	17,97964303	24,8352	316,12	23,88	23,43158
2	340	322,5487782	17,45122184		310,67	29,33	
3	310	323,6513375	-13,65133748		312,97	-2,97	
4	300	323,7618884	-23,76188836		314,3	-14,3	
5	300	323,5125754	-23,51257537		311,87	-11,87	
6	270	323,2700626	-53,27006257		310,87	-40,87	
7	285	323,4340864	-38,43408643		311,45	-26,45	
8	330	323,1651922	6,83480783		310,65	19,35	
9	340	323,5864762	16,41352377		312,39	27,61	
10	330	324,0196675	5,98033255		320,06	9,94	
11	340	321,7917177	18,20828235		326,14	13,86	
12	300	321,7145669	-21,7145669		331,72	-31,72	
13	350	320,6837152	29,31628484	66,6884	318,92	31,08	66,60857
14	395	320,7452398	74,25476024		318,73	76,27	
15	230	325,9977899	-95,99778994		313,74	-83,74	
16	200	326,0756711	-126,0756711		313,74	-113,74	
17	345	320,6401978	24,35980224		319,06	25,94	
18	300	328,4557727	-28,45577274		314,31	-14,31	
19	260	326,5903769	-66,59037688		313,76	-53,76	
20	320	328,7818531	-8,78185312		314,54	5,46	
21	310	324,1994709	-14,1994709		314,04	-4,04	
22	390	331,6631552	58,33684482		324,26	65,74	
23	260	333,2854538	-73,28545384		346,94	-86,94	
24	250	333,631042	-83,63104202		353,99	-103,99	
25	240	310,2847831	-70,28478313	54,484	309,9	-69,9	53,59074
26	320	315,5811868	4,41881316		326,78	-6,78	
27	330	312,9437065	17,05629355		310,7	19,3	
28	340	315,3108863	24,68911368		321,92	18,08	
29	350	314,8208598	35,17914016		316,22	33,78	
30	350	311,5085679	38,49143212		310,29	39,71	
31	410	309,4450062	100,5549938		309,08	100,92	
32	360	308,7850595	51,21494052		307,59	52,41	
33	400	309,3954568	90,60454317		309	91	
34	380	313,7606735	66,23932646		311,58	68,42	
35	350	316,6107892	33,3892108		356,06	-6,06	
36	340	315,5649551	24,43504486		326,45	13,55	
37	405	312,5339339	92,46606615	46,1382	319,06	85,94	45,98447
38	340	319,0716073	20,9283927		319,03	20,97	
39	325	325,8105682	-0,8105682		323,92	1,08	
40	385	315,3831637	69,61683634		318,86	66,14	
41	290	317,9208148	-27,92081479		318,92	-28,92	
42	270	316,134478	-46,134478		318,85	-48,85	
43	315	316,0249014	-1,0249014		318,85	-3,85	
44	325	314,1954486	10,8045514		318,94	6,06	
45	300	325,4680222	-25,46802222		323,27	-23,27	
46	330	324,024946	5,97505396		321,29	8,71	
47	240	329,0947695	-89,09476947		336,34	-96,34	
48	320	312,1413638	7,85863623		319,12	0,88	

Table C.3: Results for July 11 for VH polarızatıon

Parcel Number	Real Yield	Yield Produced With Backscatter	11 July Difference	RMSE	Yield Produced With ANN	Difference	RMSE
1	340	318,6267447	21,373255	26,497	334,33	5,67	28,51901
2	340	319,9543376	20,045662		328,95	11,05	
3	310	326,3074793	-16,30748		328,71	-18,71	
4	300	328,8912791	-28,89128		341,2	-41,2	
5	300	327,8396501	-27,83965		333,56	-33,56	
6	270	324,738534	-54,73853		327,19	-57,19	
7	285	325,552519	-40,55252		327,74	-42,74	
8	330	323,5962561	6,4037439		326,87	3,13	
9	340	325,6581043	14,341896		327,85	12,15	
10	330	328,0075564	1,9924437		334,48	-4,48	
11	340	318,8950857	21,104914		332,73	7,27	
12	300	318,8059821	-18,80598		333,23	-33,23	
13	350	324,8992634	25,100737	65,597	297,17	52,83	67,71997
14	395	325,3043642	69,695636		308,19	86,81	
15	230	325,916583	-95,91658		318,84	-88,84	
16	200	326,5861101	-126,5861		323,16	-123,16	
17	345	324,6047354	20,395265		289,01	55,99	
18	300	327,1463622	-27,14636		324,27	-24,27	
19	260	327,982073	-67,98207		324,61	-64,61	
20	320	327,879687	-7,879687		324,61	-4,61	
21	310	326,1026848	-16,10268		320,59	-10,59	
22	390	329,1929325	60,807068		323,43	66,57	
23	260	329,405392	-69,40539		322,68	-62,68	
24	250	329,4533152	-79,45332		322,47	-72,47	
25	240	311,8168273	-71,81683	54,424	314,64	-74,64	51,95199
26	320	312,5304999	7,4695001		317,04	2,96	
27	330	312,2834961	17,716504		315,69	14,31	
28	340	312,7081093	27,291891		321,86	18,14	
29	350	312,4900053	37,509995		316,61	33,39	
30	350	312,3044572	37,695543		315,73	34,27	
31	410	311,9217662	98,078234		315,13	94,87	
32	360	311,8601257	48,139874		314,89	45,11	
33	400	311,7831828	88,216817		314,4	85,6	
34	380	312,2378307	67,621619		315,94	64,06	
35	350	312,5931777	37,406822		318,06	31,94	
36	340	312,5724529	27,427547		317,67	22,33	
37	405	315,9175458	89,082454	45,905	320,9	84,1	44,07261
38	340	319,0989104	20,90109		322,32	17,68	
39	325	326,3870706	-1,387071		322,59	2,41	
40	385	313,3903433	71,609657		317,04	67,96	
41	290	317,6796959	-27,6797		321,93	-31,93	
42	270	317,5387459	-47,53875		321,88	-51,88	
43	315	316,834729	-1,834729		321,55	-6,55	
44	325	311,7033422	13,296658		312,12	12,88	
45	300	327,1579884	-27,15799		322,57	-22,57	
46	330	326,5848406	3,4151594		322,58	7,42	
47	240	328,2753242	-88,27532		322,53	-82,53	
48	320	313,9026389	6,0973611		318,14	1,86	

Table C.4: Results for June 29 for VV polarızatıon

Parcel Number	Real Yield	Yield Produced With Backscatter	29 June Difference	RMSE	Yield Produced With ANN	Difference	RMSE
1	340	310,055847	29,944153	30,714247	302,52	37,48	24,796
2	340	314,4275658	25,572434		310,16	29,84	
3	310	336,6877248	-26,68772		327,18	-17,18	
4	300	333,7366522	-33,73665		316,01	-16,01	
5	300	331,3276206	-31,32762		313,2	-13,2	
6	270	331,1524774	-61,15248		313,09	-43,09	
7	285	334,9290704	-49,92907		318,99	-33,99	
8	330	327,0385984	2,9614016		311,93	18,07	
9	340	337,2080987	2,7919013		330,83	9,17	
10	330	338,1917896	-8,19179		339,61	-9,61	
11	340	317,2078286	22,792171		311,11	28,89	
12	300	310,112904	-10,1129		302,73	-2,73	
13	350	317,7905373	32,209463	65,421126	309,72	40,28	65,702
14	395	321,2563958	73,743604		316,96	78,04	
15	230	319,5784607	-89,57846		316,03	-86,03	
16	200	323,3885625	-123,3886		317,12	-117,12	
17	345	320,8601702	24,13983		316,86	28,14	
18	300	325,7105873	-25,71059		317,14	-17,14	
19	260	325,1436902	-65,14369		317,14	-57,14	
20	320	327,8157589	-7,815759		317,14	2,86	
21	310	320,3247302	-10,32473		316,64	-6,64	
22	390	331,98349	58,01651		317,37	72,63	
23	260	331,8857722	-71,88577		317,34	-57,34	
24	250	336,28932	-86,28932		350,02	-100,02	
25	240	317,317395	-77,31739	54,253992	318,98	-78,98	43,836
26	320	306,5502424	13,449758		314,11	5,89	
27	330	309,2724718	20,727528		318,43	11,57	
28	340	305,7176133	34,282387		308,31	31,69	
29	350	307,4913663	42,508634		317,03	32,97	
30	350	312,9788643	37,021136		315,37	34,63	
31	410	320,1041832	89,895817		360,07	49,93	
32	360	315,1430187	44,856981		314,66	45,34	
33	400	320,3758681	79,624132		366,87	33,13	
34	380	311,220713	68,779287		317,41	62,59	
35	350	305,0099771	44,990023		298,88	51,12	
36	340	305,4672686	34,532731		305,57	34,43	
37	405	319,5335691	85,466431	43,613515	376,08	28,92	35,488
38	340	320,7426713	19,257329		309,3	30,7	
39	325	321,5351631	3,4648369		345,66	-20,66	
40	385	320,1286293	64,871371		311,1	73,9	
41	290	320,2851953	-30,2852		307,42	-17,42	
42	270	320,219032	-50,21903		308,57	-38,57	
43	315	321,4557193	-6,455719		343,8	-28,8	
44	325	320,9733894	4,0266106		318,38	6,62	
45	300	322,3245823	-22,32458		345,08	-45,08	
46	330	322,3296351	7,6703649		344,97	-14,97	
47	240	322,9194377	-82,91944		288,47	-48,47	
48	320	320,3462718	-0,346272		306,75	13,25	

Table C.5: Results for July 5 for VV polarızatıon

Parcel Number	Real Yield	Yield Produced With Backscatter	Difference	RMSE	Yield Produced With ANN	Difference	RMSE
1	340	314,5837864	25,416214	28,243	331,77	8,23	26,934
2	340	319,2012272	20,798773		313,21	26,79	
3	310	329,6342656	-19,634266		323,8	-13,8	
4	300	328,2965345	-28,296535		317,47	-17,47	
5	300	331,458305	-31,458305		343,73	-43,73	
6	270	328,6451832	-58,645183		318,69	-48,69	
7	285	329,8427655	-44,842766		325,29	-40,29	
8	330	326,5889028	3,4110972		314,13	15,87	
9	340	329,8802917	10,119708		325,58	14,42	
10	330	329,7592889	0,2407111		324,67	5,33	
11	340	317,7815513	22,218449		314,7	25,3	
12	300	316,1208273	-16,120827		319,74	-19,74	
13	350	319,6054466	30,394553	66,107	307,35	42,65	63,968
14	395	320,3012368	74,698763		310,14	84,86	
15	230	322,1729111	-92,172911		314,67	-84,67	
16	200	326,9812229	-126,98122		316,24	-116,24	
17	345	321,2830862	23,716914		313,1	31,9	
18	300	325,1436544	-25,143654		316,14	-16,14	
19	260	325,7484957	-65,748496		316,19	-56,19	
20	320	329,0171276	-9,0171276		316,3	3,7	
21	310	322,0355659	-12,035566		314,49	-4,49	
22	390	330,9811335	59,018866		316,93	73,07	
23	260	332,7624734	-72,762473		326,06	-66,06	
24	250	332,4396968	-82,439697		322,31	-72,31	
25	240	311,9418509	-71,941851	54,478	306,6	-66,6	48,019
26	320	312,5789942	7,4210058		308,63	11,37	
27	330	312,2244808	17,775519		305,29	24,71	
28	340	312,5541551	27,445845		307,6	32,4	
29	350	312,4931594	37,506841		306,2	43,8	
30	350	312,054872	37,945128		305,48	44,52	
31	410	311,7082379	98,291762		349,6	60,4	
32	360	311,842197	48,157803		311,76	48,24	
33	400	311,748505	88,251495		331,66	68,34	
34	380	312,474734	67,525266		305,98	74,02	
35	350	312,6480786	37,351921		314,45	35,55	
36	340	312,7124684	27,287532		327,52	12,48	
37	405	316,2136567	88,786343	45,553	300,81	104,19	45,924
38	340	318,8344817	21,165518		299,78	40,22	
39	325	323,245292	1,754708		303,55	21,45	
40	385	313,3302268	71,669773		409,59	-24,59	
41	290	315,9717959	-25,971796		301,78	-11,78	
42	270	316,7258055	-46,725806		299,9	-29,9	
43	315	323,8459489	-8,8459489		304,95	10,05	
44	325	319,9777121	5,0222879		300,16	24,84	
45	300	326,6184363	-26,618436		319,38	-19,38	
46	330	325,7691575	4,2308425		313,06	16,94	
47	240	327,9721809	-87,972181		334,56	-94,56	
48	320	318,0170105	1,9829895		299,63	20,37	

Table C.6: Results for July 11 for VV polarızatıon

Parcel Number	Real Yield	Yield Produced With Backscatter	Difference	RMSE	Yield Produced With ANN	Difference	RMSE
1	340	318,6267447	21,373255	30,925047	334,35	5,65	28,7064
2	340	319,9543376	20,045662		323,55	16,45	
3	310	326,3074793	-16,30748		332,52	-22,52	
4	300	328,8912791	-28,89128		334,56	-34,56	
5	300	327,8396501	-27,83965		334,19	-34,19	
6	270	324,738534	-54,73853		328,18	-58,18	
7	285	325,552519	-40,55252		330,78	-45,78	
8	330	323,5962561	6,4037439		324,41	5,59	
9	340	325,6581043	14,341896		331,06	8,94	
10	330	328,0075564	1,9924437		334,28	-4,28	
11	340	318,8950857	21,104914		330,94	9,06	
12	300	318,8059821	-18,80598		331,99	-31,99	
13	350	324,8992634	25,100737	65,454781	303,26	46,74	63,1325
14	395	325,3043642	69,695636		304,87	90,13	
15	230	325,916583	-95,91658		309,96	-79,96	
16	200	326,5861101	-126,5861		314,87	-114,87	
17	345	324,6047354	20,395265		302,73	42,27	
18	300	327,1463622	-27,14636		316,23	-16,23	
19	260	327,982073	-67,98207		316,54	-56,54	
20	320	327,879687	-7,879687		316,55	3,45	
21	310	326,1026848	-16,10268		311,69	-1,69	
22	390	329,1929325	60,807068		315,26	74,74	
23	260	329,405392	-69,40539		314,44	-54,44	
24	250	329,4533152	-79,45332		314,19	-64,19	
25	240	311,8168273	-71,81683	54,237667	323,46	-83,46	54,5875
26	320	312,5304999	7,4695001		303,66	16,34	
27	330	312,2834961	17,716504		307,53	22,47	
28	340	312,7081093	27,291891		331,71	8,29	
29	350	312,4900053	37,509995		303,06	46,94	
30	350	312,3044572	37,695543		306,88	43,12	
31	410	311,9217662	98,078234		319,76	90,24	
32	360	311,8601257	48,139874		321,93	38,07	
33	400	311,7831828	88,216817		324,66	75,34	
34	380	312,3783807	67,621619		304,76	75,24	
35	350	312,5931777	37,406822		307,7	42,3	
36	340	312,5724529	27,427547		305,8	34,2	
37	405	315,9175458	89,082454	44,660851	310,11	94,89	45,9171
38	340	319,0989104	20,90109		310,13	29,87	
39	325	326,3870706	-1,387071		313,13	11,87	
40	385	313,3903433	71,609657		310,07	74,93	
41	290	317,6796959	-27,6797		310,12	-20,12	
42	270	317,5387459	-47,53875		310,12	-40,12	
43	315	316,834729	-1,834729		310,12	4,88	
44	325	311,7033422	13,296658		310,02	14,98	
45	300	327,1579884	-27,15799		315,68	-15,68	
46	330	326,5848406	3,4151594		313,66	16,34	
47	240	328,2753242	-88,27532		322,31	-82,31	
48	320	313,9026389	6,0973611		310,08	9,92	

APPENDIX D: Yield and RMSE values calculated by linear regression and ANN method using coherence values for each parcel in VH and VV polarization on 29

June-5 July, 5 -11 July and 11-17 July comparison of these values with actual yield values.

Table D.1: Results for June 29- July 5 VH polarızatıon

Parcel Number	Real Yield	Yield Produced With Coherence	29 June- 5 July Difference	RMSE	Yield Produced With ANN	Difference	RMSE
1	340	325,2361435	14,7638565	24,89566	323,92	16,08	26,474173
2	340	321,096788	18,903212		321,24	18,76	
3	310	321,8501345	-11,8501345		322,44	-12,44	
4	300	320,4568485	-20,4568485		319,58	-19,58	
5	300	324,4746965	-24,4746965		323,82	-23,82	
6	270	323,526938	-53,526938		323,59	-53,59	
7	285	328,0227155	-43,0227155		324,05	-39,05	
8	330	324,1992795	5,8007205		323,77	6,23	
9	340	325,9813895	14,0186105		323,97	16,03	
10	330	341,6153545	-11,6153545		364,86	-34,86	
11	340	332,4779905	7,5220095		324,95	15,05	
12	300	323,802355	-23,802355		323,67	-23,67	
13	350	327,3566949	22,64330512	65,33171	319,32	30,68	63,510453
14	395	327,5684723	67,43152774		319,74	75,26	
15	230	326,8992944	-96,89929442		318,82	-88,82	
16	200	327,2271142	-127,2271142		319,19	-119,19	
17	345	327,9340058	17,06599418		323,35	21,65	
18	300	327,5007809	-27,50078086		319,56	-19,56	
19	260	328,0026642	-68,00266424		325,05	-65,05	
20	320	327,7202944	-7,7202944		320,51	-0,51	
21	310	327,0124358	-17,0124376		318,99	-8,99	
22	390	327,1033356	62,89666436		319,08	70,92	
23	260	327,1545877	-67,1545877		319,13	-59,13	
24	250	328,0780918	-78,0780918		327,54	-77,54	
25	240	308,7920396	-68,7920396	55,05415	308,69	-68,69	53,954298
26	320	305,9394094	14,0605906		304,86	15,14	
27	330	319,5292688	10,4707312		367,24	-37,24	
28	340	306,2406188	33,7593812		305,52	34,48	
29	350	311,7864154	38,2135846		310,31	39,69	
30	350	309,0400944	40,9599056		308,85	41,15	
31	410	318,2624175	91,7375825		347,79	62,21	
32	360	312,814071	47,185929		311,23	48,77	
33	400	309,8196952	90,1803048		309,27	90,73	
34	380	302,4577831	77,5422169		293,89	86,11	
35	350	314,5947501	35,4052499		314,85	35,15	
36	340	308,1719026	31,8280974		308,22	31,78	
37	405	316,8022762	88,1977238	43,47117	314,87	90,13	44,747484
38	340	320,0187103	19,9812897		315	25	
39	325	319,673143	5,326857		314,94	10,06	
40	385	329,3933309	55,6066691		375,29	9,71	
41	290	316,4921517	-26,4921517		314,9	-24,9	
42	270	322,5262884	-52,5262884		316,39	-46,39	
43	315	314,5516584	0,4483416		315,28	-0,28	
44	325	332,9110288	-7,9110288		392,92	-67,92	
45	300	326,1946182	-26,1946182		332,24	-32,24	
46	330	322,9693234	7,0306766		316,99	13,01	
47	240	324,3604533	-84,3604533		320,44	-80,44	
48	320	321,5604721	-1,5604721		315,57	4,43	

Table D.2: Results for July 5-July 11 VH polarızatıon

Parcel Number	Real Yield	Yield Produced With Coherence	5 July-11 July Difference	RMSE	Yield Produced With ANN	Difference	RMSE
1	340	326,52744	13,47256	26,498	336,26	3,74	28,705
2	340	319,531016	20,468984		314,06	25,94	
3	310	332,022273	-22,02227		337,03	-27,03	
4	300	335,734998	-35,735		339,03	-39,03	
5	300	315,273758	-15,27376		298,83	1,17	
6	270	315,851293	-45,85129		299,58	-29,58	
7	285	330,438177	-45,43818		336,86	-51,86	
8	330	312,105566	17,894434		297,54	32,46	
9	340	325,883901	14,116099		335,97	4,03	
10	330	315,30676	14,69324		298,88	31,12	
11	340	326,081913	13,918087		336,07	3,93	
12	300	327,088474	-27,08847		336,43	-36,43	
13	350	329,5446952	20,455305	64,767	329,73	20,27	68,269
14	395	327,6261886	67,373811		327,37	67,63	
15	230	324,5609884	-94,56099		326,04	-96,04	
16	200	333,462565	-133,4626		341,09	-141,09	
17	345	324,0464464	20,953554		325,59	19,41	
18	300	329,9783806	-29,97838		330,29	-30,29	
19	260	322,1867446	-62,18674		323,8	-63,8	
20	320	327,8614078	-7,861408		327,56	-7,56	
21	310	330,265054	-20,26505		330,63	-20,63	
22	390	329,6255518	60,374448		329,84	60,16	
23	260	327,7732006	-67,7732		327,48	-67,48	
24	250	318,6290542	-68,62905		338,28	-88,28	
25	240	312,107045	-72,10705	55,51	319,13	-79,13	51,363
26	320	306,88067	13,11933		287,85	32,15	
27	330	327,82418	2,17582		255,6	74,4	
28	340	318,09362	21,90638		320,59	19,41	
29	350	314,2166	35,7834		325,94	24,06	
30	350	314,577695	35,422305		326,37	23,63	
31	410	317,276405	92,723595		323,76	86,24	
32	360	318,150635	41,849365		320,31	39,69	
33	400	286,222235	113,77777		360,64	39,36	
34	380	332,860505	47,139495		402,27	-22,27	
35	350	308,648135	41,351865		296,2	53,8	
36	340	303,136685	36,863315		282,02	57,98	
37	405	326,453	78,547	42,144	346,06	58,94	40,537
38	340	321,1286	18,8714		330,48	9,52	
39	325	321,3986	3,6014		331,76	-6,76	
40	385	321,3284	63,6716		331,5	53,5	
41	290	320,9234	-30,9234		328,99	-38,99	
42	270	319,0442	-49,0442		307,1	-37,1	
43	315	320,7506	-5,7506		327,37	-12,37	
44	325	316,5224	8,4776		303,14	21,86	
45	300	322,1168	-22,1168		331,97	-31,97	
46	330	321,4364	8,5636		331,88	-1,88	
47	240	321,782	-81,782		332,41	-92,41	
48	320	321,7982	-1,7982		332,41	-12,41	

Table D.3: Results for July 11- July 17 VH polarızatıon

Parcel Number	Real Yield	Yield Produced With Coherence	11 July-17 July Difference	RMSE	Yield Produced With ANN	Difference	RMSE
1	340	314,476752	25,523248	26,892	304,9	35,1	26,409
2	340	319,859776	20,140224		303,99	36,01	
3	310	326,491232	-16,491232		308,93	1,07	
4	300	317,8596	-17,8596		303,97	-3,97	
5	300	327,79336	-27,79336		313,19	-13,19	
6	270	325,189104	-55,189104		306,53	-36,53	
7	285	325,001168	-40,001168		306,29	-21,29	
8	330	325,350192	4,649808		306,76	23,24	
9	340	317,644816	22,355184		303,99	36,01	
10	330	323,36344	6,63656		304,89	25,11	
11	340	323,108384	16,891616		304,76	35,24	
12	300	327,592	-27,592		312,37	-12,37	
13	350	322,882512	27,117488	72,496	294,54	55,46	70,828
14	395	307,115328	87,884672		314,77	80,23	
15	230	345,519216	-115,519216		338,38	-108,38	
16	200	332,674304	-132,674304		333,6	-133,6	
17	345	310,931728	34,068272		315,68	29,32	
18	300	300,856432	-0,856432		314,52	-14,52	
19	260	329,424912	-69,424912		327,98	-67,98	
20	320	337,646528	-17,646528		335,54	-15,54	
21	310	338,366192	-28,366192		335,65	-25,65	
22	390	312,54552	77,45448		316,58	73,42	
23	260	335,422112	-75,422112		335,06	-75,06	
24	250	319,829392	-69,829392		308,95	-58,95	
25	240	321,68066	-81,68066	57,028	336,8	-96,8	58,979
26	320	319,8658	0,1342		324,2	-4,2	
27	330	309,45238	20,54762		307,66	22,34	
28	340	318,8086	21,1914		319,12	20,88	
29	350	304,5364	45,4636		307,57	42,43	
30	350	311,83108	38,16892		308,19	41,81	
31	410	318,50906	91,49094		317,95	92,05	
32	360	309,61096	50,38904		307,68	52,32	
33	400	306,26316	93,73684		307,49	92,51	
34	380	308,0604	71,9396		307,53	72,47	
35	350	304,23686	45,76314		307,6	42,4	
36	340	308,48328	31,51672		307,56	32,44	
37	405	328,256775	76,743225	44,288	335,26	69,74	44,412
38	340	317,70479	22,29521		316,14	23,86	
39	325	330,104455	-5,104455		335,64	-10,64	
40	385	304,62668	80,37332		302,42	82,58	
41	290	324,850115	-34,850115		331,51	-41,51	
42	270	314,55796	-44,55796		314,84	-44,84	
43	315	329,02183	-14,02183		335,5	-20,5	
44	325	305,49278	19,50722		303,7	21,3	
45	300	320,721705	-20,721705		320,44	-20,44	
46	330	320,90936	9,09064		320,88	9,12	
47	240	319,826735	-79,826735		318,63	-78,63	
48	320	318,094535	1,905465		316,44	3,56	

Table D.4: Results for June 29- July 5 VV polarızatıon

Parcel Number	Real Yield	Yield Produced With Coherence	29 June- 5 July Difference	RMSE	Yield Produced With ANN	Difference	RMSE
1	340	322,9644638	17,03553616	24,62555586	314,66	25,34	22,316
2	340	322,3302895	17,66971048		353,87	-13,87	
3	310	322,5652312	-12,5652312		316,67	-6,67	
4	300	323,1708088	-23,1708088		314,82	-14,82	
5	300	323,3412677	-23,34126768		316,05	-16,05	
6	270	322,6689644	-52,6689644		315,1	-45,1	
7	285	323,0990366	-38,09903664		314,71	-29,71	
8	330	322,9033454	7,09665464		314,66	15,34	
9	340	323,060347	16,93965304		314,68	25,32	
10	330	322,4099118	7,59008824		330,89	-0,89	
11	340	323,2823921	16,71760792		315,33	24,67	
12	300	323,1309977	-23,13099768		314,75	-14,75	
13	350	324,8213088	25,1786912	66,32245552	324,87	25,13	62,758
14	395	317,5199072	77,4800928		326,08	68,92	
15	230	325,5652016	-95,5652016		324,84	-94,84	
16	200	321,1205984	-121,1205984		325,24	-125,24	
17	345	321,3331392	23,6668608		325,18	19,82	
18	300	325,6652208	-25,6652208		324,83	-24,83	
19	260	332,735328	-72,735328		306,62	-46,62	
20	320	325,1526224	-5,1526224		324,86	-4,86	
21	310	326,984224	-16,984224		324,69	-14,69	
22	390	328,8095744	61,1904256		323,69	66,31	
23	260	328,6470432	-68,6470432		323,87	-63,87	
24	250	334,0418288	-84,0418288		322,82	-72,82	
25	240	306,8629522	-66,8629522	56,06087159	336,67	-96,67	54,881
26	320	307,4703681	12,5296319		337,62	-17,62	
27	330	313,7981733	16,2018267		307,17	22,83	
28	340	309,9534309	30,0465691		332,94	7,06	
29	350	307,9709856	42,0290144		337,8	12,2	
30	350	306,3623347	43,6376653		335,06	14,94	
31	410	312,5633168	97,4366832		312,51	97,49	
32	360	313,0639343	46,9360657		309,76	50,24	
33	400	309,3259903	90,6740097		335,65	64,35	
34	380	303,3452799	76,6547201		286,89	93,11	
35	350	309,1724676	40,8275324		336,13	13,87	
36	340	311,9158515	28,0841485		317,33	22,67	
37	405	318,4406613	86,5593387	44,02687085	320,83	84,17	50,52
38	340	321,1521129	18,8478871		331,63	8,37	
39	325	322,7453804	2,2546196		330,58	-5,58	
40	385	324,0315818	60,9684182		323,95	61,05	
41	290	318,9273321	-28,9273321		325,67	-35,67	
42	270	323,6665787	-53,6665787		326,87	-56,87	
43	315	334,3501615	-19,3501615		259,2	55,8	
44	325	316,0188947	8,9811053		270,56	54,44	
45	300	322,8149048	-22,8149048		330,42	-30,42	
46	330	319,779006	10,220994		329,83	0,17	
47	240	323,023478	-83,023478		329,86	-89,86	
48	320	320,7233791	-0,7233791		331,39	-11,39	

Table D.5: Results for July 5- July 11 VV polarızatıon

Parcel Number	Real Yield	Yield Produced With Coherence	5 July-11 July Difference	RMSE	Yield Produced With ANN	Difference	RMSE
1	340	318,81459	21,18541	32,697	299,41	40,59	29,573
2	340	340,348414	-0,348414		335,71	4,29	
3	310	314,776998	-4,776998		295,43	14,57	
4	300	330,150906	-30,150906		315,29	-15,29	
5	300	320,445156	-20,445156		301,25	-1,25	
6	270	323,887462	-53,887462		305,6	-35,6	
7	285	337,0614	-52,0614		328,61	-43,61	
8	330	334,317908	-4,317908		323,02	6,98	
9	340	327,717998	12,282002		311,25	28,75	
10	330	267,490584	62,509416		276,62	53,38	
11	340	325,725084	14,274916		308,2	31,8	
12	300	333,69674	-33,69674		321,81	-21,81	
13	350	327,658762	22,341238	64,139	316,62	33,38	61,257
14	395	330,8949235	64,1050765		375,97	19,03	
15	230	325,531495	-95,531495		315,97	-85,97	
16	200	324,3471655	-124,3471655		316,72	-116,72	
17	345	327,1885505	17,8114495		316,08	28,92	
18	300	322,2400145	-22,2400145		326,97	-26,97	
19	260	326,7359405	-66,7359405		315,9	-55,9	
20	320	327,724139	-7,724139		316,75	3,25	
21	310	328,7073085	-18,7073085		323,52	-13,52	
22	390	329,5119485	60,4880515		345,22	44,78	
23	260	326,5951285	-66,5951285		315,88	-55,88	
24	250	330,002276	-80,002276		361,93	-111,93	
25	240	303,763038	-63,763038	53,995	298,91	-58,91	51,12
26	320	291,786885	28,213115		289,46	30,54	
27	330	314,502411	15,497589		315,11	14,89	
28	340	313,698504	26,301496		313,58	26,42	
29	350	327,509214	22,490786		345,43	4,57	
30	350	314,935284	35,064716		315,95	34,05	
31	410	296,362971	113,637029		292,26	117,74	
32	360	337,135485	22,864515		367,89	-7,89	
33	400	330,992811	69,007189		354,12	45,88	
34	380	289,993554	90,006446		288,58	91,42	
35	350	322,376577	27,623423		332,54	17,46	
36	340	320,150373	19,849627		327,21	12,79	
37	405	336,39174	68,60826	43,219	330,65	74,35	43,021
38	340	309,020492	30,979508		299,97	40,03	
39	325	326,700942	-1,700942		309,62	15,38	
40	385	320,680032	64,319968		304,04	80,96	
41	290	324,15878	-34,15878		306,79	-16,79	
42	270	317,94673	-47,94673		302,54	-32,54	
43	315	326,089294	-11,089294		308,87	6,13	
44	325	317,335082	7,664918		302,26	22,74	
45	300	327,465502	-27,465502		310,65	-10,65	
46	330	327,064108	2,935892		310,1	19,9	
47	240	330,447286	-90,447286		315,54	-75,54	
48	320	324,06321	-4,06321		306,7	13,3	

Table D.6: Results for July 11- July 17 VH polarızatıon

Parcel Number	Real Yield	Yield Produced With Coherence	11 July-17 July Difference	RMSE	Yield Produced With ANN	Difference	RMSE
1	340	328,662042	11,337958	26,3306	323,57	16,43	24,844
2	340	323,972373	16,027627		323,58	16,42	
3	310	322,492681	-12,492681		323,59	-13,59	
4	300	324,294564	-24,294564		323,58	-23,58	
5	300	341,692878	-41,692878		323,6	-23,6	
6	270	321,001056	-51,001056		323,64	-53,64	
7	285	322,003428	-37,003428		323,6	-38,6	
8	330	345,606902	-15,606902		323,64	6,36	
9	340	321,21585	18,78415		323,63	16,37	
10	330	344,580664	-14,580664		323,63	6,37	
11	340	321,764768	18,235232		323,61	16,39	
12	300	318,375796	-18,375796		324,18	-24,18	
13	350	327,6561866	22,3438134	65,8412	321,19	28,81	64,733
14	395	329,3039432	65,6960568		356,97	38,03	
15	230	328,5197248	-98,519725		325,3	-95,3	
16	200	328,6409494	-128,64095		327,25	-127,25	
17	345	328,2937382	16,7062618		323,09	21,91	
18	300	328,3027178	-28,302718		323,15	-23,15	
19	260	329,1782288	-69,178229		348,39	-88,39	
20	320	327,7774112	-7,7774112		321,32	-1,32	
21	310	328,1919694	-18,191969		322,49	-12,49	
22	390	326,5651652	63,4348348		321,19	68,81	
23	260	328,2653028	-68,265303		322,91	-62,91	
24	250	327,5214926	-77,521493		321,09	-71,09	
25	240	302,689918	-62,689918	56,608	313,92	-73,92	53,383
26	320	301,999116	18,000884		313,94	6,06	
27	330	320,012104	9,987896		313,84	16,16	
28	340	313,299594	26,700406		313,8	26,2	
29	350	306,613152	43,386848		313,84	36,16	
30	350	309,663108	40,336892		313,81	36,19	
31	410	300,369866	109,630134		314,01	95,99	
32	360	308,841966	51,158034		313,81	46,19	
33	400	315,085252	84,914748		313,8	86,2	
34	380	301,334382	78,665618		313,96	66,04	
35	350	320,820212	29,179788		313,86	36,14	
36	340	308,516116	31,483884		313,81	26,19	
37	405	318,3979586	86,6020414	43,2445	322,27	82,73	43,079
38	340	322,544795	17,455205		322,22	17,78	
39	325	324,994403	0,005597		322,38	2,62	
40	385	331,905797	53,094203		324,29	60,71	
41	290	315,983345	-25,983345		324,17	-34,17	
42	270	322,2560912	-52,256091		322,21	-52,21	
43	315	323,20094	-8,20094		322,25	-7,25	
44	325	318,4591988	6,5408012		322,26	2,74	
45	300	320,4188852	-20,418885		322,17	-22,17	
46	330	322,2298454	7,7701546		322,21	7,79	
47	240	328,3276196	-88,32762		322,87	-82,87	
48	320	315,2572112	4,7427888		326,57	-6,57	

APPENDIX E: Comparison of yield and RMSE values calculated by linear regression and ANN method with actual yield values when coherence and backscatter values are used together on 29 June-5 July, 5-11 July and 11-17 July.

Table E.1: Results of the 29 June-5 July, when backscatter and coherence values are used together.

Parcel Number	Real Yield	Yield Produced With ANN	Difference	RMSE Produced With ANN	Backscatter (VV)	Coherence (VV)	Linear Average RMSE
1	340	318,44	21,56	22,78356626	30,71424664	24,62555586	27,66990125
2	340	319,19	20,81				
3	310	315,08	-5,08				
4	300	307,25	-7,25				
5	300	307,42	-7,42				
6	270	314,88	-44,88				
7	285	306,93	-21,93				
8	330	314,29	15,71				
9	340	303,16	36,84				
10	330	318,23	11,77				
11	340	316,97	23,03				
12	300	320,73	-20,73				
13	350	313,47	36,53	67,90782656	65,42112633	66,32245552	65,87179093
14	395	314,08	80,92				
15	230	313,7	-83,7				
16	200	314,52	-114,52				
17	345	313,32	31,68				
18	300	330,95	-30,95				
19	260	355,6	-95,6				
20	320	335,97	-15,97				
21	310	315,36	-5,36				
22	390	293,71	96,29				
23	260	295,39	-35,39				
24	250	323,66	-73,66				
25	240	318,59	-78,59	47,36330533	54,25399179	56,06087159	55,15743169
26	320	327,66	-7,66				
27	330	313,1	16,9				
28	340	310,86	29,14				
29	350	317,94	32,06				
30	350	314,58	35,42				
31	410	322,42	87,58				
32	360	323,54	36,46				
33	400	327,59	72,41				
34	380	352,7	27,3				
35	350	320,52	29,48				
36	340	302,45	37,55				
37	405	346,08	58,92	40,19331723	43,61351475	44,02687085	43,8201928
38	340	299,45	40,55				
39	325	311,78	13,22				
40	385	312,58	72,42				
41	290	300,11	-10,11				
42	270	307,53	-37,53				
43	315	297,57	17,43				
44	325	310,76	14,24				
45	300	328,67	-28,67				
46	330	328,82	1,18				
47	240	315,04	-75,04				
48	320	300,53	19,47				

Table E.2: Results of the 5 July- 11 July image, when backscatter and coherence values are used together.

Parcel Number	Real Yield	Yield Produced With ANN	Difference	RMSE Produced With ANN	Backscatter (VV)	Coherence (VV)	Linear Average RMSE
1	340	323,76	16,24	29,49390474	28,24324366	32,69716434	30,470204
2	340	337,19	2,81				
3	310	324,66	-14,66				
4	300	329,47	-29,47				
5	300	325,65	-25,65				
6	270	327,09	-57,09				
7	285	334,42	-49,42				
8	330	331,37	-1,37				
9	340	328,3	11,7				
10	330	294,82	35,18				
11	340	328,58	11,42				
12	300	334,89	-34,89				
13	350	323,1	26,9	60,26784722	66,1068843	64,13938791	65,12313611
14	395	323,11	71,89				
15	230	322,9	-92,9				
16	200	303,36	-103,36				
17	345	323,09	21,91				
18	300	277,62	22,38				
19	260	323,18	-63,18				
20	320	324,41	-4,41				
21	310	323,11	-13,11				
22	390	332,42	57,58				
23	260	282,24	-22,24				
24	250	346,99	-96,99				
25	240	309,28	-69,28	48,71489223	54,47839662	53,99490149	54,23664905
26	320	266,03	53,97				
27	330	301,52	28,48				
28	340	300,72	39,28				
29	350	351,62	-1,62				
30	350	321,3	28,7				
31	410	368,1	41,9				
32	360	353,98	6,02				
33	400	355,82	44,18				
34	380	262,83	117,17				
35	350	348,71	1,29				
36	340	350,52	-10,52				
37	405	313,63	91,37	50,39973338	45,55346366	43,21882673	44,38614519
38	340	264,61	75,39				
39	325	326,42	-1,42				
40	385	375,65	9,35				
41	290	294,21	-4,21				
42	270	279,2	-9,2				
43	315	327,13	-12,13				
44	325	276,23	48,77				
45	300	338,16	-38,16				
46	330	334,72	-4,72				
47	240	346,94	-106,94				
48	320	291,41	28,59				

Table E.3: Results of the 11 July- 17 July image, when backscatter and coherence values are used together.

Parcel Number	Real Yield	Yield Produced With ANN	11 July-17 July Difference	RMSE Produced With ANN	Linear RMSE Values Backscatter (VV)	Coherence (VV)	Linear Average RMSE
1	340	345,23	-5,23	21,74727033	30,92504655	26,33058032	28,62781343
2	340	336,37	3,63				
3	310	311,14	-1,14				
4	300	314,25	-14,25				
5	300	326,12	-26,12				
6	270	317,49	-47,49				
7	285	302,57	-17,57				
8	330	353,8	-23,8				
9	340	310,81	29,19				
10	330	351,43	-21,43				
11	340	326,2	13,8				
12	300	310,77	-10,77				
13	350	309,03	40,97	66,61217456	65,4547807	65,84120151	65,6479911
14	395	299,5	95,5				
15	230	308,15	-78,15				
16	200	320,38	-120,38				
17	345	317,19	27,81				
18	300	326,81	-26,81				
19	260	303,83	-43,83				
20	320	329,17	-9,17				
21	310	323,39	-13,39				
22	390	325,9	64,1				
23	260	333,06	-73,06				
24	250	343,41	-93,41				
25	240	330,58	-90,58	66,82533321	54,23766736	56,60801652	55,42284194
26	320	285,11	34,89				
27	330	373,21	-43,21				
28	340	331,52	8,48				
29	350	267,79	82,21				
30	350	290,89	59,11				
31	410	337,69	72,31				
32	360	301,36	58,64				
33	400	308,03	91,97				
34	380	266,41	113,59				
35	350	366,56	-16,56				
36	340	299,12	40,88				
37	405	316,18	88,82	38,88864873	44,66085079	43,24449056	43,95267068
38	340	307,62	32,38				
39	325	334,77	-9,77				
40	385	350,78	34,22				
41	290	297	-7				
42	270	298,49	-28,49				
43	315	334,53	-19,53				
44	325	294,66	30,34				
45	300	321,39	-21,39				
46	330	322,94	7,06				
47	240	301,3	-61,3				
48	320	281,06	38,94				

APPENDIX F: Comparison of yield and RMSE values calculated by linear regression and ANN method with actual yield values when SAR and optical image values are used together on 29 June-5 July, 5-11 July and 10-17 July.

Table F.1: Results of the 29 June-5 July, when SAR and optical values are used together.

Parcel Number	Real Yield	Yield Produced With ANN	29 June-5 July Difference	RMSE Produced With ANN	30 June Index Values NDVI	NDVR1	OSAVI	IRECI	29 June Backscatter Value(VV)	29 June-5 July Coherence Value(VV)	Linear Average RMSE
1	340	334,82	5,18	25,74771025	15,99562	20,676103	16,36133	24,576	30,71424664	24,62555586	22,15812612
2	340	307,25	32,75								
3	310	287,64	22,36								
4	300	280,47	19,53								
5	300	265,79	34,21								
6	270	239,72	30,28								
7	285	276,82	8,18								
8	330	286,34	43,66								
9	340	321,11	18,89								
10	330	334,55	-4,55								
11	340	331,83	8,17								
12	300	338,34	-38,34								
13	350	329,75	20,25	33,53790679	33,34078	32,265687	32,49312	34,464	65,42112633	66,32245552	44,05120652
14	395	400,1	-5,1								
15	230	244,53	-14,53								
16	200	240,04	-40,04								
17	345	380,49	-35,49								
18	300	303,11	-3,11								
19	260	295,81	-35,81								
20	320	336,2	-16,2								
21	310	316,97	-6,97								
22	390	384,02	5,98								
23	260	317,71	-57,71								
24	250	320,84	-70,84								
25	240	259,23	-19,23	24,4326525	21,98994	21,667746	20,49868	19,516	54,25399179	56,06087159	32,3311407
26	320	333,07	-13,07								
27	330	329,13	0,87								
28	340	340,97	-0,97								
29	350	320,56	29,44								
30	350	311,56	38,44								
31	410	397,99	12,01								
32	360	346,79	13,21								
33	400	393,02	6,98								
34	380	319,45	60,55								
35	350	334,99	15,01								
36	340	335,79	4,21								
37	405	373,6	31,4	23,6101223	19,22353	20,082178	20,53813	19,043	43,61351475	44,02687085	27,75456068
38	340	356,05	-16,05								
39	325	345,61	-20,61								
40	385	385,84	-0,84								
41	290	271,54	18,46								
42	270	297,31	-27,31								
43	315	347,66	-32,66								
44	325	342,3	-17,3								
45	300	329,22	-29,22								
46	330	326,91	3,09								
47	240	250,29	-10,29								
48	320	359,98	-39,98								

Table F.2: Results of the 5-11 July, when SAR and optical values are used together.

Parcel Number	Real Yield	Yield Produce With ANN	5 July- 11 July Difference	RMSE Produced With ANN	NDVI	NDVR1	OSAVI	IRECI	5 July Backscatter Value(VV)	5 July- 11 July Coherence Value(VV)	Linear Average RMSE
1	340	347,91	-7,91	35,54972011	20,78780249	19,56924743	20,47866121	26,48694314	28,24324366	32,69716434	24,71051038
2	340	355,79	-15,79								
3	310	275,46	34,54								
4	300	285,15	14,85								
5	300	276,92	23,08								
6	270	277,88	-7,88								
7	285	303,81	-18,81								
8	330	316,9	13,1								
9	340	321,17	18,83								
10	330	223,93	106,07								
11	340	338,59	1,41								
12	300	326,69	-26,69								
13	350	334,4	15,6	35,72457278	44,8826162	41,28284079	42,86491431	42,35133602	66,1068843	64,13938791	50,27132992
14	395	392,91	2,09								
15	230	248,03	-18,03								
16	200	251,97	-51,97								
17	345	345,39	-0,39								
18	300	371,37	-71,37								
19	260	296,78	-36,78								
20	320	298,32	21,68								
21	310	312,01	-2,01								
22	390	379,13	10,87								
23	260	297,24	-37,24								
24	250	310,13	-60,13								
25	240	243,23	-3,23	26,99067648	29,9380966	27,61038253	28,00417054	23,22224787	54,47839662	53,99490149	36,20803261
26	320	303,77	16,23								
27	330	324,33	5,67								
28	340	333,93	6,07								
29	350	355,57	-5,57								
30	350	332,35	17,65								
31	410	393,2	16,8								
32	360	384,8	-24,8								
33	400	392,46	7,54								
34	380	298,34	81,66								
35	350	330,06	19,94								
36	340	346,04	-6,04								
37	405	373,15	31,85	35,69584511	33,72832981	33,29826847	31,64778837	30,08528739	45,55346366	43,21882673	36,2553274
38	340	349,12	-9,12								
39	325	366,45	-41,45								
40	385	365,1	19,9								
41	290	314,7	-24,7								
42	270	318,29	-48,29								
43	315	266,92	48,08								
44	325	269,27	55,73								
45	300	266,91	33,09								
46	330	345,98	-15,98								
47	240	222,23	17,77								
48	320	274,69	45,31								

Table F:3: Results of the 10-17 July, when SAR and optical values are used together.

Parcel Number	Real Yield	Yield Produced With ANN	10 July-17 July Difference	RMSE Produced With ANN	NDVI	NDVR1	OSAVI	IRECI	11 July Backscatter Value (VV)	11 July-17 July Coherence Value (VV)	Linear Average RMSE
1	340	344,93	-4,93	27,33411833	18,378	19,158	19,493	26,191	30,92504655	26,33058032	23,41252505
2	340	341,67	-1,67								
3	310	263,64	46,36								
4	300	280,87	19,13								
5	300	286,66	13,34								
6	270	271,53	-1,53								
7	285	255,82	29,18								
8	330	320,09	9,91								
9	340	269,92	70,08								
10	330	324,51	5,49								
11	340	347,37	-7,37								
12	300	317,26	-17,26								
13	350	341,79	8,21	32,70057275	42,94	39,474	42,336	43,358	65,4547807	65,84120151	49,90066147
14	395	385,59	9,41								
15	230	240,05	-10,05								
16	200	240,4	-40,4								
17	345	374,57	-29,57								
18	300	318,28	-18,28								
19	260	259,33	0,67								
20	320	327,68	-7,68								
21	310	278,69	31,31								
22	390	338,06	51,94								
23	260	310,38	-50,38								
24	250	308,81	-58,81								
25	240	268,8	-28,8	21,51709998	26,275	23,183	26,945	27,196	54,23766736	56,60801652	35,74087679
26	320	337,49	-17,49								
27	330	351,53	-21,53								
28	340	366,01	-26,01								
29	350	351,89	-1,89								
30	350	345,2	4,8								
31	410	385,84	24,16								
32	360	362,79	-2,79								
33	400	373,19	26,81								
34	380	367,74	12,26								
35	350	312,14	37,86								
36	340	321,03	18,97								
37	405	396,33	8,67	42,63957317	36,928	35,512	34,195	31,22	44,66085079	43,24449056	37,62670914
38	340	373,45	-33,45								
39	325	354,91	-29,91								
40	385	357,97	27,03								
41	290	348,99	-58,99								
42	270	356,24	-86,24								
43	315	344,67	-29,67								
44	325	305,89	19,11								
45	300	316,72	-16,72								
46	330	333,08	-3,08								
47	240	313,88	-73,88								
48	320	287,01	32,99								

CURRICULUM VITAE

Credentials

Name, Surname	:	İrem Ecem ASLAN
Place of Birth	:	İstanbul, Turkey
Date of Birth	:	08.08.1995
Marial Status	:	Single
Address	:	Ankara, Turkey
Telephone	:	+90 507 084 44 54
E-Mail	:	ecemasln@icloud.com

Education

BSC.	:	Erciyes University, Department of Map Engineering, Kayseri, Turkey (2019)
MSc.	:	-
PhD.	:	-